Charles University

Faculty of Science

Experimental Plant Biology

Cellular and Molecular Plant Biology

Bc. Oliver Pitoňak

Role of TCTP1 in plant reproduction

Úloha TCTP1 v rozmnožování rostlin

Diploma thesis

Supervisor: Said S. Hafidh, Ph.D.

Consultant: Prof. RNDr. David Honys, Ph.D.

Prague, 2022

Declaration

I hereby declare that I have written this thesis on my own and that I have stated all used publications and other sources. This thesis or any part of it has not been used to acquire other or the same academic title.

Prohlášení

Prohlašuji, že jsem závěrečnou práci zpracoval samostatně a že jsem uvedl všechny použité informační zdroje a literaturu. Tato práce ani její podstatná část nebyla předložena k získaní jiného nebo stejného akademického titulu.

Prague, 10th August 2022

……..

Bc. Oliver Pitoňak

Acknowledgement

I want to thank my supervisor, Dr. Said Hafidh, for his valuable advice during experimental work and preparation of this thesis. I am grateful to Prof. David Honys for giving me an opportunity to work on such an interesting project in Laboratory of Pollen Biology. Thank you to Dr. Kateřina Malínská, who explained to me the basics of confocal fluorescent microscopy. I would like to thank all members of Pollen Biology Lab for the great time we spent together. Finally, I want to thank my family and friends for their support throughout my study.

Abstract

TCTP is a conserved eukaryotic protein involved in regulation of multiple cellular processes, such as translation, cell cycle and cell death. Apart from its intracellular functions, TCTP is secreted and participates in human immune response. Dimerization via a terminal cysteine residue is critical for its extracellular function. Multiple sequence alignment of eukaryotic TCTPs revealed that terminal cysteine residue is conserved not only in animals but also in green plant lineage. In contrast to animal model organisms, knowledge about TCTP in plants is limited. *Arabidopsis thaliana* genome harbors two TCTP paralogs, *TCTP1* and *TCTP2*. *TCTP1* expression is highly upregulated in pollen. Previously published studies pointed to its role in embryo development, pollen tube growth and targeting. Using mutant characterization and analysis of subcellular localization, the role of *TCTP1* in plant reproduction was investigated in this thesis. Recombinant *Arabidopsis thaliana* TCTP1 protein was produced along with its potential interacting partners BRL2 and TTL3 in heterologous *Escherichia coli* system. *tctp-1* T-DNA line characterization pointed to TCTP1 role in pollen tube growth. It was expressed in mature pollen and pollen tube under native promoter and localized to the cytoplasm. Recombinant *At*TCTP1 formed dimers *in vitro* and mutation of terminal cysteine residue inhibited dimer formation, suggesting a similar dimerization mechanism in animal and plant TCTP. Future experiments will show if TCTP1 dimerization is important for its function in plant development and physiology.

Keywords

TCTP, pollen, male gametophyte, pollen tube, dimerization, recombinant protein expression, *Arabidopsis thaliana*

Abstrakt

TCTP je evolučně konzervovaný eukaryotní protein zapojený do regulace řady buněčných procesů, například translace, buněčného cyklu a buněčné smrti. U člověka je TCTP z buňky sekretován a účastní se imunitní odpovědi. Pro jeho extracelulární funkci je zásadní schopnost dimerizace přes terminální cysteinový zbytek. Porovnání sekvencí TCTP u různých eukaryotních organismů odhalilo, že tento zbytek je evolučně konzervován nejen u živočichů, ale i u rostlin. Na rozdíl od živočišných modelů jsou poznatky o TCTP v rostlinách omezené. V genomu huseníčku rolního (*Arabidopsis thaliana*) jsou kódovány dva paralogní geny *TCTP1* a *TCTP2*. *TCTP1* je silně exprimován v pylu. Publikované studie ukazují na jeho úlohu ve vývoji embrya a růstu pylové láčky. V této diplomové práci byla dále studována úloha *TCTP1* v pohlavním rozmnožování rostlin s využitím metod fenotypové charakterizace mutantní linie a analýzy subcelulární lokalizace. V heterologním bakteriálním systému byl exprimován rekombinantní TCTP1 z huseníčku rolního a jeho potenciální interakční partneři BRL2 a TTL3. Charakterizace mutantní linie *tctp-1* naznačila roli TCTP1 v růstu pylové láčky. TCTP1 exprimován pod kontrolou nativního promotoru lokalizoval v cytoplazmě pylu a pylové láčky. Rekombinantní *At*TCTP1 v *in vitro* podmínkách vytvářel dimery. Mutace terminálního cysteinového zbytku inhibovala dimerizaci. Další experimenty ukážou, jestli je dimerizace TCTP1 důležitá pro vývoj a fyziologii rostlin.

Klíčová slova

TCTP, pyl, samčí gametofyt, pylová láčka, dimerizace, rekombinantní exprese proteinů, huseníček rolní, *Arabidopsis thaliana*

List of abbreviations

ABA	abscisic acid
ATS	alkaline treatment solution
cDNA	complementary deoxyribonucleotide acid
CDS	coding sequence
Col-0	Columbia-0
DAPI	2-(4-amidinophenyl)-1H-indole-6-carbaximadine
dH_2O	distilled water
dNTP	deoxyribonucleotidephosphate
DTT	dithiotreitol
ER	endoplasmic reticulum
gDNA	genomic deoxyribonucleotide acid
GDP	guanine dinucleotide phosphate
GEF	guanine nucleotide exchange factor
GFP	green fluorescent protein
GTP	guanine trinucleotide phosphate
GUS	β-glucuronidase
HAP	hours after pollination
His	polyhistidine tag
HRP	horseradish peroxidase
IMAC	immobilized metal affinity chromatography
IPTG	isopropyl-β-D-thiogalactopyranoside
MBP	maltose binding protein
MD	molecular dynamics
NMR	nuclear magnetic resonance
PCR	polymerase chain reaction
PMSF	phenylmethylsulphonyl fluoride
RNAi	RNA interference
rpm	rotations per minute
SDS/PAGE	sodium dodecyl sulphate polyacrylamide gel electrophoresis
TCTP	translationally controlled tumor protein
WT	wild type
YFP	yellow fluorescent protein

Contents

Introduction

Even though the ability of plants to reproduce sexually was discovered more than 400 years ago, plant reproduction is still a highly researched topic. Two phases alternate in plant life cycle – a diploid sporophytic and a haploid gametophytic phase. Male gametophyte in angiosperms consists of only three cells. Yet its development is a complex process that involves the cooperation with sporophytic tissues and female gametophyte.

A previous study in Laboratory of Pollen Biology revealed that secretion of a well-conserved eukaryotic protein called translationally controlled tumor protein (TCTP) was highly upregulated in tobacco pollen tube after its germination on stigma (Hafidh et al., 2016b). Homologous protein *At*TCTP1 was identified in model species *Arabidopsis thaliana*. Analysis of *tctp-1* T-DNA line pointed to its possible role in male gametophyte development (Berkowitz et al., 2008). Mutant characterization was thus pursued in our laboratory and indicated a role of TCTP1 in pollen tube guidance. Our key objective question is: **Does TCTP1 have a function in pollen tube guidance and what are its interacting partners?** Potential interactors of male expressed TCTP1 in a pollinated pistil were identified by a co-immunoprecipitation experiment. Multiple sequence alignment of eukaryotic TCTPs uncovered that terminal cysteine residue critical for dimerization in human TCTP homolog is conserved in green plant lineage.

In the first part of this thesis, TCTP1 function in model species *Arabidopsis thaliana* is investigated, using mutant characterization and analysis of its subcellular localization in the male gametophyte. In the second part, heterologous bacterial protein expression is utilized to verify if TCTP1 can self-associate and if it interacts with selected candidates BRL2 and TTL3 *in vitro.*

Goals of the thesis

- Phenotypic characterization of *tctp-1* T-DNA insertion line with focus on pollen tube growth and guidance
- Analysis of subcellular localization of TCTP1 in *Arabidopsis thaliana* mature pollen and pollen tubes
- Optimization of recombinant *At*TCTP1 expression in *E. coli* and its purification
- Verification of *At*TCTP1 dimerization *in vitro*
- Recombinant expression of selected potential TCTP1 interacting partners BRL2 and TTL3 and in vitro pull-down experiment

Literature review

Male gametophyte development

Male gametophyte development is a complex process which can be divided into a developmental and a functional phase (Hafidh et al., 2016a). Developmental phase takes place in the stamen and leads to the formation of a mature pollen grain. The functional phase is initiated as soon as a pollen grain lands on a receptive stigma. It germinates and a pollen tube grows through female sporophytic tissues towards ovules. As it reaches the female gametophyte, it bursts and releases the gametes to ensure successful fertilization. In this section, both phases of male gametophyte development are briefly introduced.

Developmental phase

The life of a male gametophyte begins in the anther, which is a part of a flower organ called stamen. A microspore mother cell undergoes meiotic division to produce four haploid microspores in a tetrad. In some plant species, microspores remain joined in a tetrad throughout their development until they are transferred onto a stigma, for example *Erica sp.* (Sarwar and Takahashi, 2014). In *Arabidopsis thaliana*, individual microspores are released from the tetrad.

Prior to the first mitotic division (pollen mitosis I or PMI), microspore becomes polarized. Smaller vacuoles are joined in a single vacuole and the nucleus migrates to the germ cell pole. Mutants with an impaired microspore polarization (such as *gemini pollen1 (gem1))* exhibit decreased gametophytic transmission (Park et al., 1998). Proper microtubule organization is implicated in microspore polarization. Polarized microspore divides asymmetrically into a larger vegetative and a smaller generative cell, giving rise to two distinct cell lineages. Novel regulators of PMI are emerging and broaden our knowledge about genetic regulation of the process (Oh et al., 2020).

The generative cell divides symmetrically in the second mitotic division (pollen mitosis II or PMII) into two male gametes, called the sperm cells. In 30% angiosperms including *Arabidopsis thaliana*, PMII takes place in the anther (Brewbaker, 1967). In remaining 70% flowering plants, the generative cell divides after germination. Vegetative cell and sperm cells are specialized in different functions. This functional distinction is reflected in their epigenetic and transcriptomic profile of vegetative cell and sperm cell (Borges et al., 2008; Borg and Berger, 2015). Whereas chromatin is highly condensed in the sperm cell, it is rather diffuse in the vegetative cell. mRNA transcripts encoding proteins involved in pollen tube growth accumulate in cytoplasmic granules and can be quickly utilized after germination (Honys et al., 2009) Prior to maturation and release from the anthers, pollen undergoes dehydration.

Mature pollen has a unique cell wall structure composed of two layers – a gametophyte-derived intine and a sporophyte-derived exine. Intine composition is comparable with sporophytic primary cell wall and contains cellulose, hemicelluloses, pectin, and cell wall associated proteins. Two layers can be distinguished in the exine – a nexine composed mainly of arabinogalactan proteins, and a sexine that contains the sporopollenin. Pollen cell wall components are deposited at specific timepoints during the developmental phase (summarized in Cascallares et al., 2020).

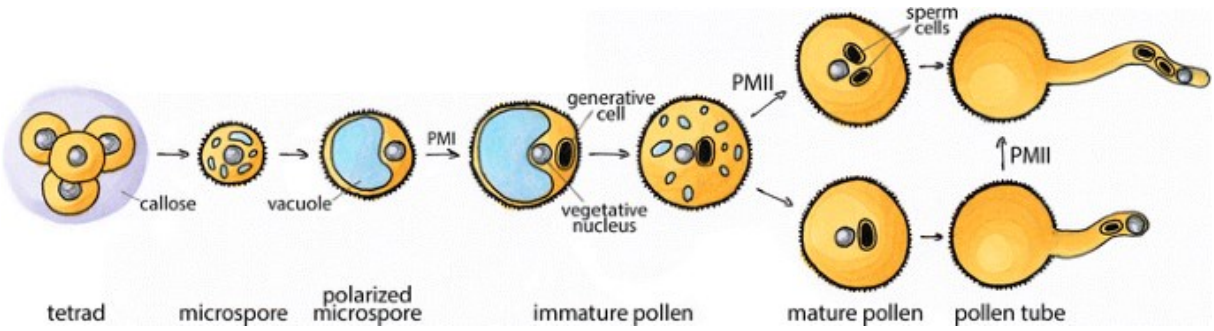

***Figure 1**. **Developmental phase of male gametophyte development**. Adapted from (Honys et al., 2009). PMI – pollen mitosis I, PMII – pollen mitosis II*

Functional phase

When a pollen grain lands and adheres to the stigma, it needs to be hydrated and metabolically activated. Apart from a self-incompatibility response present in some plant species (summarized in Fujii et al., 2016), plants possess a basal compatible response pathway (Doucet et al., 2016). Communication between pollen and stigma is crucial in this process. Molecules on pollen surface mediate the interaction with papilla cells. In turn, cellular responses are initiated in the stigma. For example, PCP-Bs (Pollen coat protein B-class peptides), a class of cysteine rich peptides present in the pollen coat are critical for pollen hydration (Wang et al., 2017). Upon compatible pollination, their interaction with receptor kinases ANJ (ANJEA) and FER (FERONIA) localized in papilla plasma membrane leads to a decrease in levels of ROS (reactive oxygen species) in the papillae (Liu et al., 2021a). In addition, actin cytoskeleton undergoes a rearrangement and concentrates around the contact site with the pollen (Rozier et al., 2020). Secretory vesicles fuse with the papilla plasma membrane at the contact site and release cargo to promote hydration (Safavian and Goring, 2013). Calcium is exported via an ATPase pump from the papilla cell (Iwano et al., 2014). Emerging pollen tube penetrates papilla cell wall and grows through the apoplast to the ovary.

Along with root hairs, pollen tubes present a unique model system to study unidirectional tip growth. Growth of both root hairs and pollen tubes is impaired in *tip1* mutant, which suggests existence of some common mechanisms in these systems (Schiefelbein et al., 1993) Pollen tube cytoplasm is highly

polarized and cellular processes are localized to its tip. Three regions can be distinguished in a growing pollen tube – a non-growing shank containing sperm cells and the vegetative nucleus, a subapical region rich in organelles, and a growing apex with a so-called clear zone. The clear zone contains numerous vesicles that form a dome-like structure (summarized in Hepler and Winship, 2015). These vesicles fuse with plasma membrane and release cargo required for pollen tube growth, such as cell wall components. Exocytosis is polarly localized to the tip by the exocyst complex (Bloch et al., 2016). Vesicle transport is mediated by actin cytoskeleton. Material is secreted in excess and the process of endocytosis maintains a dynamic balance at the tip. Cell wall must remain intact until pollen tube reaches the micropyle. As a pollen tube expands, cell wall experiences mechanical stress and new cell wall material needs to be incorporated. Mutation of genes involved in cell wall integrity signaling pathway typically leads to premature pollen tube burst (Mecchia et al., 2017). RAPID ALKALINIZATION FACTOR4 (RALF4) and RALF19 are expressed in the pollen tube and secreted to the cell wall along with LEUCIN-RICH REPEAT EXTENSINS (LRXs) (Mecchia et al., 2017; Fabrice et al., 2018). They interact and bind to receptor like kinase in pollen tube plasma membrane to activate downstream signaling pathways (summarized in Vogler et al., 2019). Activity of other key players in pollen tube growth is modulated, including ROP (RHO OF PLANTS) GTPases, H^+ ATPases and Ca^{2+} channels. Ion dynamics is critical for pollen tube growth. For example, mutations in H^+ ATPases (AHA6, AHA8 and AHA9) result in pollen tube growth defects and decrease in transmission (Hoffmann et al., 2020).

On the way from stigma to the micropyle of an ovule, a pollen tube needs to pass through multiple tissues: transmitting tract, septum epidermis and funiculus. Extensive communication with female tissues guides the way of a growing pollen tube. An example of a chemical signal directing the pollen tube is concentration gradient of γ-aminobutyric acid (Palanivelu et al., 2003). Passage through stigma and style confers competence on pollen tube to respond to ovular guidance signals (Palanivelu and Preuss, 2006). Transcriptome and secretome of pollen tubes that passed through stigma and style differs largely from pollen tubes germinated *in vitro* (Qin et al., 2009; Hafidh et al., 2016b). Transmitting tract consists of cells that secrete extracellular matrix rich in glycoproteins, glycolipids, and polysaccharides and undergo programmed cell death. Proper transmitting tract development is crucial for pollen tube growth (Crawford et al., 2007). At some point, a pollen tube needs to turn towards an ovule and grow on the surface of a funiculus towards the micropyle. *mpk3 mpk6* double mutant pollen tubes do not turn towards the ovules but can normally target ovules in a semi-in vivo assay (Guan et al., 2014). MPK3 and MPK6 thus play a role in funicular but not in micropylar guidance and it is sensible to distinguish these two phases. On the other hand, LURE peptides secreted by the synergid cell and perceived by PRK6 receptor kinase in the pollen tube participate in both phases (Liu et al., 2021b). As

a pollen tube passes through micropyle, communication with synergid cell leads to its burst and release of sperm cells, which fuse with the egg cell and the central cell.

Translationally controlled tumor protein

Translationally controlled tumor protein (TCTP) was discovered as a protein encoded by an abundant untranslated mRNA in murine tumor cells (Yenofsky et al., 1983). Various names are used in literature to describe TCTP – e. g. P23, fortilin, HRF (Histamine releasing factor) or MMI1 (Microtubule and mitochondria-interacting protein 1). Throughout this thesis, the term "Translationally controlled tumor protein (TCTP)" is used exclusively.

TCTP homologs have been identified and characterized in various eukaryotic organisms, including plants. It has become clear that TCTP is a multifunctional protein regulating many cellular processes. However, information about its precise molecular function is still lacking.

In this section, I would like to review a few chosen aspects of TCTP structure and function with a focus on plant TCTPs. I will address following questions:

1. What can be inferred from evolution of TCTP family?
2. How conserved are TCTP functions in different eukaryotic organisms?
3. Why is it interesting to study TCTP in male gametophyte development?

Evolution of TCTP family

TCTP genes in eukaryotic genomes

A recent study analysed the phylogeny of *TCTP* genes (Koo et al., 2020). No TCTP homologs were found in either *Archaea* or *Bacteria*. 533 candidate genes from 377 eukaryotic species were identified. The number of *TCTP* genes in an organism is lineage dependent. Most fungi, protozoans and invertebrates carry a single *TCTP* gene. In contrast, multiple *TCTP* paralogs are present in mammalian and plant species. It is noteworthy that no *TCTP* homolog has been identified in genomes of some eukaryotic organisms, such as *Chlamydomonas reinhardtii* (Gutiérrez-Galeano et al., 2014). This might be due to technical limitations in genome sequencing or a loss of *TCTP* genes. In the latter case, other proteins are thought to substitute TCTP functions (Gutiérrez-Galeano et al., 2014).

Multiple *TCTP* paralogs in mammals and plants were already documented in previous studies (Hinojosa-Moya et al., 2008) along with speculations of a possible subfunctionalization or neofunctionalization (Gutiérrez-Galeano et al., 2014). For example, *TCTP* paralogs (*CsTCTP1* and *CsTCTP2*) in *Cucumis sativus* have different functions in defense response to *Sphaerotheca fuliginea* (Meng et al., 2018). *Arabidopsis thaliana* genome harbors two *TCTP* genes (At*TCTP1* and At*TCTP2*) with different expression profiles and low redundancy (Toscano-Morales et al., 2015). Higher copy number of *TCTP* genes in plants and mammals is likely a result of whole genome duplication in these lineages (Koo et al., 2020).

Protein sequence conservation

Multiple sequence alignment of TCTP protein sequences uncovers which parts of the sequence are conserved and which are variable. Regions with high sequence similarity might be important for function in different organisms. Remarkably, nearly 9% of TCTP amino acid residues are evolutionary conserved (Hinojosa-Moya et al., 2008). Two regions are marked as signature patterns for TCTPs on PROSITE database (https://prosite.expasy.org/). These are named TCTP1 (corresponds to 48I-58E in human TCTP) and TCTP2 (129F-151Y) (Figure 2A). TCTP3 profile represents the whole TCTP domain. Interestingly, there is a TCTP homolog in a unicellular algal species *Nannochloropsis oceanica* from the *Eustigmatophyceae* family that lacks both TCTP1 and TCTP2 patterns. *No*TCTP has only 28% identity and 34% similarity to human TCTP (*At*TCTP1 has 38% identity and 56% similarity to *Hs*TCTP) but retains some of conserved TCTP functions (Yao et al., 2015). Sequences of plant TCTP homologs display 70.2-95.2% identity and 80.4-98.2% similarity, which suggests high conservation of plant TCTP structure and possibly function (Gutiérrez-Galeano et al., 2014).

Structure conservation

TCTP structure has been experimentally solved in various organisms, including *Schizosaccharomyces pombe* (Thaw et al., 2001), *Plasmodium knowlesi* (Vedadi et al., 2007), *Plasmodium falciparum* (Eichhorn et al., 2013), alga *Nannochloropsis oceanica* (Yao et al., 2019), *Mus musculus* (Doré et al., 2018) and *Homo sapiens* (Feng et al., 2007; Susini et al., 2008; Doré et al., 2018). Experimental structure of a plant TCTP has not yet been reported in literature.

First experimentally solved structure of the fission yeast homolog contains four α helices (H1-H3), four β strands (sA-sD) and a disordered loop (Figure 2B) (Thaw et al., 2001). Sheets A and B form a β-barrel like central structure that packs H1 and H3 on opposite sides. H1 helix is shorter (5 amino acid residues) than H2 and H3 helices, which form an α-helical hairpin. Sheet C protrudes from the globular structure and anchors the flexible loop. Sheet D is a shorter extension of sheet A.

TCTP1 signature pattern maps on the disordered loop region. Nuclear magnetic resonance (NMR) experiments and molecular dynamics (MD) simulations point to a great flexibility of the loop (Malard et al., 2018). Remarkably, it can extend up to β-barrel core domain and contact TCTP2 signature pattern. Calcium binding influences flexible loop conformation and might impact TCTP function. The flexible loop is known to be functional in TCTP-regulated immune response (Lee et al., 2020).

TCTP sequences do not show any similarity to other known protein families. Nevertheless, β-barrel like structure in fission yeast TCTP is similar to a human protein RABIF (Rab-interacting factor)/MSS4 (Mammalian suppressor of Sec4) (Thaw et al., 2001). In mammalian cells, RABIF is involved in vesicle trafficking and positively regulates stability of selected Rab GTPases involved in the exocytosis

(Gulbranson et al., 2017). Interestingly, interaction of *Arabidopsis thaliana* TCTP1 with 4 Rab GTPases was confirmed in a bimolecular fluorescence complementation experiment (Brioudes et al., 2010). Biological relevance of these interactions is unclear.

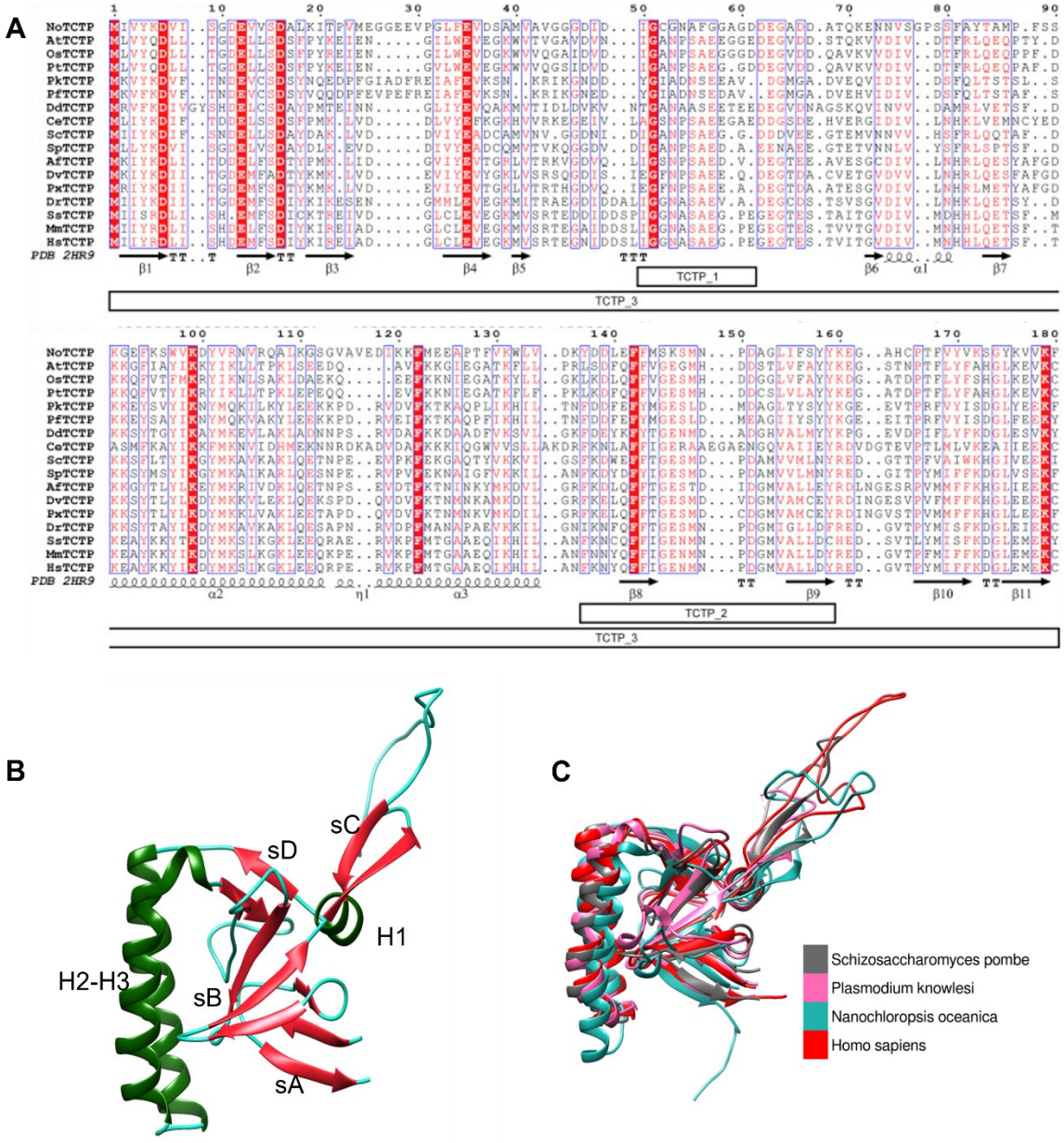

Figure 2. TCTP in evolutionary perspective*. (A) Multiple sequence alignment of TCTP sequences from various eukaryotic organisms. Human TCTP secondary structure and TCTP signature patterns under the sequences. (B) Experimentally determined structure of Schizosaccharomyces pombe TCTP. Helices are marked green, sheets are marked red and loops are marked cyan. (C) Comparison of experimentally determined TCTP structures of Schizosaccharomyces pombe, Plasmodium knowlesi, Nanochloropsis oceanica and Homo sapiens. Adapted from (Yao et al., 2019), protein structural models visualized in Chimera*

No-Nannochloropsis oceanica; At- Arabidopsis thaliana; Os-Oryza sativa; Pt-Populus trichocarpa; Pk-Plasmodium knowlesi; Pf- Plasmodium falciparum; Dd-, Dictyostelium discoideum; Ce- Caenorhabditis elegans; Sc- Saccharomyces cerevisiae; Sp- Schizosaccharomyces pombe; Af- Artemia franciscana; Dv- Drosophila virilis; Px- Plutella xylostella; Dr- Danio rerio; Ss-, Sus scrofa; Mm- Mus musculus; Hs- Homo sapiens

Even though the overall fold of TCTP is well conserved Figure 2C), structures of TCTP homologs from different organisms vary in number of defined helices and sheets (Yao et al., 2019). These differences might reflect in TCTP functions. TCTP homolog in *Plasmodium knowlesi* contains an extra helical segment on N-terminus (Vedadi et al., 2007). It is speculated that this helix might distort the structure of GTPase binding pocket in its proximity and hamper interactor binding (Hinojosa-Moya et al., 2008).

TCTP dimerization

Dimerization and/or oligomerization can be important for protein function. Self-association of TCTP was first discovered in the rat homolog (Yoon et al., 2000). Most reported TCTP solution structures are monomeric (e. g. Thaw et al., 2001). A recently reported solution structure for a dimeric *Hs*TCTP contains an intermolecular disulfide bond between C172 residues (Doré et al., 2018). TCTP dimerization by a disulfide bond is necessary for its function in immune response (Kim et al., 2009). The flexible loop region and H2 helix are critical for dimer cytokine-like activity (Lee et al., 2020). Interestingly, *At*TCTP1 associates with *Hs*TCTP and with itself in a bimolecular fluorescence experiment (Brioudes et al., 2010). This result indicates a possibly conserved mechanism of self-association in plant and animal TCTP homologs.

TCTP functions and interactors

Regulation of translation

Using yeast two hybrid screen, interaction of human TCTP with components of translational machinery was uncovered in two independent studies (Cans et al., 2003; Langdon et al., 2004). TCTP directly interacts with elongation factors eEF1A (Cans et al., 2003) and eEF1Bβ (Cans et al., 2003; Langdon et al., 2004). They are part of elongation factor eEF1 complex, which brings aminoacyl-tRNAs to the ribosome during translation (summarized in Xu et al., 2022). eEF1A is a GTPase that binds aminoacyl-tRNA in a GTP-bound state. After proper binding to the ribosome, bound GTP is hydrolyzed to GDP. GDP must be released for GTP binding and another elongation cycle to begin. eEF1B is a guanine nucleotide exchange factor required for GDP release from eEF1A. In yeast, it consists of a catalytic α subunit and a structural γ subunit. Both subunits are present in animal and plant eEF1B along with another catalytic subunit β in animals and δ in plants.

Human TCTP preferentially binds to eEF1A1 in a GDP bound state and stabilizes it (Cans et al., 2003). Furthermore, TCTP hinders guanine nucleotide exchange activity of eEF1B (Cans et al., 2003). TCTP interacts with a C-terminal central acidic region (CAR) domain of eEF1Bβ (confusingly named eEF1δ in Wu et al., 2015). α-helical loop (helices H2 and H3) and one side of β-barrel like core domain mediate the interaction of TCTP with eEF1Bβ (Wu et al., 2015). Residues critical for eEF1B binding are conserved in TCTPs throughout eukaryotes. All three catalytic subunits eEF1Bα, β and δ contain a CAR domain

with conserved amino acid residues important for TCTP binding. Fission yeast *Sp*TCTP interacts with *Sp*eEF1Bα and a highly divergent *Nannochloropsis oceanica No*TCTP interacts with *Noe*EF1Bα, which points to a highly conserved role of TCTP in regulation of translation elongation.

Cell cycle regulation

Indications of TCTP involvement in regulation of the cell cycle come from the studies of *TCTP1* in *Arabidopsis thaliana* (Brioudes et al., 2010). Leaf blade area in seedlings with silenced *AtTCTP1* expression is significantly reduced in comparison to wild type plants. As there are no differences in cell size, the reduction of leaf area is caused by a decrease in cell division rate. Knockdown of *TCTP* in BY2 tobacco cells further supports TCTP role in cell cycle regulation. RNAi-*NtTCTP* BY2 cells are significantly delayed in cell cycle progression in comparison to WT. In addition, this delay is reflected in the expression of cell cycle marker genes.

Molecular mechanism of TCTP function in cell cycle regulation has been investigated. *At*TCTP1 physically interacts with a subunit of COP9 signalosome complex, *At*CSN4 (COP9 signalosome subunit 4), to regulate G1/S transition in cell cycle (Betsch et al., 2019). COP9 complex regulates the activity of CRL (CULLIN-RING) ubiquitin ligases by neddylation, which is a posttranslational modification. CRL are E3 ubiquitin ligases known to be involved in the regulation of cell cycle. The interaction of *At*TCTP with *At*CSN4 promotes CUL1 neddylation and the progression of cell cycle.

Remarkably, TCTP function in cell cycle regulation and its molecular mechanism are conserved between plants and animals. *Drosophila melanogaster DmTCTP* expression complements cell proliferation defects in *Arabidopsis tctp* loss of function mutant and vice versa (Brioudes et al., 2010). CUL1 neddylation status is disturbed in individuals with silenced *DmTCTP* in fruit fly.

Calcium binding properties

TCTP was first discovered to bind calcium in a screen for novel calcium-binding proteins in *Trypanosoma brucei* (Haghighat and Ruben, 1992). Calcium-binding property has been confirmed for example in human (Sanchez et al., 1997, Cantrell et al., 2022), rat (Kim et al., 2000), thale cress (Hoepflinger et al., 2013) or rubber tree homologs (Li et al., 2013). However, there are contradicting results in literature for mode of calcium binding and its binding site(s) on TCTP. While some studies suggest the presence of high-affinity calcium binding sites (Sanchez et al., 1997), others report binding sites with a low affinity (Feng et al., 2007). Experimental data support the idea that there are multiple calcium binding sites on TCTP (Graidist et al., 2007). It is possible that these sites vary in their affinity towards calcium (Graidist et al., 2007). Indeed, different TCTP regions have been shown to bind calcium. First attempt to map a calcium binding region on fragments of rat TCTP identified amino acid residues 81-112 (Kim et al., 2000). This result could not be replicated in a further study (Graidist et al., 2007). Instead, E55 and E58 residues were shown to be crucial for calcium binding. These residues lie

in the flexible loop region. NMR structural study mapped a weak low-affinity calcium binding site to N131, Q132 and D150 residues (Feng et al., 2007). A recent MDbased study detected seven potential calcium binding sites (Malard et al., 2018).

There are indications in literature that calcium binding is important for TCTP function(s). For example, TCTP prevents Ca^{2+}-dependent apoptosis in U2OS human cell lines (Graidist et al., 2007). Another study suggests TCTP is involved in placental calcium transport (Arcuri et al., 2005).

Programmed cell death regulation

TCTP negatively regulates cell death in mammalian cell lines (Li et al., 2001). Similar results have been obtained for yeast (Bischof et al., 2017) and plant TCTP homologs (Hoepflinger et al., 2013). Human TCTP interacts with proteins involved in multiple apoptotic pathways: MDM2, MCL1 (induced myeloid leukemia cell differentiation protein Mcl-1), BCL-XL and IRE-1α.

MDM2 (also known as HDM2) is an E3 ubiquitin ligase that integrates stress signals and regulates P53 stability. P53 is a well-known tumor suppressor that influences countless pathways and functions in the cell, including apoptosis (summarized in Levine, 2020). TCTP directly interacts with MDM2 and increases MDM2-mediated ubiquitination of P53 (Amson et al., 2012). α-helical loop mediates the interaction of TCTP with MDM2 (Funston et al., 2012). It is noteworthy that P53 acts as a transcriptional repressor of TCTP, suggesting the existence of a regulatory feedback loop between P53 and TCTP (Amson et al., 2012). As no P53 homologs have been identified in plants, conservation of this TCTP function is unlikely.

MCL-1 and BCL-XL are members of the B cell lymphoma 2 (BCL-2) family. Proteins belonging to this family can have either pro-apoptotic or anti-apoptotic activity (Warren et al., 2019). Their interplay regulates the intrinsic apoptotic pathway, which involves cytochrome c release from the mitochondria and activation of downstream caspase pathway (summarized in Kiraz et al., 2016). Anti-apoptotic function of TCTP was indeed shown to occur at the mitochondria (Susini et al., 2008). α-helical loop (helices H2 and H3) are structurally similar to H5 and H6 helices of BCL-2 family proteins (Susini et al., 2008). Mutation in H2 and H3 helices of TCTP disturbs its anti-apoptotic function.

MCL-1 was found to delay induced apoptosis in hamster ovary cells and is considered an anti-apoptotic protein (Reynolds et al., 1994). Interaction of TCTP with MCL-1 stabilizes MCL-1 and prevents its ubiquitin-dependent proteasome degradation (Liu et al., 2005).

N-terminal region of TCTP interacts with anti-apoptotic BCL-XL protein (Yang et al., 2005). Interestingly, multiple sequence alignment uncovered a putative BH3 domain in this region (Thébault et al., 2016). Upon binding to a hydrophobic BH3 groove of BCL-XL protein, amino acid residues D16-L27 refold into

a three turn α-helix. Binding of TCTP to BCL-XL enhances its anti-apoptotic function in hindering BAX-mediated mitochondrial membrane permeabilization. This might explain results of a previous study that revealed TCTP-induced inhibition of BAX-induced apoptotic activity without their direct interaction (Susini et al., 2008).

BCL2 homologs have not been identified in plants. However, overexpression of mammalian BAX can induce programmed cell death in plant tissue (Kawai-Yamada et al., 2001). The core mechanism of programmed cell death may thus be conserved in plants and animals. *At*TCTP1 reduces cell death in *Nicotiana benthamiana* leaves co-transformed with murine BAX, which could suggest conserved function of TCTP in this process (Hoepflinger et al., 2013). Interestingly, a TCTP homolog from a parasitic nematode *Meloidogyne enterolobii* reduces cell death in BAX-transformed *Nicotiana benthamiana* leaves (Zhuo et al., 2017). Authors of the study speculate that *Me*TCTP suppresses plant immune response to promote infection.

In stress conditions, unfolded proteins accumulate in the endoplasmic reticulum (ER). Master regulator GRP78 (also known as binding protein BiP) dissociates from transmembrane proteins IRE1, PERK and ATF6, which leads to their activation and triggers unfolded protein response (UPR) (summarized in Hetz and Papa, 2018). UPR signaling pathway converges on the described intrinsic apoptotic pathway. Human TCTP directly binds to ubiquitously expressed IRE1α and inhibits its function in UPR (Pinkaew et al., 2017). TCTP thus protects cells from ER-mediated apoptotic pathway. Remarkably, IRE1 is the only UPR branch conserved in plant, yeast and animal lineages (Hollien, 2013). This suggests a possible conserved function of TCTP. *At*TCTP1 overexpressed in *Nicotiana benthamiana* leaves indeed protects cells from UPR-induced cell death (Hoepflinger et al., 2013).

Interaction with the cytoskeleton

Analyzing its subcellular localization, TCTP was found in molecular complexes with tubulin in extracts from human HeLa cells (Gachet et al., 1999). Association of TCTP with microtubular cytoskeleton in monkey COS-7 cells depends on the phase of cell cycle.

TCTP immunostaining colocalizes with microtubules in the interphase (Gachet et al., 1999). A study on *Xenopus laevis* XL2 cell line confirmed only partial colocalization of TCTP with microtubule cytoskeleton (Bazile et al., 2009). Apart from colocalizing strands, TCTP forms fiber-like structures that do not colocalize with β-tubulin. However, TCTP network is dependent on the integrity of microtubule cytoskeleton. Application of colchicine leads to changes in the TCTP network.

α-helical loop region of TCTP (amino acid residues 79-123) shows sequence similarities to a microtubule associated protein MAP-1B (Gachet et al., 1999). This stretch of amino acids is believed to be necessary and sufficient for TCTP binding to tubulin isolated from a cell extract. However, there are

contradicting results in literature. According to Bazile et al. (2009), neither recombinant nor native *Xl*TCTP have any detectable affinity for taxol-stabilized microtubules in vitro. The interaction of TCTP with microtubules might be indirect (Jaglarz et al., 2012).

In the mitotic phase, TCTP colocalizes with the mitotic spindle up to the anaphase (Gachet et al., 1999). Its association with centrosomes has been confirmed in different animal species (Jaglarz et al., 2012). From anaphase onward, TCTP localization displays a diffuse pattern (Gachet et al., 1999). A serine/threonine Polo-like kinase (PLK) is involved in metaphase-to-anaphase change of TCTP localization (Yarm, 2002). PLK phosphorylates TCTP on S46 and S64 residues. Mutation of these phosphorylation sites results in mitotic defects. This suggests the importance of TCTP phosphorylation by PLK in mitotic cell division. In addition, PLK phosphorylation plays a role in meiotic division of murine oocytes (Jeon et al., 2016). Phosphorylated TCTP promotes spindle depolymerization.

Recombinant *At*TCTP interacts with microtubules in vitro (Yong-Min et al., 2012). This interaction is increased by the presence of calcium. TCTP plays a role in microtubule depolymerization in ABA (abscisic acid)-dependent stomatal closure. ABA-induced microtubule depolymerization is accelerated in plants overexpressing TCTP in comparison to control. To my knowledge, TCTP subcellular localization during cell cycle has not been investigated in plant cells before. PLK phosphorylation sites are not conserved in plant TCTPs and PLK homologs are not present in land plants. Their function was probably acquired by different proteins, possibly AURORA kinase paralogs (Okamura et al., 2017).

Much less is known about the interaction of TCTP with actin cytoskeleton. TCTP colocalizes with actin in XL2 cells (Bazile et al., 2009). There is a region in TCTP with primary sequence homology to cofilin (Tsarova et al., 2010). This region contains a β sheet after the flexible loop and a part of helix 2. A peptide with this sequence binds to G-actin and competes for actin binding with cofilin. A possible interaction of TCTP with actin cytoskeleton would deserve more attention.

Regulation of TOR pathway

TARGET OF RAPAMYCIN (TOR) kinase is an evolutionary conserved protein involved in regulation of cell growth, proliferation, and metabolism. In animals, it forms two complexes (mTORC1 and mTORC2) activating distinct pathways (summarized in Liu and Sabatini, 2020). TCTP is reported to be involved in regulation of both pathways.

mTORC1 complex activates a downstream pathway which leads to increased translation, synthesis of lipids and nucleotides. RHEB (Ras homolog enriched in brain) directly binds to TOR kinase and activates mTORC1 pathway (Long et al., 2005). As a small GTPase, RHEB exists in an active GTP-bound state and an inactive GDP-bound state. The tuberous sclerosis complex (TSC) consisting of TSC1, TSC2 and TBC197 subunits has a GTPase activating activity towards RHEB and negatively regulates mTORC1

pathway (Inoki et al., 2003; Dibble et al., 2012). *Dm*TCTP was shown to interact with RHEB and act as its guanine nucleotide exchange factor (GEF) (Hsu et al., 2007). GEF activity towards RHEB was confirmed for *Hs*TCTP (Dong et al., 2009). The residues E12, K90 and E138 in TCTP are believed to be critical for RHEB binding. However, these results could not be replicated in other studies (e. g. Wang et al., 2008). Contrasting results could be possibly explained by usage of different model systems or very weak interaction between TCTP and RHEB (Dong et al., 2009). Multiple studies suggest that mTORC1 pathway regulates TCTP stability (Bommer et al., 2017; Jeong et al., 2021), which points to a feedback loop regulation between mTORC1 and TCTP.

mTORC2 complex influences cytoskeletal organization and activates AKT (protein kinase B) signaling pathway. Through its downstream targets, AKT signaling promotes cell proliferation, growth, and metabolic changes. Little is known about TCTP involvement in mTORC2 pathway. TCTP interacts with mTORC2 complex and hypothetically inhibits its degradation (Lin et al., 2020).

TOR signaling pathway is evolutionarily well-conserved (Tatebe and Shiozaki, 2017). Components of TORC1 complex are conserved throughout eukaryotes including plants. In contrast, TORC2 complex is not present in plants. There is no RHEB homolog in plants. However, there are indications TCTP could be involved in TOR signaling in plants (Meng et al., 2018), likely using a different molecular mechanism than in animals. Interestingly, residues critical for RHEB binding are conserved in *At*TCTP1. Possibly, these residues are important for interaction with other small GTPases.

Extracellular function

Apart from its multiple functions inside the cell, there is evidence of extracellular TCTP function(s) in literature. TCTP is present in the serum of allergic patients and induces histamine and interleukin IL-4 release from the basophils (MacDonald et al., 1995; Schroeder et al., 1996). It impacts other cells of the immune system as well. For example, recombinant *Hs*TCTP stimulates B cell proliferation and activity (Kang et al., 2001). TCTP role in immune response is summarized in Kawakami et al. (2019). Dimerization is critical for TCTP extracellular function in immune response (Kim et al., 2009).

As a secreted protein, one would expect a signal peptide in TCTP sequence. Absence of such a signal could indicate that TCTP is secreted by a non-classical pathway. Indeed, TCTP was identified in exosomes, which are a possible pathway of non-classical secretion (Amzallag et al., 2004). TCTP directly interacts with Tumor suppressor-activated pathway-6 (TSAP6) protein, which facilitates its secretion (Amzallag et al., 2004). TSAP6 protein is critical for exosome secretion and this process (Lespagnol et al., 2008).

After secretion, there must be a way how TCTP signal is transmitted into a responding cell. One possibility is a presence of a TCTP interactor (a receptor) on cell surface. Indeed, TCTP directly binds

immunoglobulin E (IgE) molecules on the surface of mast cells in FcεRI receptor, which activates allergic response in mast cells (Kashiwakura et al., 2012). Another option could be TCTP endocytosis. Remarkably, M1-H10 amino acid residues on the N-terminus form a protein transduction domain (PTD) (Kim et al., 2011). These domains share a cell-penetrating ability. TCTP enters the cell mainly via lipid raft mediated endocytosis (Kim et al., 2011). Properties of PTDs can be useful in drug delivery. For instance, TCTP PTD was recently shown to be functional in intranasal delivery of insulin in mice (Bae et al., 2019).

Extracellular function has been proposed for TCTP homologs outside mammals. *Plasmodium falciparum* TCTP secreted into the serum is thought to interfere with host´s immune response (Calderón-Pérez et al., 2014). TCTP was detected in the tobacco pollen tube secretome (Hafidh et al., 2016b). Interestingly, *Nt*TCTP colocalizes with ER, Golgi vesicle and exosome markers (Hafidh et al., 2016b). This indicates TCTP secretion is independent of a signal peptide, possibly via a non-classical pathway. It is possible other proteins (such as TSAP6) are involved in TCTP secretion in plants but have not been identified so far.

Summary

TCTP is a highly conserved essential eukaryotic protein with functions in regulation of various cellular and organismal processes. Overall TCTP fold is highly conserved, which could indicate functional conservation as well. Indeed, some TCTP functions are conserved throughout eukaryotes (such as regulation of translation elongation or calcium binding). On the other hand, some functions (such as its role in human immune response) point to a specialization of TCTP in different organisms. Its multifunctionality could be associated with a remarkably high number of interacting proteins. Some regions of TCTP (α-helical loop and disordered loop) are known to mediate interaction with multiple proteins. Post-translational modifications and calcium binding can impact TCTP structure and binding properties. Studying its interactome in different model organisms and systems provides valuable insight into TCTP functions and their possible conservation.

TCTP in plants

In contrast to animals, there are only few studies of TCTP homologs in plant species except for *Arabidopsis thaliana*. Before turning to *At*TCTP1, knowledge about TCTPs in other plant species is summarized shortly.

Plant genomes carry multiple *TCTP* paralogs (Koo et al., 2020). Studies of more than a single paralog in an organism point to a possible specialization of TCTPs. For instance, rubber tree paralogs *HbTCTP* and *HbTCTP1* exhibit a different tissue-specific expression pattern (Li et al., 2013; Deng et al., 2016). In addition, plant TCTPs might have acquired specialized functions during evolution. For example, RPF41

is a TCTP homolog in *Robinia pseudacacia* with a role in nodulation (Chou et al., 2016). *Arabidopsis thaliana* genome harbors two *TCTP* paralogs – *AtTCTP1* and *AtTCTP2*. *AtTCTP1* is highly expressed in both vegetative and reproductive tissues (Berkowitz et al., 2008). *At*TCTP2 was assumed to be a pseudogene (Berkowitz et al., 2008) but was confirmed to have a function in plant development (Toscano-Morales et al., 2015). *AtTCTP1* and *AtTCTP2* have a different tissue-specific expression pattern and are thought to be non-redundant (Toscano-Morales et al., 2015).

TCTP studies in plants usually analyze its expression in various tissues and response to biotic and abiotic stress. TCTP displays a ubiquitous expression in all plant tissues (Hinojosa-Moya et al., 2013; Li et al., 2013; Deng et al., 2016; Meng et al., 2017). *TCTP* expression is regulated by different abiotic stresses, e. g. flooding stress (Chen et al., 2014), salt stress (Deng et al., 2016; Meng et al., 2017), low temperature (Deng et al., 2016) and high temperature stress (Meng et al., 2017). This suggests that *TCTP* is involved in plant response to different stresses. Overexpression of tomato *SlTCTP* in tobacco improves its performance under salt stress (de Carvalho et al., 2017). In addition, *TCTP* expression responds to biotic stress, for example in tomato infection by a potyvirus Pepper yellow mosaic virus (PepYMV) (Bruckner et al., 2017) or in cucumber infection by a fungus *Sphaerotheca fuliginea* (Meng et al., 2018).

A connection between plant hormones and *TCTP* has been documented in literature as well. Rice *TCTP* homolog is upregulated by gibberellin treatment in the basal region of leaf sheath (Takasaki et al., 2008). TCTP is induced by ethylene treatment in tobacco (Tao et al., 2015). *Nt*TCTP directly interacts with an ethylene receptor *Nt*HK1 (HISTIDINE KINASE 1) and is necessary for its function in growth regulation and ethylene response (Tao et al., 2015). Cucumber *Cs*TCTP1 expression is upregulated by ABA treatment (Meng et al., 2017) and in turn, expression of ABA signaling pathway proteins is altered in *Cs*TCTP1 overexpressing and silenced lines (Meng et al., 2018).

TCTP1 in Arabidopsis thaliana

Arabidopsis thaliana TCTP1 gene is annotated as At3g16640 in TAIR database. Its sequence contains 4 exons and 3 introns. *TCTP1* encodes a 168 amino acid residue long protein. *At*TCTP1 has 38% identity and 56% similarity to *Hs*TCTP.

TCTP1 in *Arabidopsis thaliana* is a ubiquitously expressed gene. First characterization study analyzed its expression pattern by real time-quantitative PCR (Berkowitz et al., 2008). *TCTP1* was found to be highly expressed in all analyzed tissues except for mature seeds. Available RNA-Seq data support high expression of *TCTP1*. Relative to its median expression value, *TCTP*1 expression is particularly upregulated in mature pollen and maturing seeds (Figure 3A).

A valuable tool to study gene function is mutant analysis. Two knockout T-DNA insertion lines (named *tctp-1* and *tctp-2*) have been examined so far (Berkowitz et al., 2008; Brioudes et al., 2010; Hafidh et al., 2016b). *tctp-1* line (annotated as SAIL_28_C03) has a T-DNA insertion in the fourth exon of TCTP. *tctp-2* (annotated as GABI_901E08) has an insertion in the first exon (Figure 3B). In studies stated above, individuals homozygous for the insertion could not be generated. Berkowitz et al. (2008) observed greatly reduced transmission through the male gametophyte (6.8%) and an impaired growth of mutant pollen tubes in a pistil. In contrast, Brioudes et al. (2010) could not reproduce previously published results and attributed observed phenotype to embryo arrest and lethality of *tctp* homozygous individuals. Apart from green seeds, white seeds containing developmentally delayed embryos were observed in a silique of *tctp-1 +/-* plant (Figure 3C,D). Remarkably, embryos from such seeds could be rescued on a medium containing nutrient supplements. After the rescue, these plants exhibit retarded growth, smaller size, and male sterility. Study in our laboratory confirmed lower transmission through the male gametophyte than expected (8.9%) (Hafidh et al., 2016b). At the same time, white seeds were observed in siliques of *tctp-1 +/-* selfed plants (10.9% frequency) along with ovules that were not fertilized (12.3%). Observed phenotype was attributed to an aberrant targeting of mutant pollen tubes. Mutant characterization thus suggests that *At*TCTP1 has a role in both male gametophyte and sporophyte development.

In line with T-DNA mutant characterization results, plants with RNAi-silenced *AtTCTP1* expression grow slower and are developmentally delayed (Brioudes et al., 2010). The primary root grows shorter and lower number of lateral roots are formed in *AtTCTP1* knockdown lines (Berkowitz et al., 2008). Recently, *AtTCTP1* function in lateral root primordia initiation was confirmed (Branco and Masle, 2019). *AtTCTP1* mRNA produced in the shoot is translocated in phloem to the root and promotes lateral root formation.

AtTCTP1 function in sporophyte is well documented. Published studies are conflicting in their interpretation of *AtTCTP1* in male gametophyte. However, there are indications it could be equally important. *AtTCTP1* expression is highly upregulated in mature pollen. TCTP1 protein was detected in first published pollen proteome of *A. thaliana* (Holmes-Davis et al., 2005). In addition, *AtTCTP1* homolog *NtTCTP* was identified in the secretome of tobacco pollen tube (Hafidh et al., 2016b). Direct interaction of *Nt*TCTP with *Nt*GNL1, a well-known vesicle trafficking regulator in pollen tube was reported recently (Zou et al., 2021).

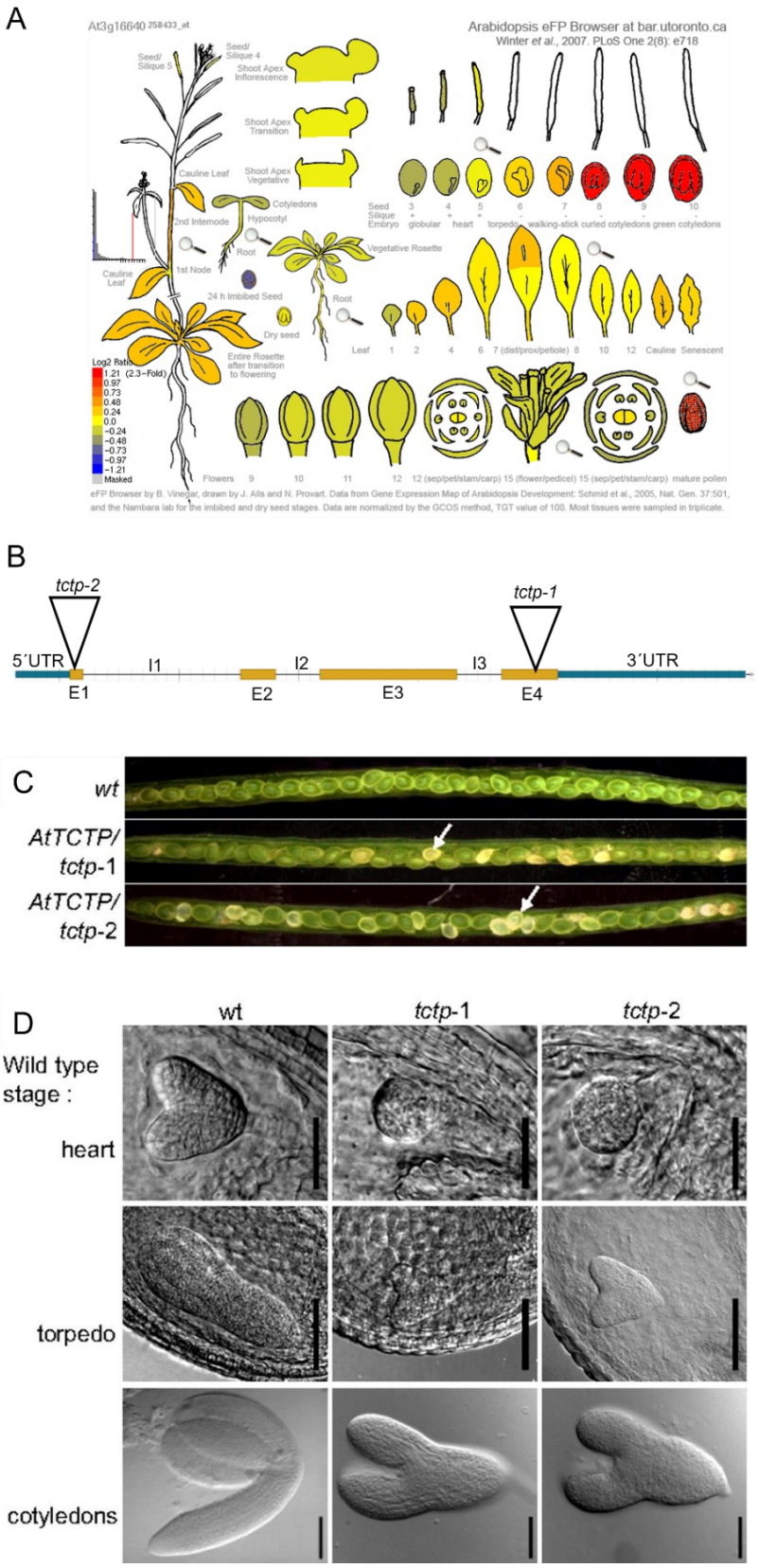

Figure 3. ***Arabidopsis thaliana TCTP1***. *(A) Relative TCTP1 expression in different developmental stages, based on RNA-seq transcriptomic data (Arabidopsis eFP browser at www.bar.utoronto.ca). Previous characterization of tctp-1 and tctp-2 (B) T-DNA insertion lines revealed defective embryo development in tctp-/- seeds (C, D). Seeds with tctp -/- delayed embryos appeared white (white arrow). Adapted from (Brioudes et al., 2010) Scale bars = 50 µm (heart stage) and 100 µm (torpedo and cotyledons stages)*

BRL2 and TTL3 as possible TCTP1 interactors

BRL2 (BRI-1 LIKE 2) and TTL3 (TETRATRICOPETIDE-REPEAT THIOREDOXIN-LIKE 3) proteins were identified as TCTP1 potential interactors in pollinated carpels prior to this diploma project (unpublished data). In this section, expression profiles and functions of BRL2 and TTL3 are introduced shortly.

BRI-1 LIKE 2 (BRL2) is annotated as At2g01950 in TAIR database and encodes a 124 kDa BRL2 protein. *BRL2* belongs to plant LRR (leucine rich repeat) kinase family (Clay and Nelson, 2002). Like other receptor kinases, it contains a signal peptide, an extracellular LRR domain, a transmembrane segment, and an intracellular kinase domain. *BRL2* has 41% sequence identity to brassinosteroid receptor BRI1 (BRASSINOSTEROID INSENSITIVE 1) and belongs to *BRI1* family along with *BRL1* and *BRL3* (Caño-Delgado et al., 2004). Whereas *BRL1* and *BRL3* complement *bri1* mutation under the control of *BRI1* promoter, *BRL2* cannot complement *bri1* mutant. Interestingly, *BRL2* expression is not affected by brassinolide treatment (Clay and Nelson, 2002). BRL2 does not bind brassinolide *in vitro* (Caño-Delgado et al., 2004). It is speculated that it binds a steroid or a protein ligand that remains to be identified. Characterization of a transposon insertion line *vh1* points to BRL2 function in vascular tissue development (Clay and Nelson, 2002). TCTP1 was detected as a potential interactor in a phage display screen (Ceserani et al., 2009). Its function in reproductive development has not been investigated.

TETRATRICOPEPTIDE THIOREDOXIN-LIKE3 (TTL3) is annotated as At2g42580 in TAIR database and belongs to a gene family composed of four members (*TTL1-4)* (Lakhssassi et al., 2012). While *TTL1, TTL3* and *TTL4* are ubiquitously expressed in most tissues, *TTL2* is expressed exclusively in pollen and is crucial for male sporogenesis (Lakhssassi et al., 2012). Mutant characterization points to a partial redundancy between *TTL1, TTL3* and *TTL4* genes in response to osmotic stress (Lakhssassi et al., 2012). TTL proteins contain six tetratricopeptide repeat domains and a thioredoxin-like domain on their C-terminus (Rosado et al., 2006). Presence of a predicted intrinsically disordered region on N-terminus of TTL3 protein suggests its potential involvement in protein-protein interactions (Amorim-Silva et al., 2019). TTL3 interacts with components of brassinosteroid signaling pathway and potentially scaffolds them at the plasma membrane (Amorim-Silva et al., 2019).

Even though BRL2 does not bind brassinolide, its interaction with TTL3 has been experimentally confirmed and suggests a cooperation of these two proteins (Ceserani et al., 2009). *TTL3* and *BRL2* expression is very low in mature pollen but both are expressed in the pistil (Figure 4).

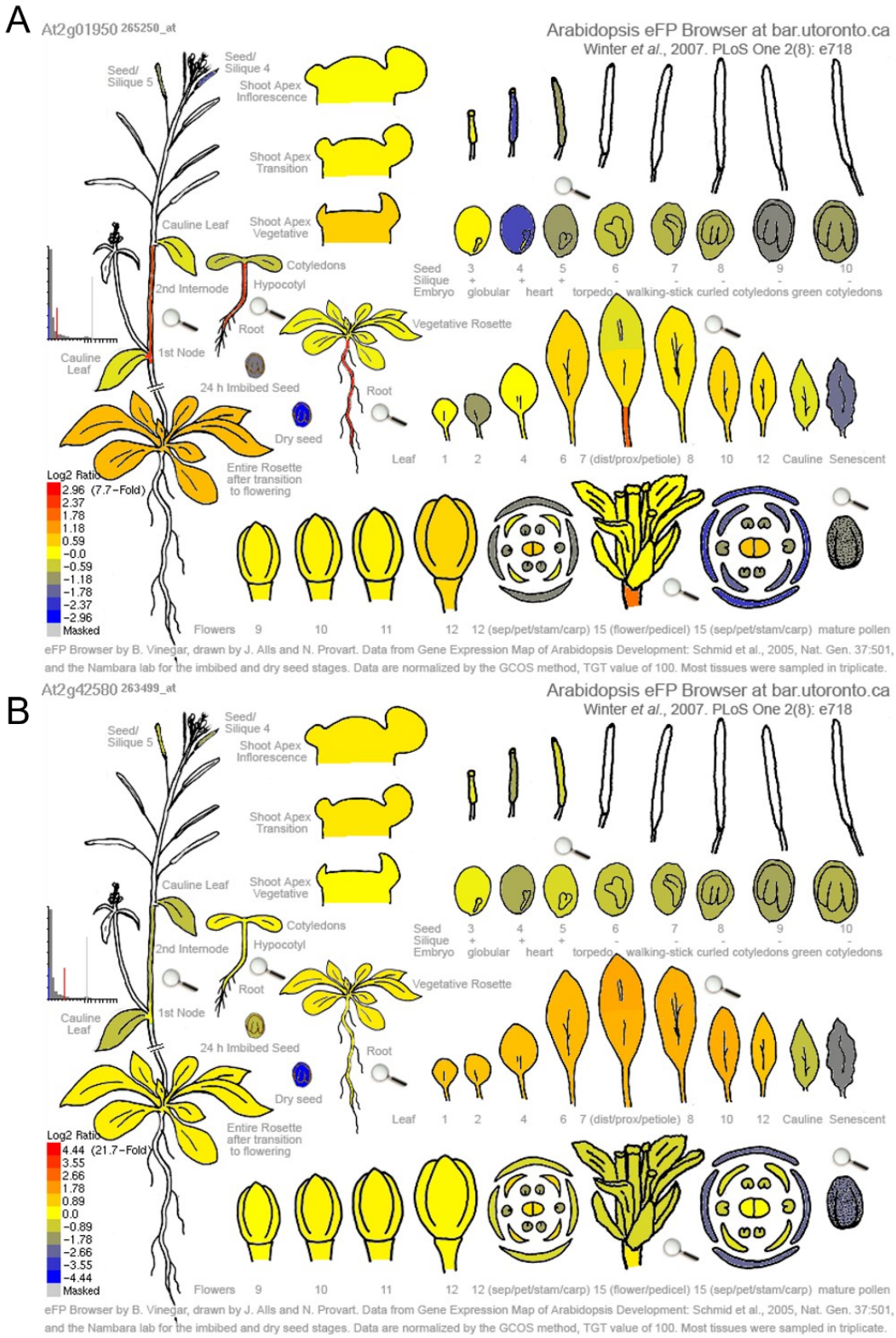

Figure 4. BRL2 (A) and TTL3 (B) expression in A. thaliana developmental stages. *Based on RNA-seq transcriptomic data (Arabidopsis eFP browser www.bar.toronto.ca).*

Material and methods

Plant material and cultivation

Plant material

Arabidopsis thaliana was a model plant organism in this thesis. Most experiments were carried out on Columbia-0 (Col-0) accession. For some crosses, male-sterile *ms1-1* plants of Landsberg erecta (Ler) accession were used as there was no need to emasculate flowers prior to crossing. For mutant characterization, SAIL_28_C03 T-DNA insertion line in Col-0 background was ordered from ABRC (Arabidopsis Biological Resource Centre).

Cultivation conditions and cultivation media

Arabidopsis thaliana plants were cultivated from seeds. Sterilized seeds germinated on a ½ MS (Murashige/Skoog) medium (0.11% MS salts (Sigma), 0.5% sucrose (Sigma), 0.4% agar (Sigma), 1 mM MES (Duchefa), 0.3 mM myo-Inositol (Sigma), pH 5.7) in *in vitro* conditions (22°C, 60% relative humidity, 16 h light – 8 h dark). Plates with MS medium were prepared one day before seed sowing. The medium was melted in a microwave, let to cool down for 45 min. Vitamins (1 mg/L pyridoxin hydrochloride (Sigma), 0.25 mg/L nicotinic acid (Sigma), 0.05 mg/L thiamine hydrochloride (Sigma)) were added to the medium along with antibiotic or herbicide selection (50 µg/ml kanamycin or 50 µg/ml Basta) before pouring into 9 cm diameter Petri plates or 12 cm square plates. After the medium solidified, it was kept in 4°C until use.

7 to 14 days after germination, seedlings were carefully transferred on Jiffy peats or in transformation pots with tweezers. They were grown in a growth room or cultivation chamber at 22°C and 60% relative humidity under long day condition (16 h light, 8 h dark). Plants were watered regularly (2-3 times per week) with water from the tap.

Seed sterilization and sowing

Seeds were frozen in -20°C 2-3 days prior to plating to destroy any insects. Seeds sterilization was carried out in a 1.5 mL or 2 mL Eppendorf tube in a flowbox. First, 1 mL 70% ethanol (Lach-Ner) was added to the tube and the suspension was incubated for 1 min on a shaker. Ethanol (Lach-Ner) was exchanged for 20% bleach (SAVO) and the seeds were incubated for 10 min on a shaker. Finally, seeds were washed 5 times with dH_2O (distilled water) for 1 min on a shaker. Seeds were transferred on MS media either with a cut yellow pipette tip or they were let to dry on a filter paper and spread out over the plate. Plates were sealed with Micropore tape (CM Company) and kept in *in vitro* growth room.

Plant crossing

For crosses, either male sterile *ms1-1* plants (Ler) or Col-0 accession plants without male sterility were used. In the latter case, it was necessary to emasculate unopened flowers as *Arabidopsis thaliana* is capable of self-pollination. Emasculation was carried out under a stereomicroscope. Flower was carefully opened with tweezers. Special attention was given to not damaging any part of the pistil. All six anthers were removed with the tweezers. 2 days later, the stigma became receptive and stigmatic papillae were visible under stereomicroscope. Flowers in this receptive condition were pollinated. Open flower with mature released pollen was collected with tweezers from the genotype to be crossed. Multiple open flowers from the same plant were used for pollination until the stigma was covered with pollen grains.

In vitro pollen tube cultivation

Arabidopsis thaliana pollen tubes were cultivated on a solid pollen germination medium according to Boavida and McCormick (2007). The medium (10% sucrose (Sigma), 0.01% boric acid (Duchefa), 5 mM $CaCl_2$ (Sigma), 1 mM $MgSO_4$ (Sigma), 5 mM KCl (Sigma), 1.5% low melting agarose (Cleaver Scientific)) was freshly prepared before each pollen tube cultivation. Prior to addition of low-melting agarose, pH of the medium was adjusted with 0.1 M KOH (Sigma) to 7.5. The medium was incubated in a container filled with hot water until low-melting agarose dissolved completely. Warm germination medium was pipetted on a microscope slide in a square-like shape. The medium was left to cool down for 30 min. Surface of the medium was gently touched with freshly collected open flowers to release pollen grains. Microscope slides with pollen were incubated in a closed box filled with wet tissues to maintain high humidity at 22^{o}C in the dark for 4 h.

Mutant characterization

Silique dissection

Arabidopsis thaliana siliques were dissected to observe seed phenotype. Double-sided tape was placed on a microscope slide. A silique was collected and transferred on the tape. Using a stereomicroscope, two valves were carefully separated from replum with an insulin needle and attached to the tape. Seeds remained attached to the placenta and their phenotype could be observed or imaged.

Aniline blue staining of *Arabidopsis thaliana* pollen tube

Aniline blue staining of *Arabidopsis* pollen tubes was performed according to Mori et al. (2006). Flowers were collected 24 HAP (hours after pollination) or 48 HAP. They were placed on a double-sided tape on a microscope glass. All flower organs except for pistils were removed using insulin needle. Pistils were carefully transferred into 100 µL Fixative solution (99.8% acetic acid (Lach-Ner)/96% ethanol (Lach-Ner) in 1:3 ratio) in a 24-well cell culture plate. After 2-hour incubation at room

temperature, the fixative was exchanged for 100 µL 70% ethanol. After 10 min incubation at room temperature, the solution was exchanged for 50% ethanol. The same treatment was repeated for 30% ethanol and dH_2O. dH_2O was exchanged for 100 µL Alkaline treatment solution (ATS) (8 M NaOH (Sigma)) and the pistils were incubated overnight at room temperature. Next day, ATS was carefully replaced with 100 µL dH_2O. Pistils were incubated at room temperature for 10 min. Finally, dH_2O was exchanged to Decolorized aniline blue solution (DABS: 0.1% aniline blue (Sigma) solution in 108 mM K_3PO_4 (Sigma) filtered through active carbon powder). Pistils were incubated in DABS for 2 h in dark at room temperature. They were stored in 4°C until microscopy. Samples were observed on a fluorescent microscope under UV light.

Blue dot assay

Flowers were collected 24 HAP. They were placed on a double-sided tape on a microscope glass. Under the stereomicroscope, remaining sepals, petals and anthers were removed. Placenta with the seeds was separated from ovary wall and carefully transferred into 100 µL Fixative solution (80% acetone (Lach-Ner)) in a 24-well cell culture plate. After 30 min incubation in room temperature, fixative solution was exchanged for β-glucuronidase (GUS) staining solution (0.1 M $NaPO_4$ pH 7.0 (Sigma), 10 mM EDTA (Duchefa), 0.1% Triton X-100 (Fluka), 1 mM 5-bromo-4-chloro-3-indolyl-beta-D-glucuronic acid, cyclohexylammonium salt (X-Gluc, Thermo Fisher Scientific), 1 mM ferrocyanide (Sigma)). The samples were incubated overnight at 37°C. For microscopy, they were mounted on slide in 20% glycerol solution and gently covered with a cover slip.

Nucleic acid and protein extraction from plant tissues

DNA extraction

DNA was extracted from the leaf tissue using CTAB DNA extraction method. A leaf fragment was harvested with tweezers into a 1.5 mL Eppendorf safe lock tube containing sterile sand and immediately frozen in liquid nitrogen. The tissue was grinded for 40 s at 4000 rpm (rotations per minute) in MagnaLyser (Roche). 150 µL CTAB extraction buffer (1.4 M NaCl (Sigma), 20 mM EDTA (Duchefa), 100 mM Tris/HCl pH 8.0 (MP Biomedicals), 3% hexadecyltrimethylammonium bromide (CTAB, Sigma)) was added to grinded leaf tissue and the mixture was vortexed and incubated at room temperature for 20 min. 150 µL 99% chloroform (Lach-Ner)/ 98% isoamylalcohol (IAA, Sigma) mixture in 24:1 ratio was added. After a brief vortex, the mixture was centrifuged at 13,000 rpm at room temperature for 10 min. Two layers formed in the tube – an upper aqueous layer and a lower green layer containing tissue debris. Upper layer was transferred with a pipette into a fresh 1.5 mL Eppendorf tube containing 120 µL isopropanol (Sigma). The mixture was vortexed, incubated at room temperature for 5 min and centrifuged at 13,000 rpm at room temperature for 10 min. Supernatant

was discarded and the pellet was washed with 500 µL 70% ethanol. After a final round of centrifugation (13,000 rpm, 10 min, room temperature), supernatant was carefully removed by vacuum driven pipette. The pellet was left to dry completely at room temperature for 2-3 h. The pellet was dissolved in 30 µL dH_2O and was used as a template in genotyping PCR.

RNA extraction and cDNA generation

RNeasy Plant Mini Kit (Qiagen) was used for RNA extraction. A maximum of 100 mg inflorescence was collected from a growing Col-0 plant, placed in a safe lock 1.5 mL Eppendorf tube and immediately frozen in liquid nitrogen. The sample was grinded with a pestle in a mortar filled with liquid nitrogen. Tissue powder was transferred to a pre-chilled 2 mL Eppendorf tube and homogenized for 40 s at 4000 rpm in MagnaLyser (Roche). 450 µL RLT buffer (in the kit) was added to the grinded tissue and vortexed. The lysate was transferred to a QIAshredder spin column placed in a 2 mL Eppendorf tube. The tube was centrifuged for 2 min at 14,500 rpm. The supernatant was carefully transferred to another 2 mL tube. 0.5 transfer volume of denatured ethanol was added to the tube, mixed with a pipette and whole volume was immediately transferred to the RNeasy spin column placed in 2 mL Eppendorf tube. The column was centrifuged at 14,500 rpm for 2 min. Flow-through was discarded and 700 µL RW1 buffer was added. The column was centrifuged at 14,500 rpm for 15 s and the flow-through was discarded. 500 µL RPE buffer was added to the column, and it was centrifuged at 14,500 rpm for 15 s. Flow-through was discarded and washing step was repeated with 500 µL RPE. The column was centrifuged at 14,500 rpm for 2 min. Finally, the column was placed into a new 1.5 mL Eppendorf tube, 30 µL RNase-free water was added and the column was centrifuged at 14,500 rpm for 1 min. RNA concentration was measured on NanoDrop (Thermo Fisher Scientific). DNA contaminations were removed with Ambion DNA-freeTM kit. A typical 50 µL reaction contained extracted RNA, 1 µL 2U rDNaseI enzyme, 5 µL 10x DNaseI reaction buffer and nuclease free water. The mixture was incubated at 37°C for 30 min. 5 µL DNase Inactivation Reagent was added for DNase enzyme inactivation. The mixture was incubated for 2 min at room temperature and centrifuged at 14,500 rpm for 1 min. Supernatant contained DNA-free RNA and was transferred to a 1.5 mL Eppendorf tube.

ImProm-IITM Reverse Transcription System (Promega) was employed to generate cDNA by reverse transcription. 1 µg purified RNA was mixed with cDNA primer (0.5 µg per reaction) in nuclease free water to final volume 5 µL. The mixture was incubated at 70°C for 5 min and immediately chilled on ice for 5 min. Reverse transcription reaction mixture contained 5x ImProm-IITM reaction buffer, 2 mM $MgCl_2$, 0.5 mM dNTP mix, 20U Recombinant RNasin Ribonuclease Inhibitor, ImProm-II™ Reverse Transcriptase and nuclease free water to final volume 15 µL. 5 µL RNA-cDNA primer mixture was added to the reaction. Reverse transcription reaction was performed in a thermocycler. The reaction

consisted of three steps – annealing for 5 min at 25°C, elongation for 60 min at 42°C and enzyme inactivation for 15 min at 70°C. Obtained cDNA was used for cloning purposes in this thesis.

Protein extraction

Proteins were extracted from mature pollen in this thesis. Plant tissue was collected in 2 mL Eppendorf tube and frozen in liquid nitrogen. Frozen tissue was grinded with a pestle in a mortar with Rapid Immunoprecipitation assay buffer (RIPA: 10 mM Tris/HCl pH 7.5 (MP Biomedicals), 150 mM NaCl (Sigma), 0.5 mM EDTA (Duchefa), 0.5% Nonidet P-40 (NP-40, Sigma), Pierce protease inhibitor (Thermo Fisher Scientific, 1 tablet per 50 ml buffer), 10 mM PMSF (Sigma)). Grinded tissue powder was transferred into a 1.5 mL Eppendorf tube and incubated on ice for 1 hr. The tube was centrifuged at 14,000 rpm at 4°C for 10 min. The supernatant containing extracted proteins was transferred into a 1.5 mL tube and frozen in -20°C until further use.

Molecular cloning

Bacterial strains and cultivation media

Three *Escherichia coli* (*E. coli*) strains were used in this work. For cloning purposes, TOP10a strain was employed to propagate and store cloned vectors. BL21-CodonPlus (DE3) RIL and BL21-CodonPlus (DE3) RIPL (Agilent) strains were utilized for recombinant protein expression. *E. coli* strains were successfully cultivated on Luria-Bertani (LB) high salt media (Duchefa) *in vitro*. TOP10a competent cells were prepared by colleagues Karel Raabe and Zahra Kahrizi.

Agrobacterium tumefaciens (*A. tumefaciens*) GV3101 strain was used for plant transformation. *Agrobacterium* cultures were cultivated in Yeast Extract Beef (YEB) medium pH 7.2 (0.6% yeast extract (MP Biomedicals), 0.5% peptone from casein tryptic digest (Sigma), 0.5% sucrose (Serva), 0.05% $MgSO_4$. $7H_2O$ (Merck)). GV3101 electrocompetent cells were prepared by Karel Raabe and Zahra Kahrizi.

Polymerase chain reaction (PCR)

Polymerase chain reaction is a common molecular biology method that was used to amplify a desired DNA sequence. Each PCR reaction contained a forward and a reverse primer (0.5 mM), a template, a mixture of deoxyribonucleotidephophates (dNTPs) (0.2 mM) and a DNA polymerase enzyme with appropriate buffer. If the PCR product was further used for cloning, a high-fidelity Phusion polymerase was used in combination with HF Buffer (Thermo Fisher Scientific). In other cases (e. g. colony PCR or genotyping PCR), Merciáza Taq polymerase (1.5 U) was used along with Merciáza buffer (Merci).

Polymerase chain reactions were run in a PCR cycler in cycles of three steps – denaturation, annealing and extension. In the denaturing step, the reaction was heated to separate template DNA strands. In

annealing step, temperature was reduced to around 50-60°C for the primers to bind to a complementary sequence in the template. Annealing temperature was determined for each primer combination using ThermoFisher Tm Calculator. In the extension step, DNA polymerase was adding dNTPs to 3´ end of the primer. The length of the extension step was determined from the length of the DNA sequence to be amplified. If Merciáza Taq polymerase was used, the length of the extension step was 1 min per 1 kb DNA. In case of Phusion polymerase, it was 1 min per 2 kb DNA. An example of a PCR reaction by Merciáza and Phusion polymerase is given in Tables 1 and 2.

Step		Temperature	Time (min:sec)
1		95°C	0:15
30x repeat	2	95°C	0:30
	3	50-60°C	0:30
	4	68°C	1 min/1kb
5		68°C	10:00
6		4°C	∞

Table 1. Merciáza polymerasePCR reaction cycle

Step		Temperature	Time (min:sec)
1		98°C	0:10
30x repeat	2	98°C	0:30
	3	50-60°C	0:30
	4	72°C	1 min/2kb
5		72°C	5:00
6		4°C	∞

Table 2. Phusion polymerase PCR reaction cycle

Agarose gel electrophoresis

To visualize DNA bands from PCR or restriction digest, samples were loaded and run on gel electrophoresis. The gel was prepared 30 min before sample loading in Thermo Scientific™ Owl™ EasyCast™ electrophoresis system (Thermo Fisher Scientific). 60 ml 1x Tris-acetate EDTA buffer (TAE) (40 mM Tris (MP Biomedicals), 20 mM acetic acid (Merck), 1 mM EDTA (Merck), pH 8.0) was measured and added to an Erlenmeyer flask. Desired amount of agarose (Lanza) (0.6 g for 1% agarose gel) was weighed and added to the Erlenmeyer flask. The mixture was heated in a microwave. When the agarose dissolved completely, it was left to cool down for 10 min. 1 drop of ethidium bromide (PanReac Applichem) was added. The mixture was poured into the gel chamber and the comb was placed on top to create wells in the gel. When the gel solidified, it was topped up with 1x TAE buffer. Samples containing OrangeG loading dye (45% sucrose with a tip of small spatula of the OrangeG powder (Sigma)) were loaded into separate wells. The gel was run at 90 V until the orange line migrated nearly to the bottom of the gel. The gel was imaged under UV light using ethidium bromide filter.

DNA isolation from an excised gel band

For cloning, it was necessary to cut out a DNA band with correct size from the gel. For further use of DNA contained in the gel slice, DNA was extracted using GeneJET Gel Extraction Kit (Thermo Fisher Scientific). Prior to cutting, a 1.5 mL Eppendorf tube was weighed using analytical scales. The gel band was cut with a scalpel cleaned with denatured ethanol and placed in the tube. The tube was weighed, and mass of the gel slice was calculated. Binding Buffer was added in the tube in 1:1 ratio, e. g. 100 µL Binding Buffer was added to 100 mg agarose gel. The tube was incubated at 60°C until agarose gel was dissolved completely. The mixture was briefly vortexed and transferred to a GeneJET Purification

Column. The column was centrifuged at 14,500 rpm for 1 min and the flow-through was discarded. DNA was washed with 750 µL Wash buffer and the column was centrifuged at 14,500 rpm for 1 min. The flow-through was discarded and the column was centrifuged for another minute at 14,500 rpm. After transferring to a 1.5 mL Eppendorf tube, 20 µL Elution buffer was added and the column was incubated at room temperature for 2 min. The tube was centrifuged at 14,500 rpm for 1 min. Concentration of eluted DNA was measured on NanoDrop (Thermo Fisher Scientific).

Plasmid isolation from *E. coli*

GeneJET Plasmid MiniPrep kit (Thermo Fisher Scientific) was used for plasmid isolation. Vectors were isolated from a 5 mL bacterial culture grown overnight in a shaker at 37°C and 180 rpm. Bacterial suspension was first centrifuged in a 2 mL Eppendorf tube at 8,000 rpm for 2 mins. Supernatant was discarded and bacteria were resuspended in 250 µL Resuspension Buffer containing RNAse A. Bacterial cells were lysed by adding 250 µL Lysis Buffer and chromosomal DNA was precipitated with 350 µL Neutralization Buffer. The tubes were gently flipped up-and-down after addition of each buffer. The mixture was centrifuged at 14,500 rpm for 5 min. Supernatant was carefully transferred into a GeneJET Purification Column and centrifuged at 14,500 rpm for 1 min. The flow-through was discarded and 500 µL Wash Buffer was added. The column was centrifuged at 14,500 rpm for 1 min, flow-through was discarded and the washing step was repeated. The column was centrifuged at 14,500 rpm for another 1 min and transferred into a 1.5 mL Eppendorf tube. To elute plasmid DNA from the column, 30 µL Elution Buffer was added and the column was incubated at room temperature for 2 mins. Finally, the tube was centrifuged at 14,500 rpm for 2 min. The column was discarded, and the concentration of eluted DNA was determined on NanoDrop (Thermo Fisher Scientific).

Restriction digest

For restriction cloning and confirmation of insert presence, PCR amplicons or vectors were digested by enzymes called restriction endonucleases. These enzymes recognize and cut a specific dsDNA sequence called restriction site. The digestion reaction contained 0.3 U selected restriction enzyme(s) (Thermo Fisher Scientific), 1x appropriate buffer (Buffer B, Buffer G, Buffer R, Buffer O or Tango Buffer) (Thermo Fisher Scientific) and up to 2 µg of DNA to be digested. If two buffers were used for digest, optimal buffer was selected using ThermoFisher DoubleDigest Calculator tool. The digestion reaction was incubated at 37°C for 1-2 h.

E. coli TOP10a competent cell transformation

30 µL of TOP10a competent *E. coli* cells were taken out of -80°C freezer and let thaw on ice. DNA to be transformed was added to bacterial suspension. The mixture was gently swirled and incubated on ice for 30 min, swirling every 10 min. The cells were heat-shocked for 30 seconds in a 42°C water bath. 250 µL Super Optimal Broth with Catabolite repression (SOC medium: 0.5 mM yeast extract powder (MP Biomedicals), 2 mM tryptone (Sigma), 10 mM KCl (Serva), 2.5 mM $MgCl_2$ (Sigma), 20 mM glucose (Serva)) was added, and the mixture was incubated in a shaker at 37°C at 200 rpm for 60 min. The cells were plated on a LB agar medium containing appropriate antibiotic selection (Table 3).

Antibiotic	Stock concentration (mg/ml)	Final concentration (µg/ml)
Kanamycin	50	50
Spectinomycin	50	50
Ampicillin	100	100
Chloramphenicol	34	34
Gentamycin	50	50
Rifampicin	50	50
Basta	50	50

Table 3. Commonly used antibiotics

A. tumefaciens GV 3101 competent cell transformation

A. tumefaciens was transformed by the electroporation method. 30 µL competent cell aliquot was removed from -80°C freezer and put on ice to thaw. 100 ng of purified plasmid DNA was added to the bacterial cells. The cells were pipetted into a pre-chilled electroporation cuvette. The cuvette was inserted into the electroporator (Eppendorf Eporator) and electrical field pulse was applied. 1 mL pre-chilled YEB medium was added immediately to the cuvette. Bacteria were resuspended and the suspension was transferred into a fresh 1.5 mL Eppendorf tube. The tube was incubated in a shaker for 2 h at 28°C at 160 rpm. 50 µL of the suspension was plated on YEB agar medium containing rifampicin, gentamycin and selection for transformed plasmid. Plates were incubated for 48 h at 28°C.

Plasmid verification and storage

After each cloning reaction, presence of DNA fragment of interest in correct orientation and sequence was verified. First, around 20 bacterial colonies were tested for construct presence in a colony PCR. Each colony was gently touched with a white spatula tip and added into a prepared PCR reaction as a template. Vector-specific primers were used in PCR amplification. PCR product was run on 1% agarose gel electrophoresis and 2-3 positive colonies were chosen based on correct band size. These clones were grown overnight in a 5 mL culture in LB medium at 37°C at 180 rpm. Plasmid DNA was isolated using described plasmid isolation protocol. Isolated plasmid DNA was digested by a chosen restriction enzyme. Restriction digest was run on 0.8% agarose gel and if the pattern corresponded to Benchling

simulation, it was sent for DNA sequencing. Sequencing reaction contained 500 ng plasmid DNA, a sequencing primer in final concentration 10 mM and dH_2O to final volume 10 µL. Sequencing was carried out as a service at Eurofins Genomics. Sequencing results were aligned with simulated sequence using MAFFT algorithm in Benchling software (www.benchling.com).

After sequence verification, each construct was stored in the form of glycerol stock in -80°C freezer. Bacterial colony with confirmed sequence was used to set up a 5 mL culture in LB medium. The culture was grown in a shaker at 37°C overnight at 180 rpm. 700µL culture was mixed with 300 µL 80% sterile glycerol (Lach-Ner) in a cryovial tube. Cryovial tubes were stored in -80°C.

Restriction cloning

Restriction cloning takes advantage of restriction endonucleases. Restriction sites are added to DNA fragment of interest during PCR amplification. PCR product of insert as well as cloning vector are digested using the same restriction enzymes. Finally, insert DNA is ligated into the vector DNA. Ligation reaction is transformed into *E. coli* competent cells.

PCR amplification of DNA fragment of interest

Primers for PCR amplification contained around 20-nucleotide long sequence complementary to DNA fragment of interest on the 3´ end and a restriction site sequence with an upstream 4-nucleotide buffer sequence at the 5´ end. DNA fragment of interest was amplified in a PCR reaction with Phusion polymerase (Thermo Fisher Scientific). PCR product was run on agarose gel electrophoresis, band of correct size was cut out and gel extracted.

Restriction digest, ligation and E. coli transformation

Both insert and vector were digested using the same restriction enzymes. Restriction digest was run on 1% agarose gel, bands of desired size were cut out and gel extracted. Concentration of purified DNA was measured on NanoDrop (Thermo Fisher Scientific). Insert and cloning vector were ligated using T4 DNA ligase (Thermo Fisher Scientific). Each ligation reaction was prepared in total volume 10 µL and contained digested cloning vector (10 ng), digested insert (10 ng), 1x T4 DNA ligase buffer and 1.5 U T4 DNA ligase enzyme (Thermo Fisher Scientific). The reaction was incubated at 22°C for 60 min. 5µL of the ligation product was used to transform *E. coli* TOP10a competent cells.

Gateway® cloning

Gateway® cloning technology is based on site-specific recombination mechanism of λ phage integration into the bacterial chromosome (Hartley et al., 2000). It consists of two reactions – so-called BP reaction and LR reaction. In BP reaction, DNA fragment of interest flanked by attB sites recombines with a donor vector (pDONR) containing attP sites (Figure 5A). This results into an entry vector (pENTR)

containing DNA fragment of interest flanked by attL sites. In LR reaction, attL sites of the entry vector recombine with attR sites of a destination vector (pDEST). DNA fragment of interest is flanked by attB sites in the resulting expression vector (pEXPR) (Figure 5B). There are multiple att site variants and recombination is att-site specific, e. g. attB1 site recombines only with attP1 site and not attP2 site. Each recombination reaction can thus proceed in an orientation. Up to 4 recombination reactions can be combined in one LR reaction. It is thus possible to combine different DNA fragments in one expression vector (Figure 5C).

PCR amplification of DNA fragment of interest

Chosen attB sites (for example attB1) were added to DNA fragment of interest during its amplification. PCR primers were designed to have attB sequence on 5´ end and gene-specific sequence on 3´ end. For example, TCTP coding sequence was amplified using TCTP1-attB1-F and TCTP1-attB2-R primers (Table 6). As attB sequence is too long to be contained in a single primer with gene-specific sequence, two consecutive PCR reactions were performed. In the second reaction, attB1-F and attB2-R primers were used (Table 6). PCR product was run on an agarose gel electrophoresis, DNA band of correct size was cut and gel eluted.

BP reaction

To create an entry Gateway vector, BP reaction was performed. 100 ng PCR product was combined with 150 ng donor vector (pDONR P1P2 or pDONR P4B1) and Tris-EDTA buffer pH 8.0 (TE: 1mM Tris (MP Biomedicals), 1mM EDTA (Duchefa)) to final volume 8 µL. BP Clonase II Mix (Thermo Fisher Scientific) was taken out of -80°C, let to thaw on ice, briefly vortexed and 2 µL were added to the prepared mixture. BP reaction was incubated for 16 h at 25°C. Finally, 1 µL proteinase K (Thermo Fisher Scientific) was added and the reaction was incubated for 10 min at 37°C. 2µL of the recombination reaction was used to transform *E. coli* TOP10a competent cells. Bacteria were plated on LB agar medium containing 50 µg/mL kanamycin (Duchefa). Bacteria transformed with a non-recombined donor vector were killed by the expression of *ccdB* gene. Construct presence was verified as described above.

LR reaction

To create an expression Gateway vector, an entry vector recombined with a chosen destination vector in LR reaction. Each reaction contained 100 ng entry vector, 150 ng destination vector, 2 µL LR Clonase Enzyme mix and TE buffer pH 8.0 to final volume 10 µL. The mixture was incubated for 16 h at 25°C. Recombination was stopped by 10 min incubation with 1 µL proteinase K at 37°C. *E. coli* TOP10a competent cells were transformed with 2 µL of the recombination reaction. Bacteria were plated on

LB agar medium containing spectinomycin (100 µg/mL). Construct presence was confirmed as described.

In case of MultiSite LR reaction, 3 entry vectors were used in an LR reaction with a destination vector. The reaction contained 10 femtomoles of each entry vector, 20 femtomoles of destination vector, 2 µL LR Clonase II Plus Enzyme Mix and TE buffer to final volume 10 µL. The reaction was performed as described.

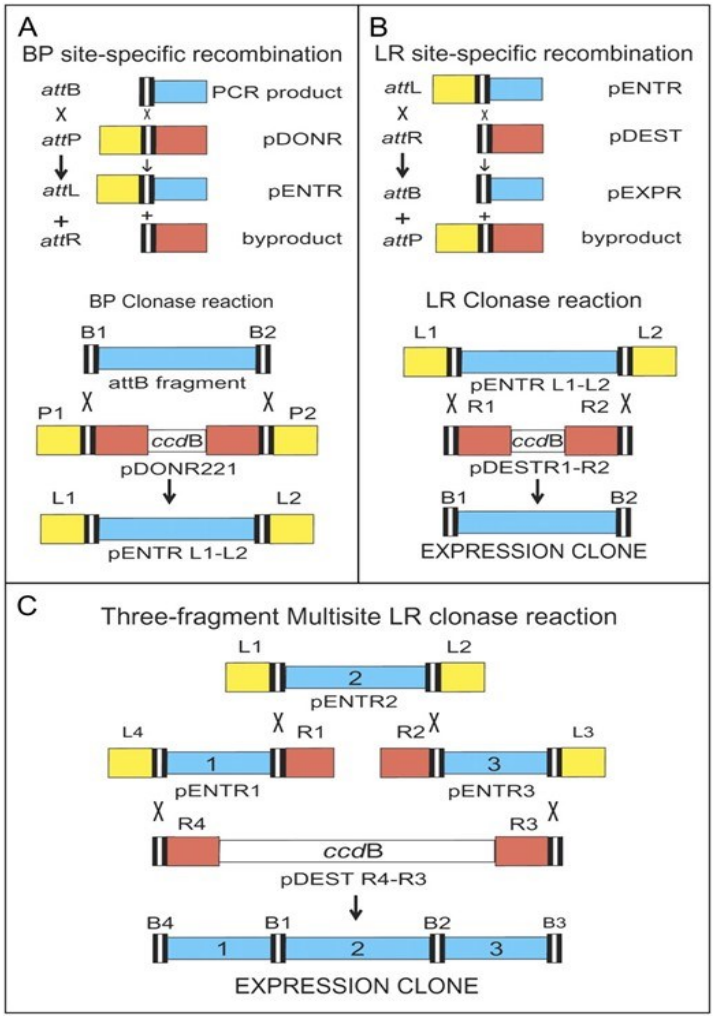

***Figure 5*. Outline of Gateway cloning technology.** *(A) In a BP reaction, attB sites on a PCR product recombine with attP sites in donor vector, resulting in an entry clone with attL sites. (B) In an LR reaction, attL sites of an entry vector recombine with attR sites of destination vector to generate expression clone. (C) multiple entry clones can be combined in a Multisite LR reaction. Adapted from (Karimi et al., 2007)*

Site-directed mutagenesis

QuikChange II XL Site-Directed Mutagenesis Kit (Agilent) was used to create a substitution in an entry Gateway vector. A PCR reaction was mixed in a 0.5 mL Eppendorf tube. It consisted of 2.5 µL 10× Reaction buffer, 10 ng plasmid template, 0.2 mM reverse and forward primer containing the mutation, 0.5 µL dNTP mix, 1.5 µL QuikSolution reagent, 0.5 µL *PfuUltra* high fidelity DNA polymerase and dH_2O to final volume 25 µL. Reaction was run in a thermocycler according to Table 4. After amplification, 1 µL DpnI restriction enzyme (10 U/µL) was added to the reaction to digest template plasmid DNA. The reaction was mixed with a pipette and incubated at 37°C for 60 min in a thermocycler. 2 µL mixture were used to transform *E. coli* TOP10 competent cells.

Step		Temperature	Time (min:sec)
1		95°C	1:00
18x repeat	2	95°C	0:50
	3	60°C	0:50
	4	68°C	1 min/1kb
5		68°C	7:00
6		4°C	∞

Table 4. PfuUltra polymerase PCR reaction cycle

All created vectors are summarized in Table 5 and used primer sequences are stated in Table 6.

Entry Gateway vectors prepared in this work				
Name	**Primers**	**Template**	**Donor vector**	**Antibiotic resistance**
pENTR-L1-TCTP1(CDS)-L2	TCTP1-attB1-F, TCTP1-attB2-R	Inflorescence cDNA	pDONR P1P2	Kan
pENTR-L1-TCTP1(gDNA)-L2	proTCTP1-attB1-F, TCTP1-attB2-R	Genomic DNA	pDONR P1P2	Kan
pENTR-L4-pTCTP1-R1	proTCTP1-attB4-F, proTCTP1-attP1-R	Genomic DNA	pDONR P4B1	Kan

Expression Gateway vectors prepared in this work					
Name	**Entry vector(s)**			**Destination vector**	**Antibiotic resistance**
pTCTP1-TCTP1(gDNA)-GFP	pENTR-L1-TCTP1(gDNA)-L2			pK7FWG,0	Spec
pTCTP1-TCTP1(cDNA)-GFP	pENTR-L4-pTCTP1-R1	pENTR-L1-TCTP1(CDS)-L2	pENTR-R2-GFP-L3 (Said Hafidh´s collection)	pK7m34GW	Spec
pLat52-TCTP1(cDNA)-GFP	pENTR L4-pLat52-R1 (Said Hafidh´s collection)	pENTR-L1-TCTP1(CDS)-L2	pENTR-R2-GFP-L3 (Said Hafidh´s	pK7m34GW	Spec
pDEST-periHisMBP-TCTP1	pENTR-L1-TCTP1(CDS)-L2			pDEST-periHisMBP	Amp

Vectors prepared by restriction cloning					
Name	**Primers**	**Template**	**Vector**	**Restriction enzymes**	**Antibiotic resistance**
pET29-TCTP1	TCTP1-BglII-F, TCTP1-XhoI-R	pENTR-L1-TCTP1(CDS)-L2	pET29	BglII, XhoI	Kan
pET29-BRL2 (ECD)	BRL2(ECD)-BglII-F, BRL2(ECD)-XhoI-R	pENTR-L2-BRL2(CDS)-L3 (Said Hafidh´s collection)			
pET29-BRL2 (KD)	BRL2(KD)-BglII-F, BRL2(KD)-XhoI-R	pENTR-L2-BRL2(CDS)-L3 (Said Hafidh´s collection)			
pET29-TTL3	TTL3-BglII-F, TTL3-XhoI-R	pENTR-L2-TTL3-L3 (Said Hafidh´s collection)			
pET29-TCTP1 C168S	TCTP1-BglII-F, TCTP1-C168S-XhoI-R	pENTR-L1-TCTP1(CDS) C168S-L2			

Vector prepared by site-directed mutagenesis			
Name	**Primers**	**Template**	**Antibiotic resistance**
pENTR-L1-TCTP1(CDS) C168S-L2	TCTP1-C168S-F, TCTP1-C168S-R	pENTR-L1-TCTP1(CDS)-L2	Kan

Table 5. Vectors generated in this work

Primer name	Sequence (5´-3´)	Purpose
TCTP1-attB1-F	ACAAAAAAGCAGGCTTAATGTTGGTGTACCAAGATC	Gateway cloning
TCTP1-attB2-R	AAGAAAGCTGGGTGGCACTTGACCTCCTTC	Gateway cloning
proTCTP1-attB4-F	ATAGAAAAGTTGGGTGCTGACCCAACCCAAGTGTC	Gateway cloning
proTCTP1-attP1-R	GTACAAACTTGTCCCCGGTCGCTTATTGATTGTTTTC	Gateway cloning
proTCTP1-attB1-F	ACAAAAAAGCAGGCTTACTGACCCAACCCAAGTGTC	Gateway cloning
attB1F	GGGGCAACTTTGTACAAAAAAGCAGGCT	Gateway cloning
attB2R	GGGGCAACTTTGTACAAGAAAGCTG	Gateway cloning
attB4F	GGGGACAACTTTGTATAGAAAAGTTGGGTG	Gateway cloning
attB1rR	GGGGCAACTTTTTTGTACAAACTTG	Gateway cloning
TTL3-BglII-F	ATAAAGATCTTATGTCTCATTCTAGAAGAC	Restriction cloning
TTL3-XhoI-R	AGAACTCGAGGTGTAAGAGGAAATGC	Restriction cloning
BRL2-ECD-BglII-F	ATAAAGATCTTATGACTACTTCACCAATCC	Restriction cloning
BRL2-ECD-XhoI-R	CGTGCTCGAGACGTTTCCCTTCCTCTGTTCC	Restriction cloning
BRL2-KD-BglII-F	GGAGAGATCTTGCGGATGATGCGAAGATGC	Restriction cloning
BRL2-KD-XhoI-R	AGAACTCGAGGTGCAAGCTGTTACTGTGAC	Restriction cloning
pET29seq-R	GCTAGTTATTGCTCAGCGG	Restriction cloning
pET29seq-F	AGGTTGAGGCCGTTGAG	Restriction cloning
TCTP1-BglII-F	AAGCAGATCTTATGTTGGTGTACCAAGACC	Restriction cloning
TCTP1-XhoI-R	AAGCCTCGAGCGACTTGACCTCCTTCA	Restriction cloning
TCTP1-C168S-XhoI-R	AAGCCTCGAGGGACTTGACCTCCTTCA	Restriction cloning
M13-R	CAGGAAACAGCTATGACCATG	Construct verification
M13-F	TGTAAAACGACGGCCAGT	Construct verification
eGFP-R2	AACAGCTCCTCGCCCTTGC	Construct verification
pDEST-periHisMBP-seqF	GCTTGCTGCAACTCTCTCAG	Construct verification
pDEST-periHisMBP-seqR	CGATTAAGTTGGGTAACG	Construct verification
TCTP1-C168S-F	GTTTGAAGGAGGTCAAGTCCCACCCAGCTTTCTTG	Site-directed mutagenesis
TCTP1-C168S-R	CAAGAAAGCTGGGTGGGACTTGACCTCCTTCAAAC	Site-directed mutagenesis

Table 6. Primers used in this work

Plant transformation

Floral dip

Primary inflorescence was cut prior to transformation to encourage branching. When secondary inflorescences started to form flowers, 5 ml YEB medium containing antibiotic selection was inoculated with a single *A. tumefaciens* colony or with a glycerol stock containing construct to be transformed. The culture was grown overnight at 28°C at 160 rpm. Following day, 200 µL grown culture was used to inoculate 200 mL fresh YEB medium in a 500 mL flask. The culture was grown overnight at 28°C at 160 rpm. Overnight culture was centrifuged in 250 mL Beckman centrifuge tubes for 20 min at 3,900 rpm at room temperature. Supernatant was carefully discarded. The pellet was gently resuspended in Infiltration medium (0.022% MS salts (Sigma), 5% sucrose (Sigma), 1 mL/L Gamborg´s Vitamin Solution (Sigma), 0.05% MES (Duchefa), 10 µg/L benzylaminopurine) with a 5 mL pipette. Bacterial suspension was carefully transferred into a 1 L beaker. Immediately before dipping flowers into the infiltration medium, 300 µL/L Silwet Star (AgroBio) was added to the suspension. Inflorescences were placed into the bacterial suspension for 45 s. Plants were covered with a porous black autoclave bag overnight. The cover was removed following day and the plants were cultivated until seed harvesting.

Transformant selection

Because transformation efficiency by floral dip is low (usually around 1%), there would be a need to screen a great number of plants without selection. T-DNA cassettes used in this thesis contained kanamycin resistance gene under the control of sporophytic 35S promoter. To select individuals carrying the transgene, seeds harvested from transformed plants were selected on MS medium containing kanamycin (50 µg/mL). Around 15-20 selected plants were transferred on Jiffy peats and cultivated. Presence of the transgene was further verified by a genotyping PCR.

Recombinant protein expression

BL21-Codon Plus (DE3)-RIP and BL21-Codon Plus (DE3)-RIPL *E. coli* strains were utilized for recombinant protein expression. These strains carry a T7 RNA polymerase gene under the control of *lac* promoter in their genome. In the absence of an inducer called isopropyl-β-D-thiogalactopyranoside (IPTG), T7 RNA polymerase transcription is blocked by a lac repressor. In its presence, lac repressor cannot bind to lac promoter and T7 RNA polymerase is expressed. If gene encoding protein of interest is driven by T7 promoter, addition of IPTG to bacterial culture ideally results in its expression. T7 promoter activity is considered very strong and can result in recombinant protein accumulation up to 50% of total cellular proteins (Studier and Moffatt, 1986).

E. coli BL21-Codon Plus competent cell transformation

100 µL of BL21-Codon Plus (DE3)-RIL or BL21-Codon Plus (DE3)-RIPL cells (Agilent Technologies) were taken out of -80°C freezer alongside XL10-Gold β-mercaptoethanol (ME) mix supplied in the same kit. XL10-Gold β-ME mix was diluted with dH_2O in 1:10 ratio. 2 µL of diluted β-ME was added to the BL21 competent cells. The mixture was incubated on ice for 10 min, swirling every 2 min. 50 ng of expression plasmid DNA was added to the tube and incubated on ice for 30 min. The cells were heat-shocked in a water bath at 42°C for 20 seconds. After 2 min incubation on ice, 900 µL preheated SOC medium was added to the bacteria. After transformation, BL21 cells were incubated in a shaker at 37°C for 60 min at 220 rpm. 50 µL and 100 µL of the bacterial suspension were plated on a LB agar medium containing antibiotic selection for the expression plasmid. Plates were incubated overnight at 37°C. Presence of the expression plasmid was confirmed by colony PCR. Glycerol stocks were prepared for 2 positive colonies per construct.

Induction of recombinant protein expression

Glycerol stock of BL21 cells was used to inoculate a 5 mL LB broth medium containing antibiotics selecting for the expression plasmid (kanamycin or ampicillin) and the plasmid carrying tRNA genes (chloramphenicol). Bacterial culture was grown overnight in a shaker at 37°C at 180 rpm. Next day, 0.5 mL culture was pipetted into a 100 mL Erlenmayer flask containing 9.5 mL fresh LB broth medium supplemented with the same antibiotic selection. The flask was incubated at 37°C at 220 rpm. Optical density of the culture was measured regularly and when it reached 0.8 (usually after 1.5-2 h), IPTG (ICN Biomedicals) in desired concentration (stock solution 24 mg/mL) was added to the culture. The culture was incubated in a shaker at 220 rpm for desired time at desired temperature. For each recombinant protein, IPTG concentration, incubation time and temperature after induction were optimized for high recombinant protein yield.

Bacterial protein extraction

Bacterial culture was centrifuged for 10 min at 4°C at 4,000 rpm. Most of the supernatant was discarded, a little amount was used to resuspend the pellet and transfer the suspension to a 1.5 mL safe-lock Eppendorf tube. This tube was centrifuged for 30 s at 14,000 rpm and the rest of the medium was discarded.

Proteins from the periplasmic fraction were extracted according to Malherbe et al. (2019). The pellet was washed with 340 µL Phosphate-buffered saline (PBS: 137 mM NaCl (Sigma), 2.7 mM KCl (Sigma), 24.2 mM Na_2HPO_4 (Sigma), 5.2 mM KH_2PO_4 (Merck)) and centrifuged at 14,000 rpm at 4°C for 3 min. Supernatant was discarded and the pellet was resuspended in 360 µL Spheroplast buffer (0.1 M Tris/HCl pH 8.0 (MP Biomedicals), 500 mM sucrose (Serva), 0.5 mM EDTA pH 8.0 (Duchefa)) and

incubated on ice for 5 min. The mixture was centrifuged at 14,000 rpm at 4°C for 3 min. The supernatant was discarded, and the pellet was resuspended in 160 µL 1 mM $MgSO_4$ (Sigma). The mixture was incubated on ice for 15 s and 8 µL 20 mM $MgSO_4$ was added. The mixture was centrifuged at 14,000 rpm at 4°C for 3 min. Supernatant containing proteins from the periplasm was carefully transferred into an Eppendorf tube.

To isolate proteins from the soluble fraction, centrifuged bacterial pellet was frozen in liquid nitrogen. Frozen pellet was grinded in a mortar with a pestle into white powder and the powder was transferred into a sterile 1.5 mL Eppendorf tube with a cut blue pipette tip. 250 µL Rapid Immunoprecipitation assay buffer (RIPA: 10 mM Tris/HCl pH 7.5 (MP Biomedicals), 150 mM NaCl (Sigma), 0.5 mM EDTA (Duchefa), 0.5% NP-40 (Sigma), Pierce protease inhibitor (Thermo Fisher Scientific, 1 tablet per 50 ml buffer), 10 mM phenylmethylsulphonyl fluoride (PMSF, Sigma)) was added to grinded bacteria and the mixture was incubated for 60 min on ice. Finally, it was centrifuged at 4°C at 14,000 rpm for 10 min. The supernatant (soluble protein extract) was carefully transferred to a 1.5 mL Eppendorf tube. The pellet was either discarded or kept for analysis of the insoluble fraction.

His-tag purification

100 µl Ni-NTA agarose beads were transferred into 1.5 mL Eppendorf tube. The tube was centrifuged for 1 min at 3,000 rpm at 4°C. Flow-through was discarded and the beads were gently resuspended in 400 µl Equilibrium buffer (20 mM Tris/HCl pH 7.5 (MP Biomedicals), 250 mM NaCl (Sigma)). After 1 min centrifugation at 3,000 rpm, 1 mL protein sample containing His-tagged protein was added to the beads. The tube was incubated for 1 hr on a turning wheel at 4°C. Beads bound proteins tagged with a His-tag. After the incubation, the tube was centrifuged for 1 min at 3000 rpm at 4°C and the flow-through was kept for analysis. As there might be non-specific interactions between the beads and other bacterial proteins, the beads were washed three times with 400 µl equilibrium buffer containing 50 mM imidazole (Sigma) and centrifuged for 1 min at 3000 rpm at 4°C after each wash. Last washing fraction was stored for analysis. 100 µl elution buffer (20 mM Tris/HCl pH 7.5 (MP Biomedicals), 250 mM NaCl (Sigma), 500 mM imidazole (Sigma)) was added to the column and it was centrifuged for 1 min at 3000 rpm at 4°C. The eluate was stored at -20°C for further analysis.

S-tag purification

S-protein agarose beads (Novagen) were used to capture proteins carrying the S-tag. 100 µL beads were added to 200 µL protein extract in a 1.5 mL Eppendorf tube, gently resuspended with a pipette tip and incubated on an orbital shaker at room temperature for 1 hr. The mixture was centrifuged at 2,000 rpm and the supernatant was carefully discarded. The beads were washed three times with Bind/Wash Buffer (20 mM Tris/HCl pH 7.5 (MP Biomedicals), 150 mM NaCl (Sigma), 0.1% NP-40 (Sigma)

and centrifuged at 2,000 rpm for 10 min. Finally, proteins bound to the beads were eluted either with 3 M $MgCl_2$ (Sigma) or 3 M guanidine thiocyanate (GuSCN) (Sigma). Eluate was stored along with collected washing fractions in -20°C until further use.

MBP purification

Proteins bearing MBP (maltose binding protein) tag were purified with MBP-Trap agarose beads (Chromotek). 25 µL bead slurry was transferred with a blue cut tip into a 1.5 mL Eppendorf tube. 150 µL Dilution buffer (10 mM Tris/HCl pH 7.5 (MP Biomedicals), 150 mM NaCl (Sigma), 0.5 mM EDTA (Duchefa)) was added, beads were gently resuspended with a pipette tip and the tube was centrifuged at 4°C at 5,000 rpm for 5 min. Equilibration step was repeated three times. 200 µL bacterial protein extract was diluted with 300 µL Dilution buffer. Diluted protein extract was added to the beads. After a gentle resuspension, beads were incubated at 4°C on a turning wheel for 1 hr. To minimize non-specific protein binding, beads were washed three times with Wash buffer (10 mM Tris/HCl pH 7.5 (MP Biomedicals), 150 mM NaCl (Sigma), 0.05 % NP40 (Sigma), 0.5 mM EDTA (Duchefa)). After each wash, beads were centrifuged at 4°C at 5,000 rpm for 5 min. Beads were resuspended in 80 µL 3X SDS buffer (0.15M Tris/HCl pH 6.8 (MP Biomedicals), 30% v/v glycerol (Lach-Ner), 6% SDS (Serva), 0.15M DTT (Sigma), 0.03% bromophenol blue (Sigma)). To elute proteins bound to the beads, beads were boiled at 95°C for 5 min. The eluate was shortly centrifuged and was either used immediately for SDS/PAGE or stored in -20°C until further use.

SDS/PAGE and Western blot

SDS/PAGE

Electrophoretic protein separation was performed in Mini-PROTEAN Tetra Cell system (Biorad). Prior to gel casting, glass plates were cleaned with ethanol. A thicker bottom glass and a thinner cover glass plates were put in a casting frame and placed on a casting stand. First, the resolving gel (10-12% acrylamide/bisacrylamide solution 37.5:1 (Biorad), 0.125 M Tris/HCl pH 8.8 (MP Biomedicals), 0.1 M SDS (Serva), 0.1% ammonium persulfate (Sigma), 0.2% tetramethylethylendiamin (TEMED, Carl ROTH)) was prepared in a beaker. Immediately after the addition of TEMED, gel was pipetted between the glass plates approximately 2 cm under the top edge. 60 µL isopropanol (Sigma) was added on top of the gel. After 30 min, isopropanol was vacuum sucked. Stacking gel (5% acrylamide/bisacrylamide solution 37.5:1 (Biorad), 0.125 M Tris/HCl pH 6.8 (MP Biomedicals), 0.1 M sodium dodecylsulfate (SDS, Serva), 0.06% ammonium persulfate (Sigma), 0.2% TEMED (Carl ROTH)) was prepared and pipetted on top of the resolving gel until the glass chamber was full. 10-well or 15-well comb was quickly put into the chamber. After 30 min, the comb was carefully removed from the gel and the glass chamber was filled with dH_2O. The glass plate was transferred from the casting stand into the electrophoresis stand.

Prior to loading, 3x SDS sample buffer (0.15M Tris/HCl pH 6.8 (MP Biomedicals), 30% v/v glycerol (Lach-Ner, 6% SDS (Serva), 0.15M DTT (Sigma), 0.03% bromophenol blue) was added to protein samples and the mixture was boiled at 95°C for 10 min at 300 rpm. Samples and PageRuler™ Prestained Protein Ladder (Thermo Fisher Scientific) were loaded into the wells of gel in the electrophoresis stand. Electrophoresis stand was placed into the tank and filled with Electrode buffer (25 mM Tris (MP Biomedicals), 192 mM glycine (PanReac Applichem), 0.1% SDS (Serva)). Electrophoresis tank was filled up to a mark indicating number of run gels. Electrophoresis was run at 75 V until blue band on the gel reached the boundary between resolving and stacking gel (around 20 min) and the voltage was increased to 150 V until blue band reached bottom of the gel.

Polyacrylamide gel was carefully removed from the glass chamber and gently placed into a plastic box containing dH_2O. It was washed in dH_2O at room temperature 3 times for 5 min and ready for Coomassie brilliant blue (CBB) staining or transfer to a membrane.

CBB G-250 staining

To visualize protein bands on a gel after SDS/PAGE electrophoresis, gel was stained with CBB G-250. The gel was incubated with CBB G-250 staining solution (5% aluminium sulphate hydrate (Sigma), 0.02% CBB G-250 (Sigma), 10% ethanol (Lach-Ner), 2% ortho-phosphoric acid (Roth)) at room temperature overnight. Following day, staining solution was exchanged for destaining solution (10% ethanol (Lach-Ner) , 2% ortho-phosphoric acid (Roth)) until blue background was washed away from the gel.

Wet transfer

Protein bands were transferred from a polyacrylamide gel onto a nitrocellulose membrane using wet transfer method. After SDS/PAGE, a gel was placed into Blotting buffer (20% v/v methanol (Lach-Ner), 25 mM Tris (MB Biomedicals), 192 mM glycine (PanReac Applichem)) for 30 min. The buffer was exchanged every 10 min. At the same time, nitrocellulose membrane was immersed into blotting buffer with 2 blotting papers (Whatman) and 4 filter papers. A stack was built in the following order on the black side of holder cassette – a blotting paper, 2 filter papers, gel, membrane, 2 filter papers and a blotting paper. The cassette was closed tightly and inserted into an electrode module. Electrode module was placed into a blotting tank. The tank was filled with blotting buffer up to the line “Blotting” and ice container was put inside to prevent overheating. Transfer was run at constant current (350 mA) for 1 h.

Western blot

The membrane was washed three times 5 min with Tris Buffered Saline with Tween (TBST: 10 mM Tris (MP Biomedicals), 150 mM NaCl (Sigma), 0.05% Tween 20 (Sigma)). It was blocked at room

temperature for 30 min in 5% milk powder (Bohemilk) in TBST and washed for 5 min with TBST. The membrane was incubated with primary antibody solution (10,000x dilution in 0.5% bovine serum albumin (BSA, Sigma) in TBST) overnight at 4°C at 100 rpm. Next day, it was washed three times 5 min with TBST and incubated with secondary antibody solution (20,000x dilution in 0.5% BSA (Sigma) in TBST). Finally, the membrane was washed three times 5 min in TBST. Used antibodies and their dilutions are summarized in Table 7.

Type	Name	Supplier	Dilution	Product number
primary	Rabbit anti-GFP	Agrisera	1 : 10,000	AS152987
primary	Rabbit anti-His	antibodies-online.com	1 : 10,000	ABIN398410
secondary	Goat anti-Rabbit HRP	Agrisera	1 : 20,000	AS09602

Table 7. Antibodies used in this work

Chemiluminiscence assay

AgriseraECL SuperBright Two-Component system (Agrisera) was used as a substrate for HRP in chemiluminiscence assay. 100 µL of Solution A was mixed with equal volume of Solution B and spread over the membrane in a cellophane foil. The membrane was incubated in dark for 1 min, exposed and imaged using a gel imaging system with detector of luminescence.

Microscopy and image analysis

Imaging was carried out at the Imaging facility at the Institute of Experimental Botany. Images were obtained on ZEISS Stemi 508 stereomicroscope, fluorescent Zeiss Axio Imager with ApoTome microscope and confocal Nikon Spinning Disk microscope. Detailed information can be found on http://www.ueb.cas.cz/cs/if/equipment. GFP (green fluorescent protein)/YFP (yellow fluorescent protein) fluorescence was excited with 488 nm laser. DAPI fluorescence was excited with 405 nm laser was used. Acquired images were processed in Fiji (ImageJ) software.

DAPI staining

DAPI (2-(4-amidinophenyl)-1H-indole-6-carbaximadine) is a fluorescent dye which binds to AT rich sequences in DNA. DAPI staining in this thesis was used for microscopic observation of vegetative and sperm nuclei in mature pollen. DAPI solution was added to GUS buffer (0.1 M $NaPO_4$ pH 7.0 (Sigma), 10 mM EDTA (Duchefa), 0.1% Triton X-100 (Fluka)) prior to microscopic slide preparation (8 µL DAPI/10 mL GUS).

Statistical testing

RStudio (R 4.1.2 version) was used for statistical analysis of acquired data and their graphical visualization. χ^2 (chi-squared) goodness-of-fit test was used to statistically evaluate differences between expected and observed frequencies of mutant allele transmission. Mean and standard deviation of measurements are presented as mean ± standard deviation in the text. Two-tailed Welch´s

t-test was used to evaluate differences in mean of two independent samples. Prior to the test, normal distribution of acquired data was assessed with a q-q plot. Welch´s test does not require homogeneity in variances and this parameter was thus not tested.

Software

Online Benchling software (www.benchling.com) was used for sequencing alignment. Protein structural models downloaded from RCSB PDB (Protein Data Bank) were visualized in UCSF Chimera, product version 1.16. Tables were created in Microsoft Excel and figures were assembled in Microsoft PowerPoint.

Results

tctp-1 mutant characterization

Previous characterization of *tctp-1* T-DNA insertion line (SAIL_C03_28) led to conflicting results for TCTP1 involvement in reproductive development. Characterization of this T-DNA insertion line was thus pursued with a special focus on the male gametophyte and events prior to fertilization.

tctp-1 SAIL allele is a Lat52-GUS trap line

tctp-1 mutant allele has a T-DNA insertion in the fourth exon of *TCTP1* and belongs to the SAIL collection collectively known as blue-SAIL collections. It contains a functional Basta resistance gene and therefore was selected for on a medium containing Basta herbicide. Presence of the insertion was further verified by genotyping PCR in a few selected plants. It was possible to discriminate between the mutant and wild type pollen and pollen tubes as the T-DNA insertion carried a GUS construct under pollen-specific Lat52 promoter. All experiments were carried out with heterozygous *tctp-1 +/-* individuals because *tctp-1* homozygous mutation is embryo lethal.

Reciprocal crosses of *tctp-1* revealed lower mutant transmission through male gametophyte

To verify transmission of the mutant allele through both female and male gametophyte, *tctp-1 +/-* plants were crossed with male sterile *ms1-1* plants and wild type Col-0 plants. Pistils were pollinated 48 h after flower emasculation where necessary. Mature seeds were harvested and plated on MS medium containing Basta herbicide. Resistant plants were easily discriminated from sensitive individuals (Figure 6A) Basta-sensitive and Basta-resistant seedlings were counted and the transmission of mutant allele through male and female gametophyte was determined.

ms1-1 x *tctp-1 +/-* (♀female x ♂male, same format here forth) and Col-0 x *tctp-1 +/-* crosses showed significantly lower mutant allele transmission than the expected 50% Mendelian segregation ratio (Table 6). Of the total population, only 16.81% (n = 458 seeds) of progeny from ms1-1 x *tctp-1 +/-* cross (p-value<0.001) and 24.49% (n = 196 seeds) progeny from Col-0 x *tctp-1 +/-* cross germinated as resistant seedlings on MS-Basta medium (p-value<0.001). In contrast, 48% (n = 125 seeds) of the seedlings from *tctp-1 +/-* x Col-0 cross were resistant to Basta, a ratio not significantly different from the expected 50% transmission (p-value = 0.65). Data are summarized in Figure 6B.

A

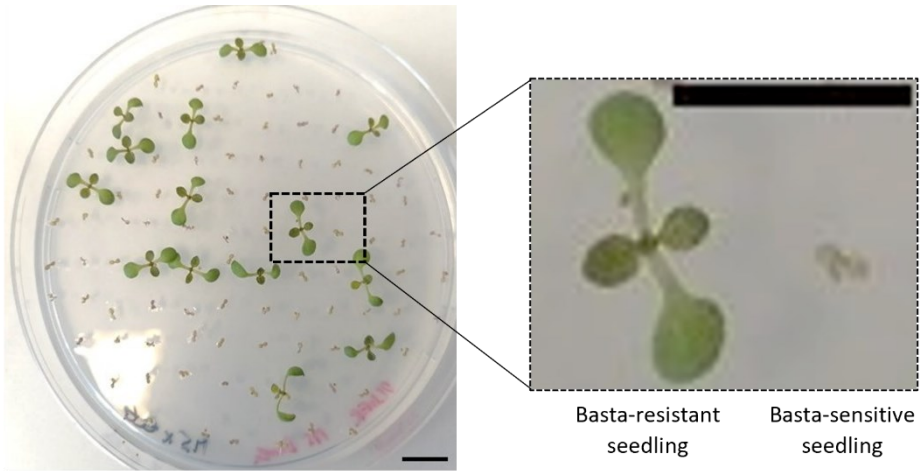

B

Cross (♀ x ♂)	Basta^R/Basta^S	*tctp-1* transmission	χ^2 value	p-value
ms1-1 x *tctp-1 +/-*	77/381	16.81%	201.78	**<0.001**
Col-0 x *tctp-1 +/-*	48/148	24.49%	51.02	**<0.001**
tctp-1 +/- x Col-0	60/65	48.00%	0.20	**0.65**

Figure 6. Transmission of tctp-1 allele is significantly reduced through the male gametophyte. *(A) Basta-resistant and Basta-sensitive seedlings have a distinct phenotype on MS-Basta medium. (B) tctp-1 allele transmission through male gametophyte is significantly lower than expected 50% but is unchanged through female gametophyte. Scale bar = 1 cm.*

The experiment thus suggests, while mutant *tctp-1* allele transmission through female gametophyte is not different from the expected Mendelian 1:1 ratio, the transmission through the male gametophyte is significantly reduced.

tctp-1 pollen fertilizes differently between apical and basal half of the silique

Lower mutant allele transmission could result from defects in pollen germination, pollen tube growth and/or ovule targeting by the pollen tube. To have a more detailed insight into the observed phenotype, reciprocal crosses of *tctp-1 +/-* plants with *Col-0* were performed. Obtained mature siliques were harvested and dissected with a sterile blade in the middle measured by a ruler. Seeds from the apical and basal half of the silique were collected separately and plated on MS medium containing Basta selection. Basta-sensitive and Basta-resistant seedlings were then quantified.

The transmission of *tctp-1* allele did not differ between the apical (50.68%, n = 73 seeds) and basal (44.23%, n=52 seeds) half of the silique in *tctp-1 +/-* x Col-0 cross. However, it was lower in the basal part of the silique (9.83%, n=61 seeds) than in the apical part (25.81%, n = 62 seeds) in the reciprocal cross Col-0 x *tctp-1 +/-*, when plant carrying the mutation was used as a pollen donor (Figure 7). This result suggests impaired growth of mutant pollen tubes.

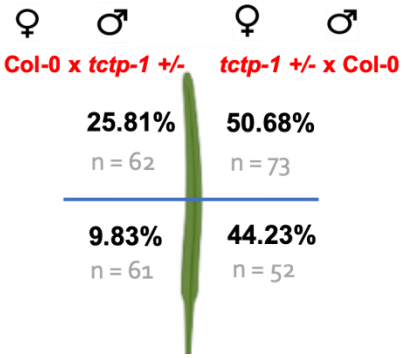

APICAL PART				
Cross	Number of seeds	Transmission(%)	χ^2 value	p-value
tctp-1 +/- x Col-0	73	50.68	0.014	**0.91**
Col-0 x tctp-1 +/-	62	25.81	14.516	**<0.001**

BASAL PART				
Cross	Number of seeds	Transmission(%)	χ^2 value	p-value
tctp-1 +/- x Col-0	52	44.23	0.692	**0.41**
Col-0 x tctp-1 +/-	61	9.83	39.36	**<0.001**

Figure 7. tctp-1 allele transmission through male gametophyte is lower in basal half of the silique

Distribution of aborted seeds in *tctp-1 +/-* siliques was not uniform

If mutant pollen tube growth is unaffected, uniform distribution of seeds carrying the male-transmitted *tctp-1* allele is expected. When dissecting *tctp-1 +/-* siliques, two seed classes were observed – wild-type looking green seeds and white seeds. White seeds carry a male-transmitted as well as a female-transmitted *tctp-1* allele. In total, 15 siliques (n = 5 plants) containing green seeds were dissected under stereomicroscope (Zeiss), as shown in Figure 8A. Siliques were imaged and

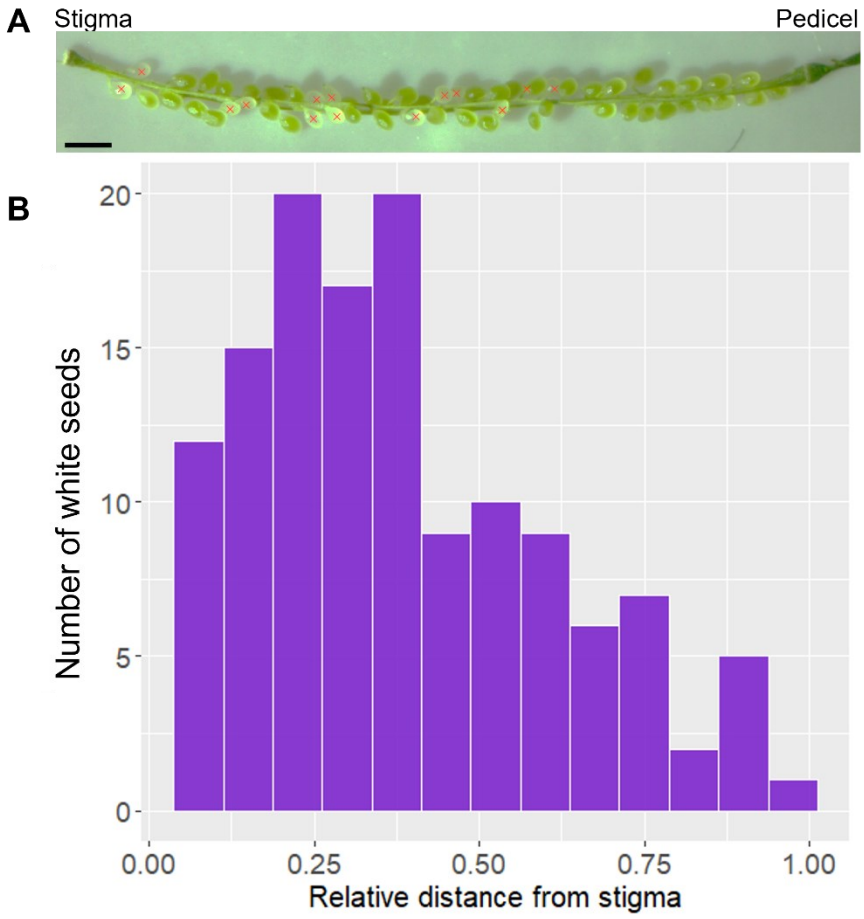

Figure 8. White seeds are not uniformly distributed in a tctp-1 +/- silique. *(A) Dissected placenta bearing white seeds (marked by red cross) and green seeds (unmarked). Scale bar = 1 mm. (B) White seeds were predominantly observed in apical half of tctp-1 +/- silique.*

position of all white seeds was marked in the image with a red cross. Relative distance of each white seed from the stigma was determined with Fiji software and values for all 133 white seeds were plotted in a histogram. White seeds were predominantly observed in the apical part of *tctp-1 +/-* siliques (Figure 8B). This result further supports the hypothesis that *tctp-1* pollen tube growth is impaired.

Aniline blue staining revealed no differences between *tctp-1 +/-* and Col-0 pollen tube targeting

Aniline blue staining of callose was performed to see if there are any observable differences in pollen tube targeting between mutant and wild type pollen. *tctp-1 +/-* pollen was used to pollinate *ms1-1* pistils. As a negative control, *ms1-1* pistils were pollinated with Col-0 pollen. Pollinated flowers were

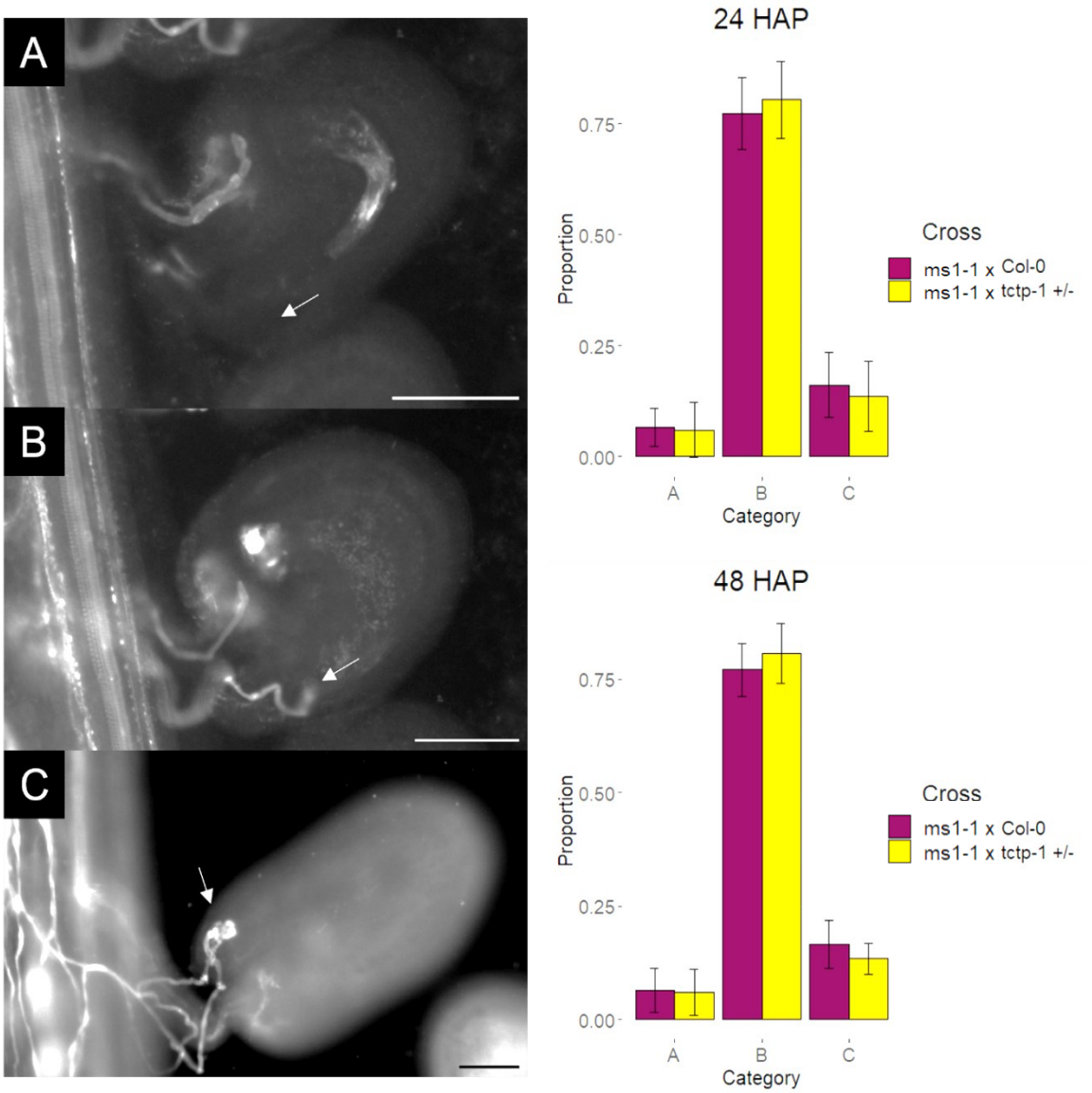

Figure 9. Aniline blue staining of pistils from ms1-1 x tctp-1 +/- cross and control ms1-1 x Col-0 cross *collected 24 HAP and 48 HAP. Stained pistils were observed on fluorescent Zeiss Axiovert microscope and each ovule was assigned a category A, B or C based on number of pollen tubes targeting the ovule. Proportion of each category was estimated. No statistically significant differences were found between ms1-1 x tctp-1 +/- cross and control ms1-1 x Col-0 cross. HAP – hours after pollination Scale bar = 50 µm.*

collected 24 h after pollination (HAP) and 48 HAP. Pistils were separated from remaining floral organs and stained for callose according to aniline blue staining protocol. Stained pistils were observed under UV light on a fluorescent Zeiss ApoTome microscope. It was possible to track individual pollen tubes.

Each ovule was categorized into one of three phenotypic categories based on number of pollen tubes targeting the ovule – no pollen tube targeting (type A), targeting by one pollen tube (type B) or targeting by 2 pollen tubes (type C). Proportion of each category in a pistil was estimated (Figure 9).

24 HAP, a total of 340 ovules (n = 13 pistils) from *ms1-1* x Col-0 cross and 523 ovules (n = 19 pistils) from *ms1-1* x tctp-1 +/- cross were counted and placed into categories A, B or C. Proportion of ovules in category A was 5.96±6.22% in *ms1-1* x *tctp-1 +/-*, which was not significantly different from 6.53±4.29% in control cross (p-value = 0.76). Proportion of ovules in category B was 80.44±8.66% in *ms1-1* x *tctp-1 +/-*, which was not significantly different from 77.34±8.17% in control cross (p-value = 0.31). Similarly, no significant difference was observed in the proportion of ovules in category C in *ms1-1* x *tctp-1 +/-* cross (13.59±7.83%) and control cross (16.12±7.24%) (p-value = 0.36).

48 HAP, a total of 331 ovules (n = 12 pistils) from *ms1-1* x Col-0 cross and 423 ovules (n = 14 pistils) from *ms1-1* x *tctp-1* +/- cross were counted and placed into categories A, B or C. Proportion of ovules in category A was 6.46±5.11% in *ms1-1* x *tctp-1 +/-*, which was not significantly different from 7.85±6.29% in control cross (p-value = 0.55). Proportion of ovules in category B was 86.38±6.59% in *ms1-1* x *tctp-1 +/-*, which was not significantly different from 84.87±5.91% in control cross (p-value = 0.54). No significant difference was observed in the proportion of ovules in category C in *ms1-1* x *tctp-1 +/-* cross (7.17±3.49%) and control cross (7.28±5.52%) (p-value = 0.95).

No differences in pollen tube targeting were observed between *ms1-1* x *tctp-1 +/-* and the control cross.

Blue dot assay showed reduced ovule targeting by *tctp-1* pollen tubes

The *tctp*-1 SAIL T-DNA insertion carries a Lat52-GUS construct. It is thus possible to track mutant and pollen grains and pollen tubes using GUS staining. Blue dot assay was performed to evaluate ovule targeting by mutant pollen tubes. *ms1-1* pistils were pollinated by heterozygous *tctp-1 +/-* pollen. As a negative control, *ms1-1* pistils were pollinated with pollen from heterozygous Lat52-GUS +/- in wild-type background. 24 HAP, pollinated pistils were collected and dissected under a stereomicroscope. Pistils were stained with GUS staining solution overnight at 37°C. Stained samples were observed on a microscope under transmitting light (Figure 10). Pollen grains and tubes which carried pLat52-GUS construct stained blue.

Each ovule was assigned a category (Figure 11). In category A, there was no blue-stained pollen tube visible in the funiculus and in the micropyle. In category B, blue-stained pollen tube targeted the ovule. A blue dot was visible in the micropylar pole, indicating a burst of the tube. In category C, blue pollen tube reached the funiculus but either did not reach the micropyle at all or did not burst. No blue dot

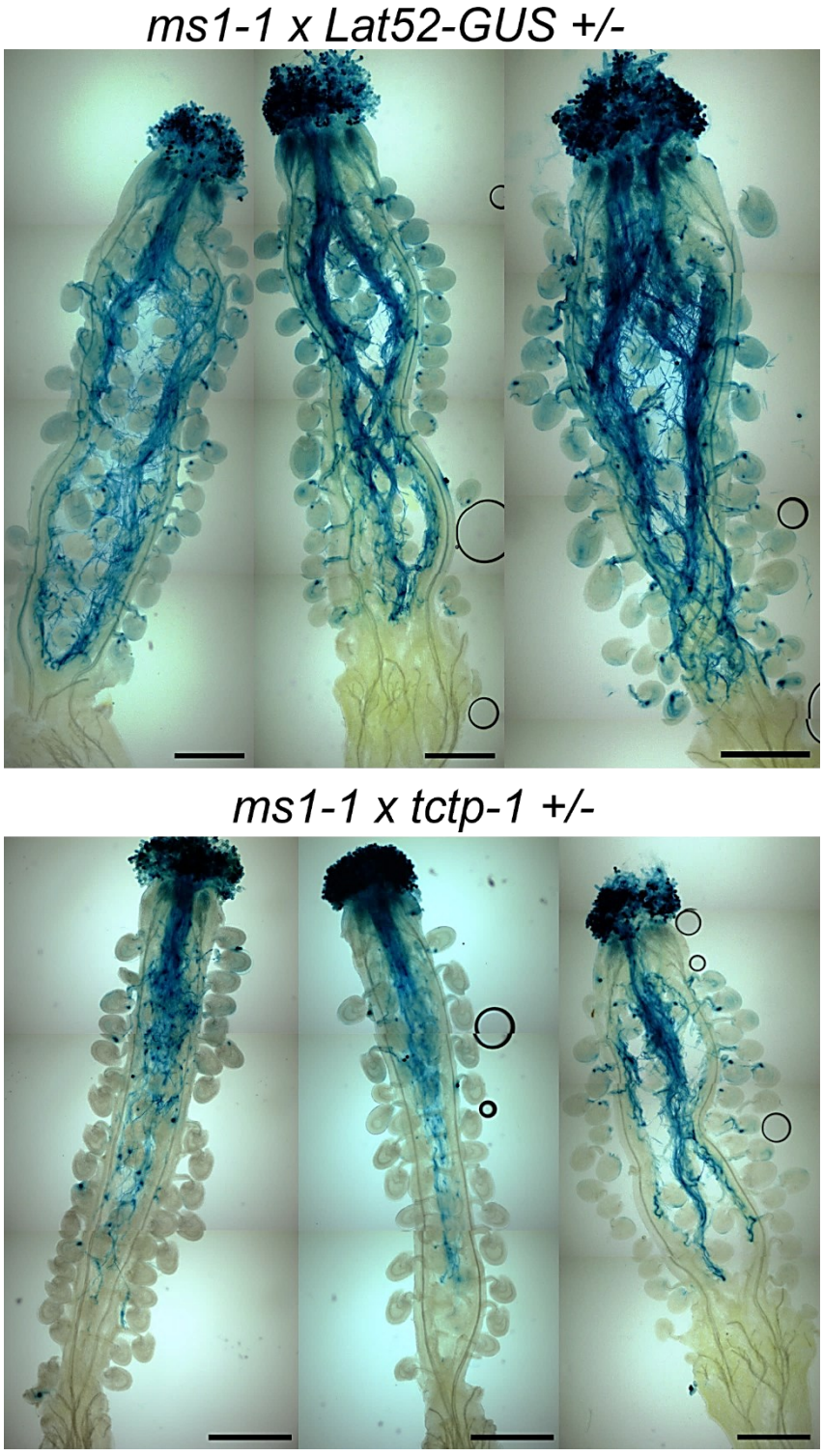

Figure 10. GUS staining of pistils from ms1-1 x tctp-1 +/- cross and control ms1-1 x Lat52-GUS +/- cross*. Three replicates shown. Pollen tubes carrying GUS stained blue. Scale bar = 500 µm.*

was observed in this case. A total of 1,025 ovules (n = 42 pistils) from *ms1-1* x Lat52-GUS +/- cross and 1,015 ovules (n = 38 pistils) from *ms1-1* x *tctp-1* +/- cross were counted and placed into categories A, B or C. Proportion of ovules within each pistil was estimated (Figure 11).

Proportion of ovules in category A was 77.05±8.28% in *ms1-1* x *tctp-1* +/- cross, which was significantly higher than 45.62±6.76% in the control cross (p-value < 0.001). In contrast, proportion of category B ovules was significantly lower in *ms1-1* x *tctp-1 +/-* cross (17.79±6.30) than in the control cross (47.91%±7.55%) (p-value < 0.001). There was no significant difference in proportion of ovules in category C between the mutant (5.16±4.61%) and the control cross (6.46%±5.58%) (p-value = 0.26).

Obtained result would be expected even if only pollen tube growth but not its targeting is affected. No differences were observed in frequency of defective targeting events (category C). However, based on very low transmission of mutant allele and outcompeting of mutant pollen tubes by wild type, such events might be too rare to detect in this experimental setup.

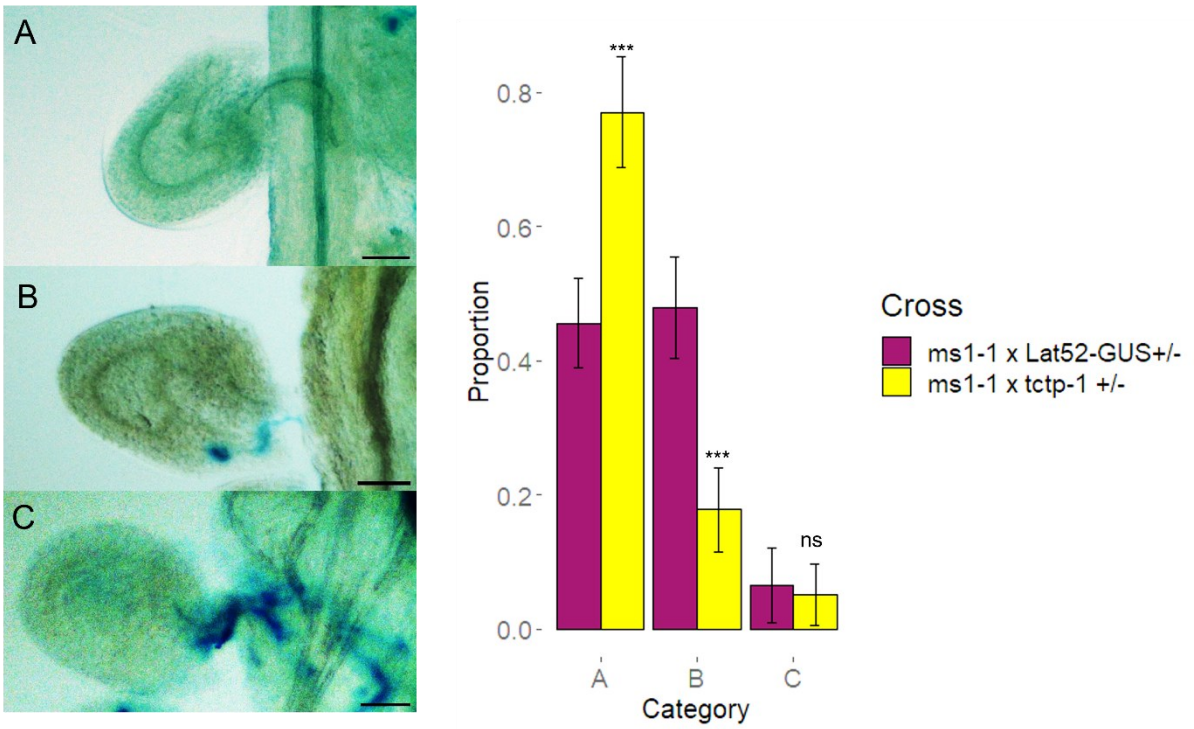

Figure 11. Blue dot assay. *Ovules from ms1-1 x tctp-1 +/- cross and control ms1-1 x Lat52-GUS +/- cross were assigned a category A, B or C based on targeting of blue-stained pollen tubes. tctp-1 pollen tubes targeted significantly lower number of ovules than control Lat52-GUS pollen tubes. *** p-value < 0.001, ** p-value < 0.01, p-value < 0.05, ns – p-value > 0.05. Scale bar = 50 µm.*

TCTP1 localization in male gametophyte

C-terminal GFP-tagged TCTP1 was previously reported to be functional and complemented *tctp-1* mutant phenotype (Brioudes et al., 2010; Hoepflinger et al., 2013). Here, we used both native promoter and Lat52 pollen-specific promoter to drive the expression of TCTP1-GFP/YFP. Because expression of cDNA-based TCTP1 construct under native promoter was very weak, genomic DNA based construct was prepared. Created constructs are schematically depicted in Figure 12.

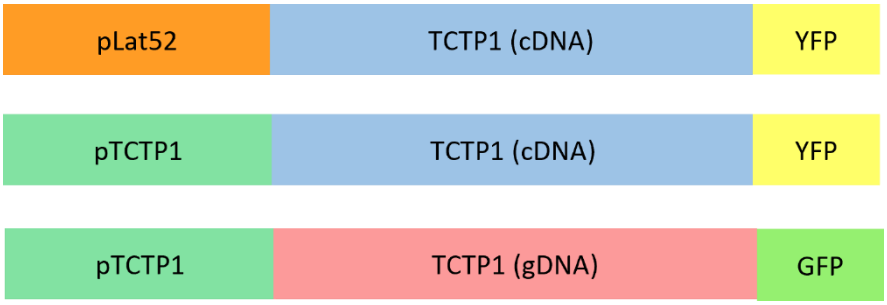

***Figure 12. Constructs created for analysis of subcellular TCTP1 localization in male gametophyte**. YFP – yellow fluorescent protein, GFP – green fluorescent protein, gDNA – genomic DNA, cDNA – complementary DNA*

TCTP1 localized in the cytoplasm of mature pollen and pollen tubes of pLat52-TCTP1-YFP transformed plants

Plants containing pLat52-TCTP1-YFP construct were selected on MS medium containing kanamycin (50 µg/mL) and were grown on Jiffy peats. The presence of the construct was verified by PCR genotyping. After bolting, mature pollen grains were observed on a Zeiss ApoTome fluorescent microscope to confirm YFP signal.

Three single insertion lines containing pLat52-TCTP-YFP transgene were selected and grown into the third generation. Flowers were collected approximately 1 week after bolting and pollen grains were observed on a fluorescent confocal microscope (Nikon Spinning Disk). In parallel, pollen germination medium was freshly prepared and pollen tubes were cultivated for microscopic observation on the same microscope.

Fluorescent signal was observed in the cytoplasm of mature pollen grains, with a slight concentration around vegetative cell nucleus (Figure 13A). Cytoplasmic fluorescent signal was also observed in growing pollen tubes. Signal concentrated in the emerging pollen tube but was later uniformly distributed in the growing pollen tube (Figure 13B, 13C).

Lat52-TCTP1-YFP construct was crossed into *tctp-1* mutant background

To verify if pLat52-TCTP1-YFP construct can complement *tctp*-1 mutant phenotype, three selected single insertion lines were crossed with *tctp-1* +/- plants. As *tctp-1* mutant allele has lower transmission through the male gametophyte but unchanged transmission through the female gametophyte, pollen

from pLat52-TCTP-YFP plants was used to pollinate emasculated *tctp-1* +/- flowers. Plants carrying the mutation were selected on MS medium supplemented with Basta herbicide and presence of the pLat52-TCTP1-YFP construct was verified by fluorescent microscopy. Preliminary analysis suggests that pLat52-TCTP1-YFP cannot rescue the *tctp*-1 phenotype. However, this analysis is incomplete due to time restrains. Seeds of fluorescence positive plants were harvested and currently, second generation is growing. In this generation, plants homozygous for the pLat52-TCTP1-YFP transgene were selected based on fluorescence and will be used to further analyze phenotypic rescue of *tctp-1 +/-* plants upon pLat52-TCTP1-YFP expression.

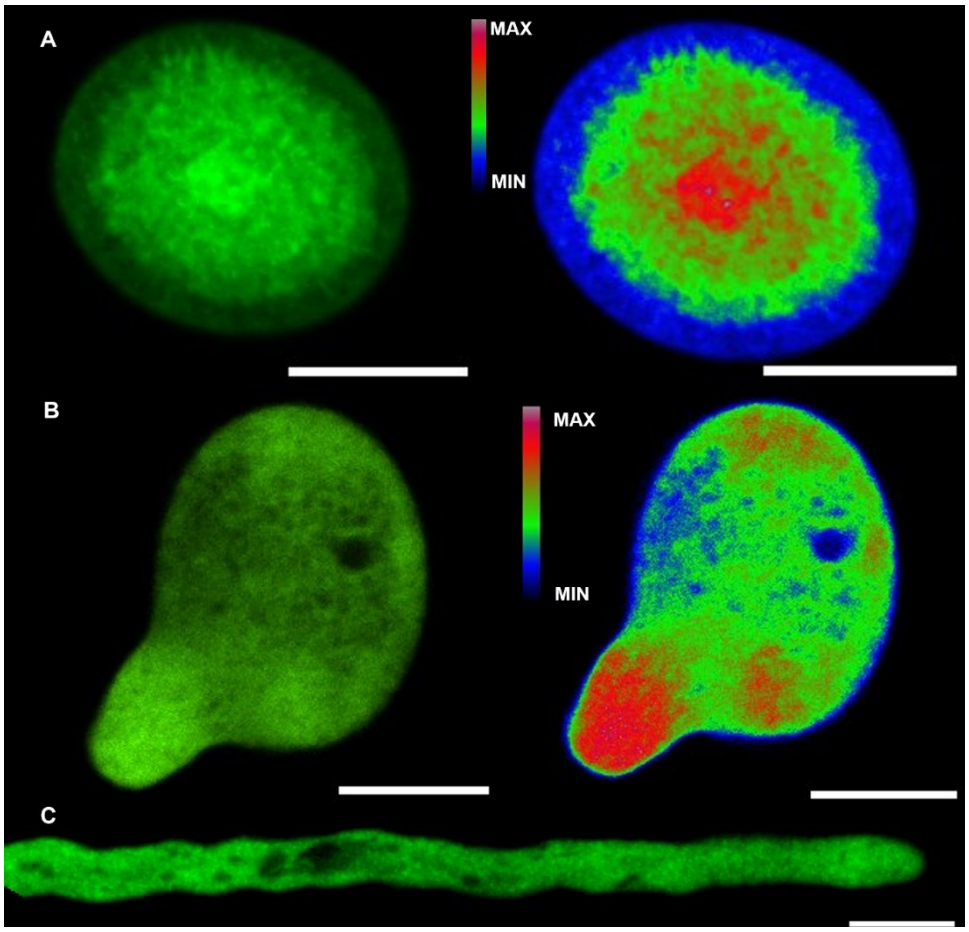

Figure 13. Subcellular localization of TCTP1-YFP under pLat52 promoter. *(A) Maximum intensity projection of mature pollen grain showed signal accumulation around vegetative nucleus. (B) Signal concentrated in the emerging pollen tube and was uniformly distributed in cytoplasm of growing*

Spliced TCTP1 coding region was not expressed by its native promoter in pollen

To verify that a native promoter can drive TCTP1 expression, 2.5 kb sequence upstream of start codon was used to generate pTCTP1-TCTP1(cDNA)-YFP construct and transformed into both Col-0 and *tctp-1* +/- plants.

20 Col-0 plants transformed with pTCTP1-TCTP1(cDNA)-YFP were selected on a medium supplemented with kanamycin and transferred on Jiffy peats. Construct presence was confirmed with by genotyping

PCR. Approximately 1 week after bolting, flowers from these plants were collected for confocal microscopy of mature pollen. However, in contrast to pLat52-TCTP-YFP construct, no fluorescent signal was observed in mature pollen grains except for pollen cell wall autofluorescence (Figure 14B). Seeds from T1 generation lines with confirmed construct presence by genotyping were harvested and plated on MS medium. 7 days after germination, seedlings were screened for fluorescent signal on a confocal fluorescent microscope. Weak fluorescent signal was observed (Figure 14A).

Similarly, *tctp-1 +/-* progeny transformed with the same construct was selected on MS medium with kanamycin and 20 plants were grown on Jiffy peats. Construct and mutant allele presence was verified by PCR genotyping. Shortly after bolting, flowers were collected for confocal microscopy. Same as Col-0 transformants, no fluorescent signal was observed except for pollen cell wall autofluorescence. Seeds from PCR-positive *tctp-1 +/-*plants were harvested and germinated on Basta selection. After transfer on Jiffy peats, DNA from 81 plants originating from three independent transgenic lines was extracted. No homozygous *tctp-1* plants could be recovered following PCR genotyping. This result suggests that the construct cannot complement pre-fertilization or the embryo lethal *tctp-1* mutant phenotype.

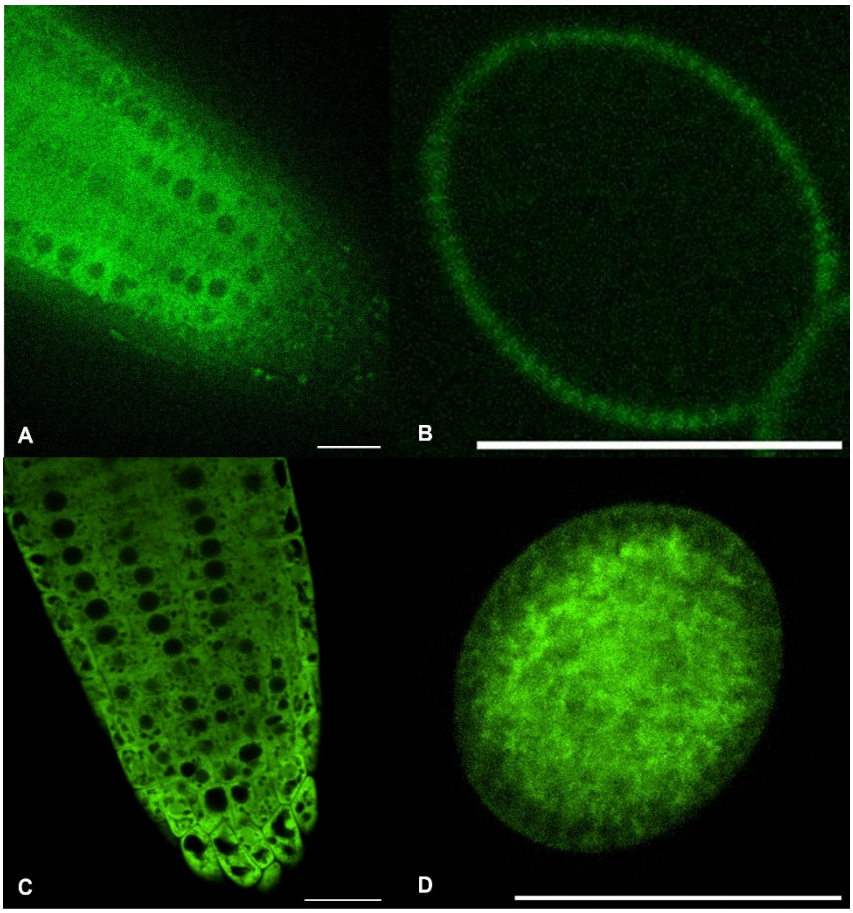

Figure 14. Subcellular localization of TCTP1-YFP/GFP under native pTCTP1 promoter*. (A) Fluorescent signal was weak in root tip and only pollen autofluorescence was observed in mature pollen (B) in lines transformed with cDNA-based TCTP1-YFP construct. In contrast, strong signal was observed in cytoplasm of root tip cells (C) and mature pollen in genomic based TCTP1-GFP construct (D). Scale bar = 20 µm.*

Non-spliced TCTP1 strongly expressed under native promoter in pollen

Intron sequence might be involved in regulation of gene expression. As my work with a TCTP1 cDNA-based construct was unsuccessful, a genomic based (unspliced TCTP1) construct including a 2.5 kb putative promoter sequence, pTCTP1-TCTP1(gDNA), was constructed. This construct was recombined with a destination vector to produce a C-terminal GFP fusion TCTP1 protein, pTCTP1-TCTP1(gDNA)-GFP. Prepared construct was transformed into Col-0 and *tctp-1 +/-* plants.

7 days after germination, a few selected resistant seedlings were used for confocal fluorescent microscopy. A strong cytoplasmic fluorescent signal was observed at the root tip (Figure 14C).

20 plants were transferred on Jiffy peats and grown further. 1 week after bolting, potential single insertion lines were selected based on counting of GFP-positive pollen grains on a standard fluorescence microscope. Work continued with lines showing 1:1 ratio of GFP-positive:GFP-negative pollen grains. Flowers from multiple such lines were collected for mature pollen confocal microscopy (Figure 14 D). In parallel, pollen tubes were germinated on a freshly prepared medium for confocal fluorescent microscopy.

A signal with similar localization as the pLat52-TCTP1-YFP was observed. Fluorescent signal appeared cytoplasmic in both mature pollen and growing pollen tubes, with a slight accumulation around the vegetative nucleus in mature pollen (Figure 15). Fiber-like structure were observed in pollen tubes.

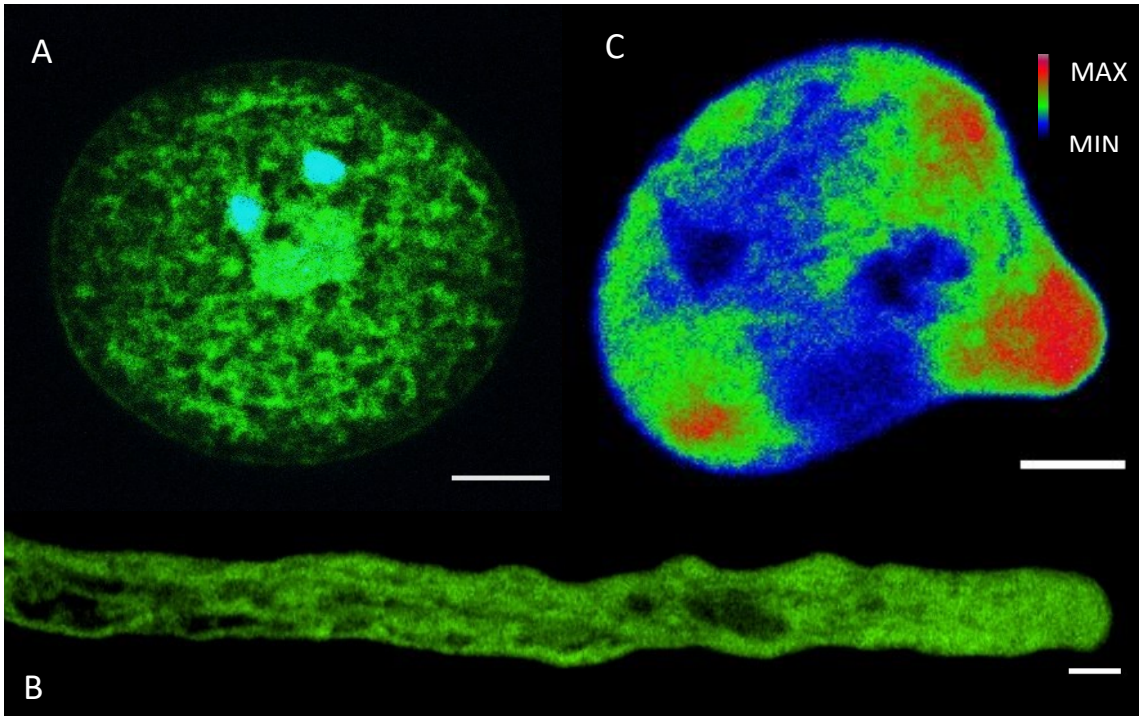

Figure 15. Subcellular localization of TCTP1 in mature pollen and pollen tube*. Slight accumulation of fluorescent signal was observed around vegetative nucleus in mature pollen stained with DAPI (A). Signal was observed in emerging pollen tube (B) and showed cytoplasmic localization in pollen tube (C) Scale bar = 10 µm.*

TCTP1-YFP/GFP fusion protein is detectable by Western blot

To confirm that observed fluorescent signal pattern is produced by a TCTP1-YFP(GFP) fusion protein, total protein was extracted from mature pollen of pLat52-TCTP1-YFP and pTCTP1-TCTP1(gDNA)-GFP transgenic lines. As a negative control, protein was extracted from mature pollen of untransformed Col-0 plants. Protein concentration was measured on NanoDrop and equal protein amount was boiled with SDS sample buffer and loaded on two SDS/PAGE gels. After gel electrophoresis, one gel was stained with CBB G250 for a total protein stain and the other one was used for Western blot. First, proteins were transferred on a cellulose membrane using wet transfer method. The membrane was blocked and incubated with primary anti-GFP antibody at 4^{o}C overnight. Following morning, primary antibody was exchanged for secondary anti-rabbit HRP-conjugated antibody for 1 hr incubation at room temperature. The membrane was washed, incubated with SuperBright solution, exposed using chemiluminescence and imaged.

A protein band with size between 55 and 70 kDa was detected with anti-GFP antibody in lanes containing protein extracts from mature pollen of all tested transgenic lines (Figure 16). No GFP signal was detected in control Col-0 pollen extract. Detected protein band corresponded to a fusion TCTP1-GFP protein in analysed samples. It had a higher apparent molecular weight than expected for TCTP1-GFP fusion protein (47 kDa). This difference could be due to a biological cause (such as post-translational modifications) or due to a partial denaturation prior to protein electrophoresis. Another surprising result was the slight difference between apparent molecular weight of Lat52-driven TCTP1-YFP CDS and the native driven TCTP1-GFP from genomic context. This could be explained by a possible alternative splicing of *TCTP1* in pollen.

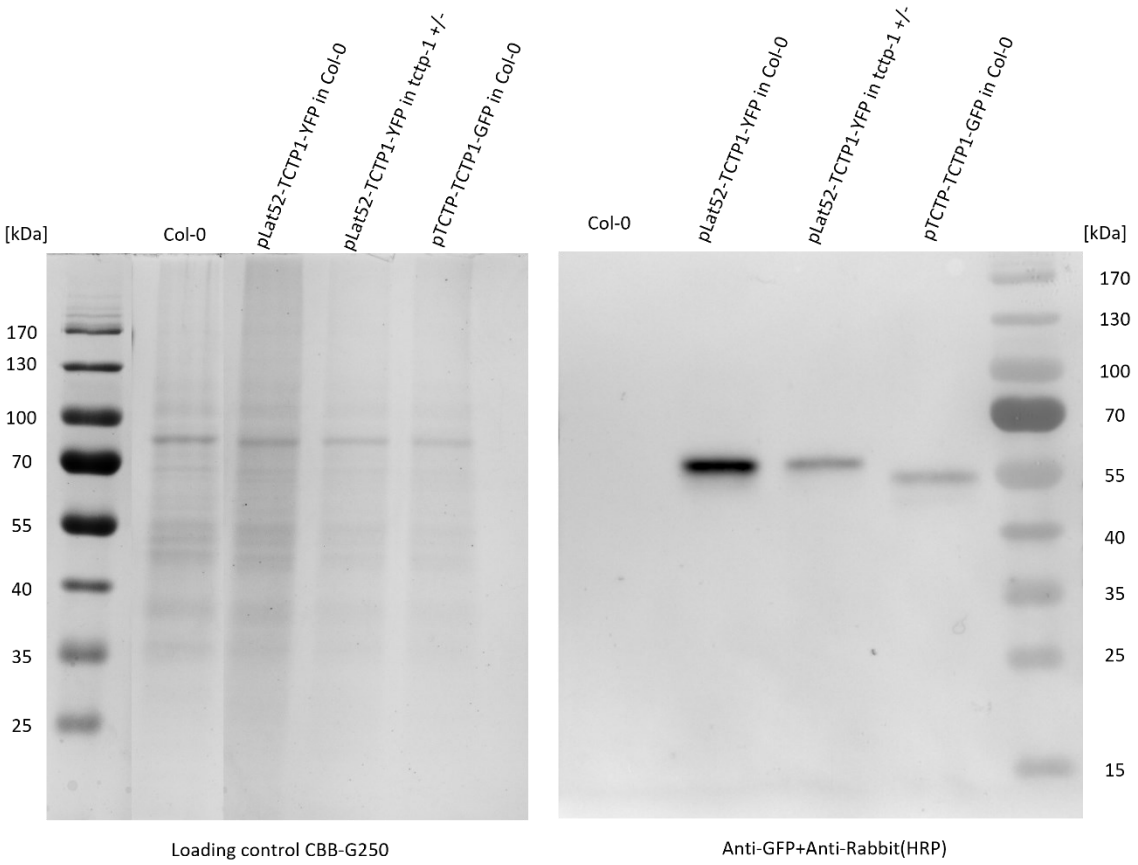

Figure 16. Western blot with anti-GFP antibody detected TCTP1-YFP/GFP fusion protein*. SDS/PAGE loading control stained with CBB-G250 and membrane after signal development. Col-0 protein extract from mature pollen was used as a negative control. Signal was detected in all three lines carrying TCTP1-YFP/GFP constructs.*

TCTP1 recombinant expression in *E. coli*

Recombinant protein expression in a heterologous bacterial system is widely used in research to obtain high amount of protein of interest. Recombinant protein can be further utilized to uncover its interacting partners, in structural studies, biochemical assays or to generate antibodies. One goal of my diploma thesis was to generate a working *E. coli* system expressing recombinant TCTP1 from *Arabidopsis thaliana*.

*At*TCTP1 heterologous protein expression in two vector systems

Based on literature, recombinant TCTP homolog from the rubber tree (*Hevea brasiliensis*) was successfully expressed in *E. coli* using pET28 vector system (Li et al., 2013). As a part of this thesis, a similar pET29 vector system was chosen for expression of TCTP1 from *Arabidopsis thaliana*. TCTP1 coding sequence was cloned in frame with an N-terminal S-tag and a C-terminal His tag. These biochemical tags have low molecular weight, which makes them less likely to interfere with protein folding and disturb its native conformation and function.

Reductive conditions in bacterial cytosol are not considered ideal for folding of proteins containing disulfide bridges. Proteins that require disulfide bonding in bacteria are secreted to the periplasm instead. As disulfide bonding might be important for TCTP1 function, TCTP1 was cloned into a pDEST-HisMBP vector containing signal for export into the periplasm. TCTP1 was tagged with an N-terminal HisMBP tag (Figure 17).

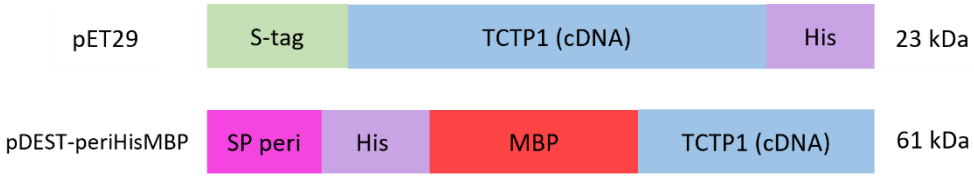

Figure 17. Constructs created for recombinant AtTCTP1 expression in E. coli *with predicted molecular weight of tagged TCTP1. His – polyhistidine rag MBP – maltose binding protein, SP peri – export signal into the periplasm*

TCTP1 was soluble at 20°C induction

Different recombinant proteins are optimally expressed under different conditions, such as temperature and time of incubation. Conditions for expression of each individual recombinant protein should thus be optimized. BL21 CodonPlus competent cells were transformed with prepared constructs. Three different combinations of temperature and incubation time were tested for TCTP1 expression using pET29-TCTP1 system: 6 h 37°C, 20 h 20°C and 20 h 37°C. Protein expression was either uninduced (as a negative control) or induced with 0.4 mM or 1 mM IPTG. Soluble protein fraction was extracted and analyzed by SDS/PAGE gel followed by CBB-G250 total protein stain (Figure 18).

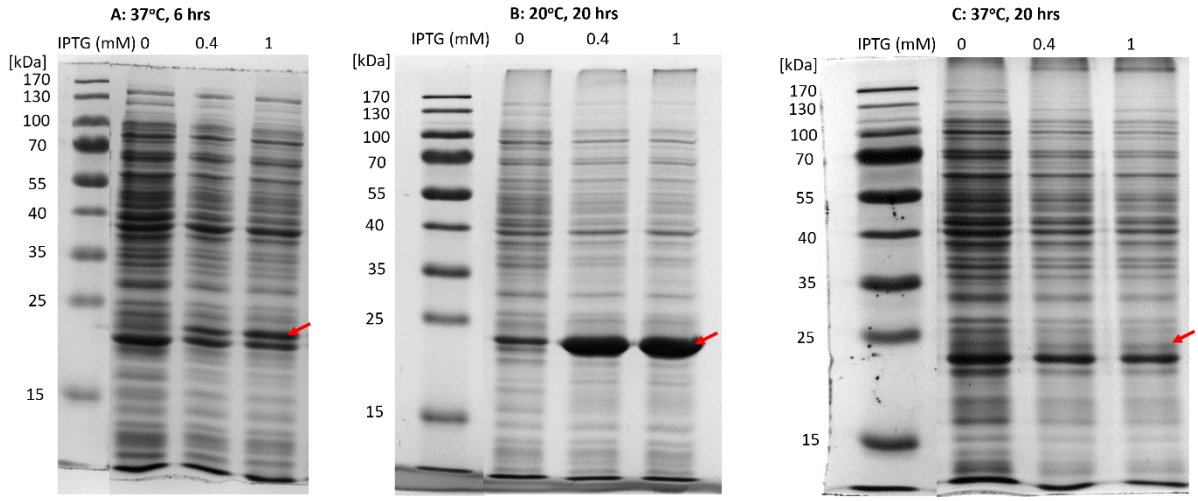

Figure 18. Optimization of expression conditions for AtTCTP1 expression in E. coli. *CBB-G250 stained SDS/PAGE gels with soluble protein extract from 3 different cultivation conditions (A – 6 hr incubation at 37°C, B - 20 hr incubation at 20°C, C - 20 hr incubation at 37°C). Protein extract from uninduced bacterial culture as a negative control. Position of TCTP1 protein band marked with a red arrow.*

A band with apparent molecular weight between 15 kDa and 25 kDa appeared stronger in the induced bacterial extract at 37°C after 6 hr incubation. The size corresponded to the predicted recombinant TCTP1 molecular weight (23 kDa). A significantly stronger band with the same size was observed at 20°C after 20 hr incubation. In contrast, no changes were observed in band pattern at 37°C after 20 hr incubation. Longer incubation at high temperature could cause insolubility of the recombinant protein. There was no observable difference in protein production when using 0.4 mM IPTG and 1 mM IPTG. For all subsequent experiments, TCTP1 expression was induced with 0.4 mM IPTG for 20 h at 20°C.

Western blot and mass spectrometry confirmed His-tagged TCTP1 expression

To verify that the observed prominent band is indeed a His-tagged recombinant protein, Western blot with primary rabbit anti-His antibody and a secondary anti-rabbit antibody conjugated with horseradish peroxidase (HRP) was performed.

Total bacterial extract from uninduced and induced culture was boiled in non-reducing SDS buffer and run on an SDS/PAGE gel. Electrophoretically separated proteins were transferred on a cellulose membrane and incubated with the antibodies. Membrane was incubated with SuperBright solution, exposed using chemiluminiscence and imaged.

A band with apparent molecular weight between 15 kDa and 25 kDa was detected in both uninduced and induced sample (Figure 19). However, the signal was much stronger in the induced sample. Expression of the recombinant protein in the uninduced culture could result from leaky expression from the T7 promoter. Another strong band with apparent molecular weight between 40 kDa and 55 kDa was also detected. According to size, it could be a TCTP1 dimer (predicted at 46 kDa).

To verify that the strong band is indeed *Arabidopsis thaliana* TCTP1, the band was cut out of the SDS/PAGE gel and sent for liquid chromatography mass spectrometry sequencing (LC-MS/MS), which was carried out as a service at the protein facility in BIOCEV, Prague. Protein sequencing confirmed the band was indeed *At*TCTP1 (Figure S1).

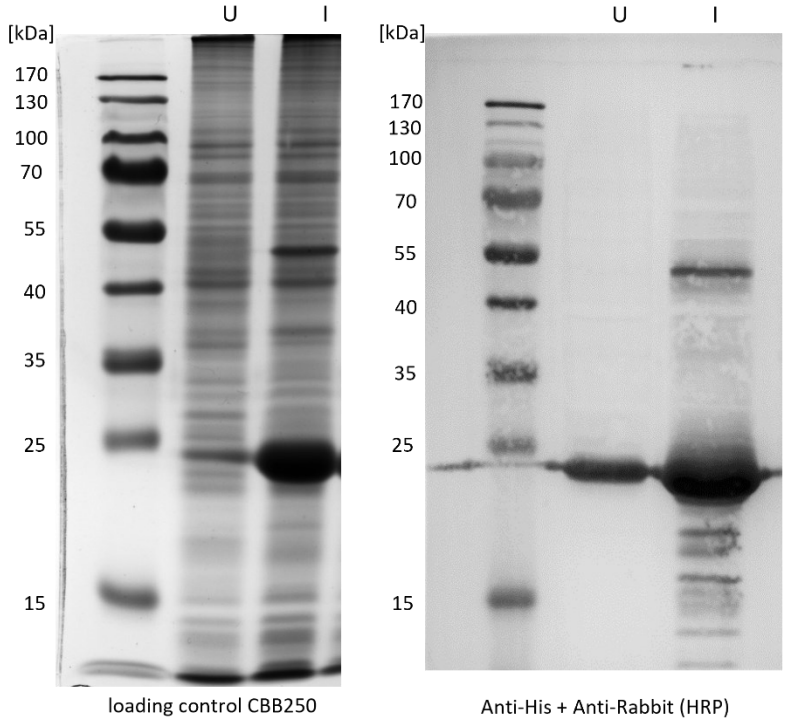

Figure 19. Western blot with anti-His primary antibody. *CBB-G250 stained SDS/PAGE loading control and blotting membrane after signal development. Signal was detected in protein extract from uninduced culture (U), suggesting leaky expression of recombinant His-tagged protein. Signal was much stronger in protein extract from induced culture (I) and both monomeric and dimeric TCTP1 bands were detected. U – uninduced sample, I – induced sample, HRP – horseradish peroxidase*

periHisMBP-TCTP1 expression showed a complex pattern in the periplasm

To test protein expression in the cloned pDEST-periHisMBP system, recombinant HisMBP-TCTP1 expression was induced at 20°C for 20 h with 0, 0.4 and 1 mM IPTG. Proteins were extracted from the periplasmic and the cytoplasmic fraction separately. An aliquot of each extract was boiled with 3x SDS sample buffer and each sample was loaded on an SDS/PAGE gel. Gel with electrophoretically separated proteins was stained with CBB-G250.

A difference between band patterns of cytoplasmic and periplasmic fraction suggested that fractionation was successful. A strong protein band with size between 55 kDa and 70 kDa was observed in induced extracts in both periplasmic and cytoplasmic fraction (Figure 20). The size corresponded to HisMBP-tagged TCTP1 (predicted 61 kDa). Another band appeared only in the periplasmic fraction between 35 kDa and 40 kDa. This result suggested a possible cleavage of HisMBP-TCTP fusion recombinant protein in the periplasm.

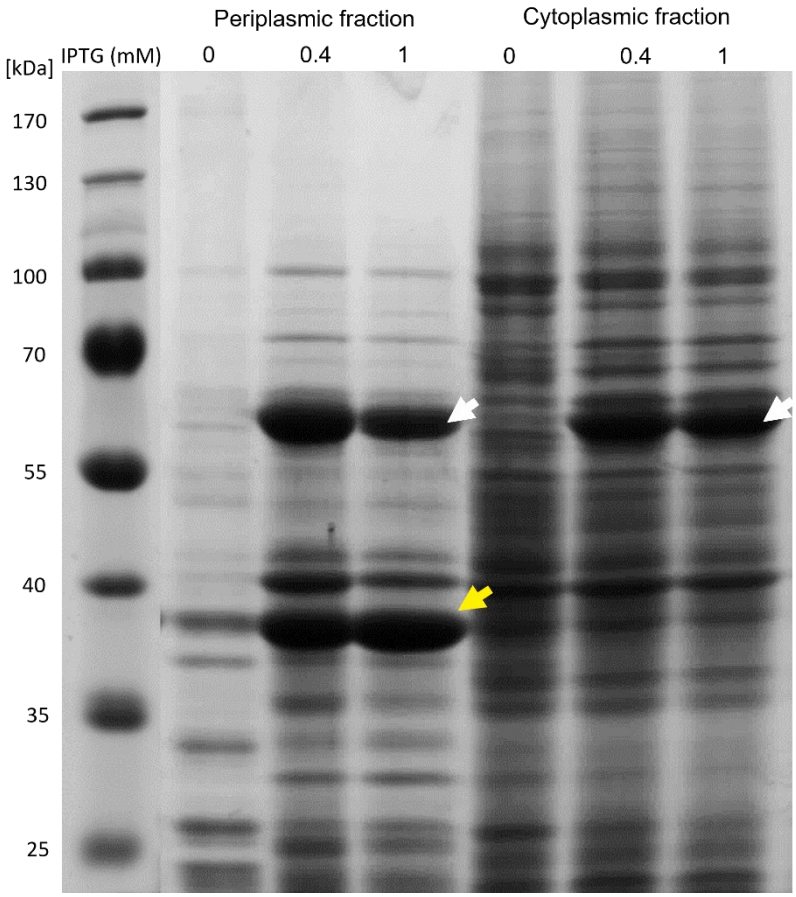

Figure 20. pDEST-periHisMBP expression in periplasmic and cytoplasmic soluble fraction. *CBB-G250 stained SDS/PAGE gel with extracts from periplasmic and cytoplasmic fraction. HisMBP-TCTP1 fusion protein marked with a white arrow and a cleaved HisMBP tag marked with a yellow arrow.*

His-tagged *At*TCTP1 was purified using immobilized metal affinity chromatography (IMAC)

For further use in *in vitro* interaction experiments or biochemical assays, it is necessary to purify an expressed recombinant protein. Since TCTP1 was tagged with a polyhistidine tag (6x Histidine) in both expression systems, nickel charged (Ni^{2+}) coupled with nitriloacetic acid based immobilized metal affinity chromatography (IMAC, Ni-NTA) purification system was tested with extracts from both expression systems.

Protein extracts were incubated with Ni-NTA agarose beads for 1 hr at 4°C. The beads were washed three times and bound proteins were released from the beads with elution buffer containing 500 mM imidazole. An aliquot of eluted protein was boiled with SDS non-reducing buffer. Samples were loaded on a polyacrylamide gel, which was stained with CBB G-250 after SDS/PAGE electrophoresis.

In pET29 system, two bands corresponding to TCTP1 monomer (between 15 and 25 kDa) and dimer (between 40 and 55 kDa) were purified (Figure 21A). In pDEST-periHisMBP system, there was a difference between the periplasmic and the cytoplasmic fraction. Two bands (size 35-40 kDa and 55-

70 kDa) were purified from the periplasmic fraction. Only the higher size band (corresponding to HisMBP-TCTP) was purified from the cytoplasm fraction. This result further supports cleavage of HisMBP tag in the periplasm.

MBP-Trap efficiently purified MBP-tagged TCTP

MBP-trap (Chromotek) was tested for purification of HisMBP-TCTP1 protein. Total protein extract from induced BL21 cells transformed with pDESTperiHisMBP-TCTP1 was incubated with agarose beads for 1 hr at 4^{o}C. Beads were washed three times, 3x SDS sample buffer was added to the beads and the mixture was boiled. High temperature released captured proteins from the beads. Eluate was loaded and run on SDS/PAGE. Polyacrylamide gel was stained with CBB G-250 and imaged.

MBP-Trap efficiently captured two protein bands with apparent molecular weights between 35-40 kDa and 55-70 kDa, which corresponded to Ni-NTA eluate from the periplasmic fraction of pDESTHisMBP-TCTP1 (Figure 21B). Therefore, both results complement the two purification systems used to purify recombinant TCTP1 expression.

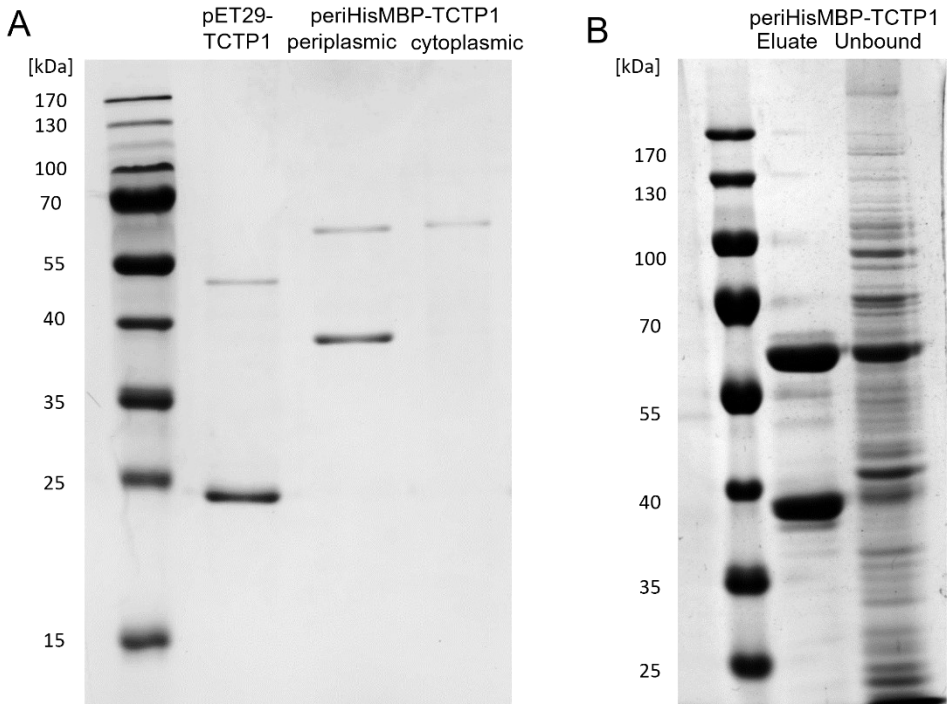

Figure 21. Purification of tagged TCTP with Ni-NTA IMAC and MBP-trap. *CBB-G250 stained SDS/PAGE gels. (A) Ni-NTA agarose beads captured both monomeric and dimeric TCTP1 band from pET29 expression system, His-MBP tagged TCTP1 from pDEST expression system in both periplasmic and cytoplasmic fraction. In addition, cleaved tag was purified from the periplasmic fraction. (B) Cleaved tag and HisMBP-TCTP1 were purified from total soluble extract of pDEST expression system.*

Recombinant TCTP1 could not be purified efficiently using S-protein agarose

S-protein agarose beads (Novagen) were tested for S-tagged TCTP1 purification. Total protein extract from induced BL21 cells transformed with pET29-TCTP1 was incubated with S-protein agarose beads for 1 hr at 4^{o}C under agitation. The beads were washed three times and bound proteins were released using two elution agents – guanidine thiocyanate and magnesium chloride. Unbound fraction, initial and final wash and eluates were boiled with 3x SDS sample buffer and loaded on a polyacrylamide gel. Gel was stained with CBB-G250 after SDS/PAGE and imaged.

Weak protein band with size corresponding to TCTP1 was purified using S-protein agarose beads. However, the intensity of the band in the eluate was comparable to washing fractions (Figure 22). This could result from low affinity of the tagged protein to the beads in tested conditions (protein did not bind to the beads) or inefficient elution (protein remained bound to the beads after incubation with elution agents). Therefore, S- protein agarose was not used in follow up experiments.

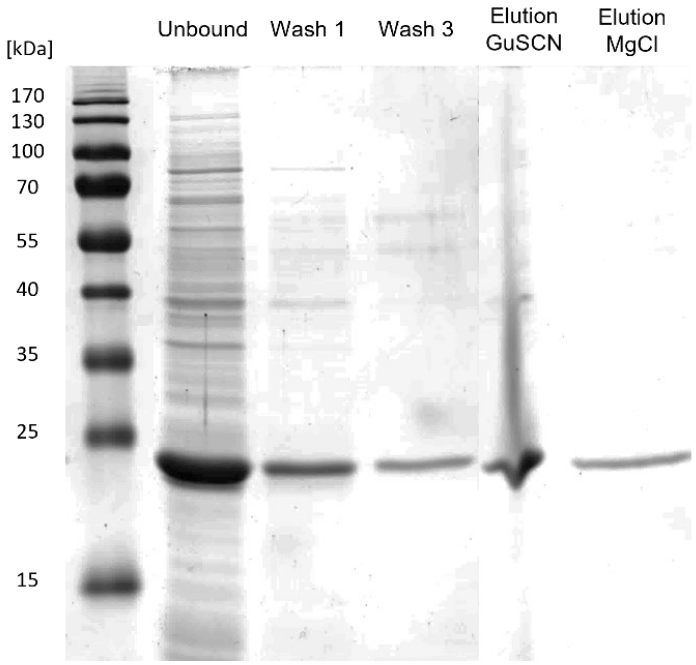

Figure 22. Purification of S- tagged TCTP with S-protein agarose. *CBB-G250 stained SDS/PAGE gel with unbound, initial washing (Wash 1), last washing (Wash 3) and eluate fractions. Two elution agents ($MgCl_2$ and GuSCN) were tested. Efficient TCTP1 purification could not be achieved using S-protein agarose beads.*

*At*TCTP1 dimerization

Human TCTP is known to dimerize via a terminal disulfide bridge. This dimerization is crucial to its function in immune response. *At*TCTP1 dimerizes with *Hs*TCTP in a bimolecular fluorescence complementation (BiFC) experiment (Brioudes et al., 2010). A goal of my thesis was to further investigate *At*TCTP1 dimerization and pinpoint critical amino acids for its dimerization, using recombinant TCTP1 expressed in *E. coli*.

MSA of eukaryotic TCTPs gave insight into possible *At*TCTP1 dimerization mechanism

The interaction of TCTP from *Homo sapiens* and *Arabidopsis thaliana* suggests that they might dimerize using a similar mechanism. TCTP sequences from different eukaryotic species were downloaded from the Uniprot database and were aligned using ClustalW (https://www.ebi.ac.uk/Tools/msa/clustalo/). Interestingly, a terminal cysteine residue (C168 in *Arabidopsis* TCTP1 and C172 in human TCTP) was conserved not only in analysed animal species, but also in green plant lineage (Figure 23A). Terminal cysteine residue was not conserved in other eukaryotic organisms, such as yeast.

*At*TCTP1 dimerizes via a cysteine disulfide bridge

To verify if recombinant *At*TCTP1 can dimerize in pET29 system, we expressed the protein as described previously. Bacterial protein extract was boiled with non-reducing SDS buffer, proteins were separated on SDS-PAGE and Western blot was performed with anti-His antibody. Apart from the monomeric 23 kDa band, a dimeric band (46 kDa) was identified (Figure 19). *At*TCTP1 in pET29 system thus appeared as a promising tool to study dimerization of TCTP1 protein.

To further verify that TCTP1 dimerization is mediated by the conserved cysteine disulfide bridge, combinations of oxidizing agent (hydrogen peroxide) and reductive agent (DTT) were applied on total protein extract. DTT as a reducing agent was expected to disrupt disulfide bridges. In contrast, hydrogen peroxide as an oxidant was expected to protect disulfide bridges from reduction. This experiment was inspired by a recent study of human TCTP dimers (Lee et al., 2020). Recombinant *At*TCTP1 was expressed, and total protein was extracted from bacterial cells. Equal amount of protein input was boiled with 3x SDS buffer, which was either non-reducing (did not contain DTT) or was reducing (contained 0.15 M DTT). Hydrogen peroxide (H_2O_2) was added to the samples in concentrations 0-400 mM prior to boiling.

Dimeric TCTP band was not observed in reducing SDS buffer with 100 mM H_2O_2. However, dimeric band was observed in reducing SDS buffer with higher concentrations of hydrogen peroxide – 200 mM and 400 mM. Dimeric band of similar intensity appeared in samples treated with non-reducing SDS buffer and all tested hydrogen peroxide concentrations (Figure 23C). This result confirmed that *At*TCTP1 dimerizes via a disulfide bridge.

Mutated C168S TCTP1 did not dimerize *in vitro*

To verify our hypothesis that terminal cysteine residue is involved in TCTP1 dimerization, a mutant variant of TCTP1 recombinant protein was created using site directed mutagenesis in a Gateway pENTR-TCTP1 vector. Terminal cysteine residue was substituted for a serine (C168S) residue. Serine is an amino acid with similar chemical properties to cysteine but cannot form disulfide bridges. pENTR-TCTP1(C168S) was used as a template to clone the mutated TCTP1 sequence into pET29 vector.

pET29-TCTP1 (C168S) mutant protein was expressed along with a wild type TCTP1 protein, total protein was extracted from bacterial cells and boiled either with non-reducing SDS buffer (without DTT) or reducing SDS buffer (containing 0.15 M DTT). Proteins were separated using SDS/PAGE electrophoresis. Dimeric band was observed in the induced sample with the wild type TCTP1 sequence but was not observed in C->S substituted mutant recombinant TCTP1 (Figure 23D). This result confirmed our hypothesis of a conserved TCTP dimerization mechanism in human and *Arabidopsis*.

Figure 23 (following page). Arabidopsis thaliana TCTP1 dimerization. *(A) Multiple sequence alignment of eukaryotic TCTPs.. (B) Homology model of AtTCTP1 dimer with a highlighted disulfide bond. (C) Recombinant TCTP1 was incubated with different concentrations of reductive DTT and oxidative hydrogen peroxide to confirm dimer formation is mediated by a disulfide bond. (D) Mutant TCTP1 C168S (labelled S168) did not form a dimer in vitro, while wild type TCTP1 (labelled C168) did. Monomeric band labelled with a blue arrow and a dimeric band with a red arrow.*

PLAKN – Plasmodium knowlesi, PLAF7 – Plasmodium falciparum, DICPU – Dictyostelium purpureum, CAEEL – Caenorhabditis elegans, HUMAN – Homo sapiens, DROME – Drosophila melanogaster, YEAST – Saccharomyces cerevisiae, CHABU – Chara braunii, MARPO – Marchantia polymorpha, PHYPA – Physcomitrium patens, SELML – Selaginella moellendorfii, MAIZE – Zea mays, ARATH – Arabidopsis thaliana, SOLTU – Solanum tuberosum, TOBAC – Nicotiana tabacum, AMBTC – Amborella trichopoda, ORYSJ – Orysa sativa (japonica), DTT-dithiotreitol

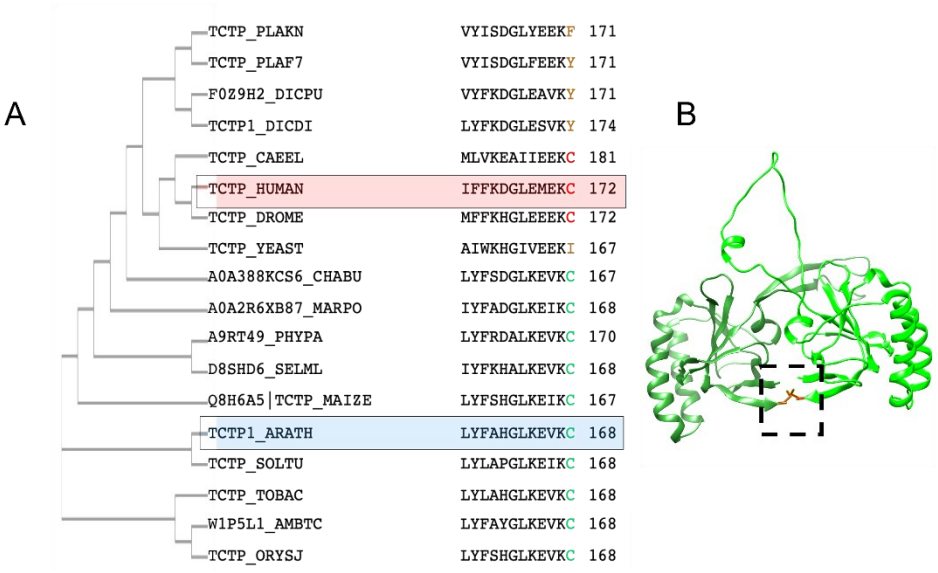
A
TCTP_PLAKN VYISDGLYEEKF 171
TCTP_PLAF7 VYISDGLFEEKY 171
F0Z9H2_DICPU VYFKDGLEAVKY 171
TCTP1_DICDI LYFKDGLESVKY 174
TCTP_CAEEL MLVKEAIIEEKC 181
TCTP_HUMAN IFFKDGLEMEKC 172
TCTP_DROME MFFKHGLEEEKC 172
TCTP_YEAST AIWKHGIVEEKI 167
A0A388KCS6_CHABU LYFSDGLKEVKC 167
A0A2R6XB87_MARPO IYFADGLKEIKC 168
A9RT49_PHYPA LYFRDALKEVKC 170
D8SHD6_SELML IYFKHALKEVKC 168
Q8H6A5|TCTP_MAIZE LYFSHGLKEIKC 167
TCTP1_ARATH LYFAHGLKEVKC 168
TCTP_SOLTU LYLAPGLKEIKC 168
TCTP_TOBAC LYLAHGLKEVKC 168
W1P5L1_AMBTC LYFAYGLKEVKC 168
TCTP_ORYSJ LYFSHGLKEVKC 168
B

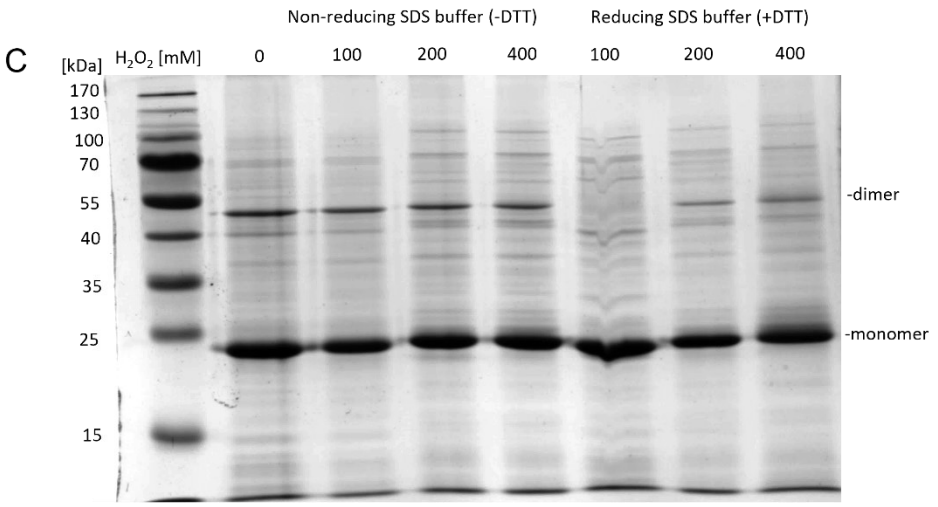
C
Non-reducing SDS buffer (-DTT)
Reducing SDS buffer (+DTT)
[kDa]
H2O2 [mM]
0
100
200
400
100
200
400
170
130
100
70
55
40
35
25
15
-dimer
-monomer

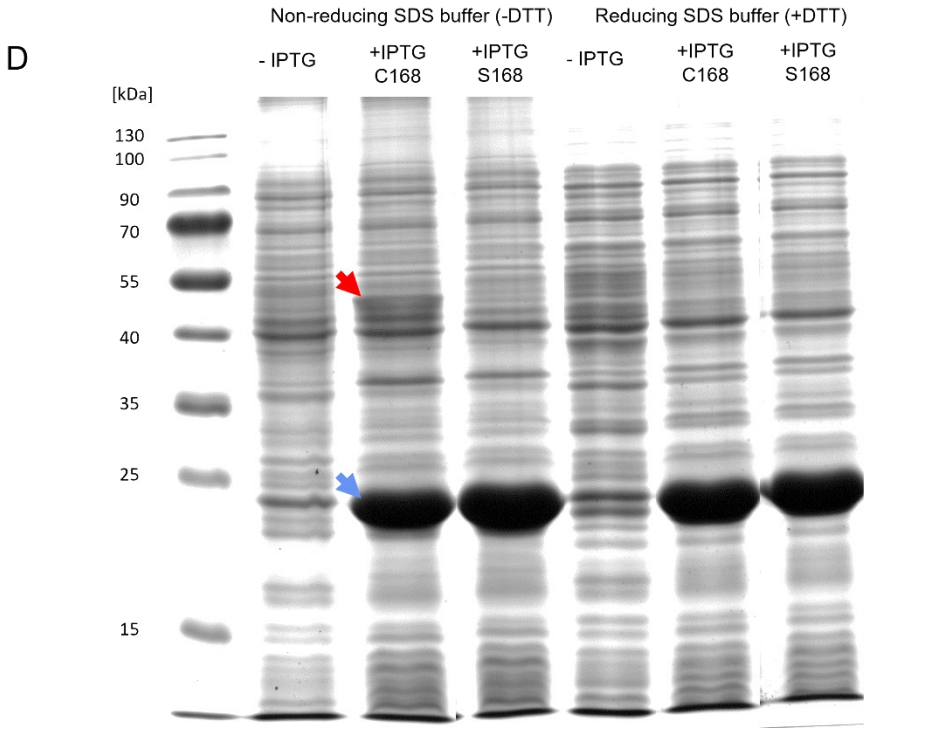
D
Non-reducing SDS buffer (-DTT)
Reducing SDS buffer (+DTT)
- IPTG
+IPTG C168
+IPTG S168
- IPTG
+IPTG C168
+IPTG S168
[kDa]
130
100
90
70
55
40
35
25
15

Recombinant expression of TCTP1 potential interacting partners

BRL2 and TTL3 were selected as possible TCTP1 interacting partners based on a co-immunoprecipitation experiment previously performed in our laboratory. My goal was to express them in *E. coli* system, purify them and perform *in vitro* pull-down experiment with TCTP1.

TTL3 and BRL2 expression in pET29 expression system

For recombinant protein expression, coding sequences of *BRL2* and *TTL3* were cloned in pET29 expression system (Figure 24). BRL2 is a transmembrane protein, which might be challenging to express in *E. coli*. To avoid expression of the hydrophobic membrane spanning segment, extracellular and intracellular kinase domains were cloned as separate fragments (Figure 24), according to Agha et al. (2017). Cloned constructs were transformed in BL21-Codon Plus(DE3) RIPL competent cells.

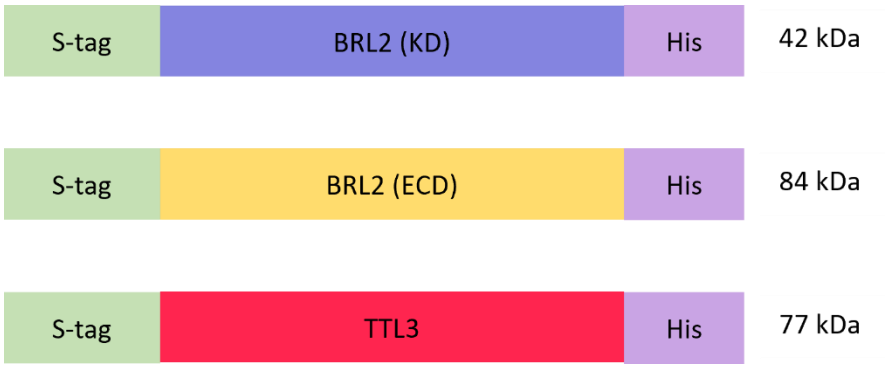

Figure 24. Constructs created for recombinant expression of potential TCTP1 interacting partners in E. coli *with predicted molecular weight of tagged BRL2 and TTL3. His – polyhistidine tag, KD – kinase domain, ECD – extracellular domain*

Induced expression of BRL2 intracellular domain and TTL3 at 20°C incubation

Conditions of BRL2 and TTL3 expression were optimized in a similar way as TCTP1. Different concentrations (0, 0.1, 0.4 and 1 mM) of IPTG were tested to induce recombinant protein expression in two different conditions – 6 hr incubation at 37° C and 20 hr incubation at 20°C.

Expression of a protein with apparent molecular weight between 40 and 55 kDa was induced by IPTG in pET29-BRL2(KD) transformed bacterial cells at 20 hr 20°C incubation (Figure 25). Molecular size of this protein band corresponded to expected 42 kDa. To verify that this band is indeed *At*BRL2 kinase domain, the band was excised from the gel and sent for LC-MS/MS protein sequencing at BIOCEV. Sequencing results confirmed it to be *At*BRL2 and identified peptides aligned only with intracellular domain sequence of BRL2 (Figure S1).

In the same conditions, expression of a protein with apparent molecular weight between 70 and 100 kDa was induced by IPTG in pET29-TTL3 transformed *E. coli* cells (Figure 25). Observed size corresponds

77 kDa expected for expressed TTL3. LC-MS/MS sequencing results indeed confirmed that expressed protein is *At*TTL3 (Figure S1).

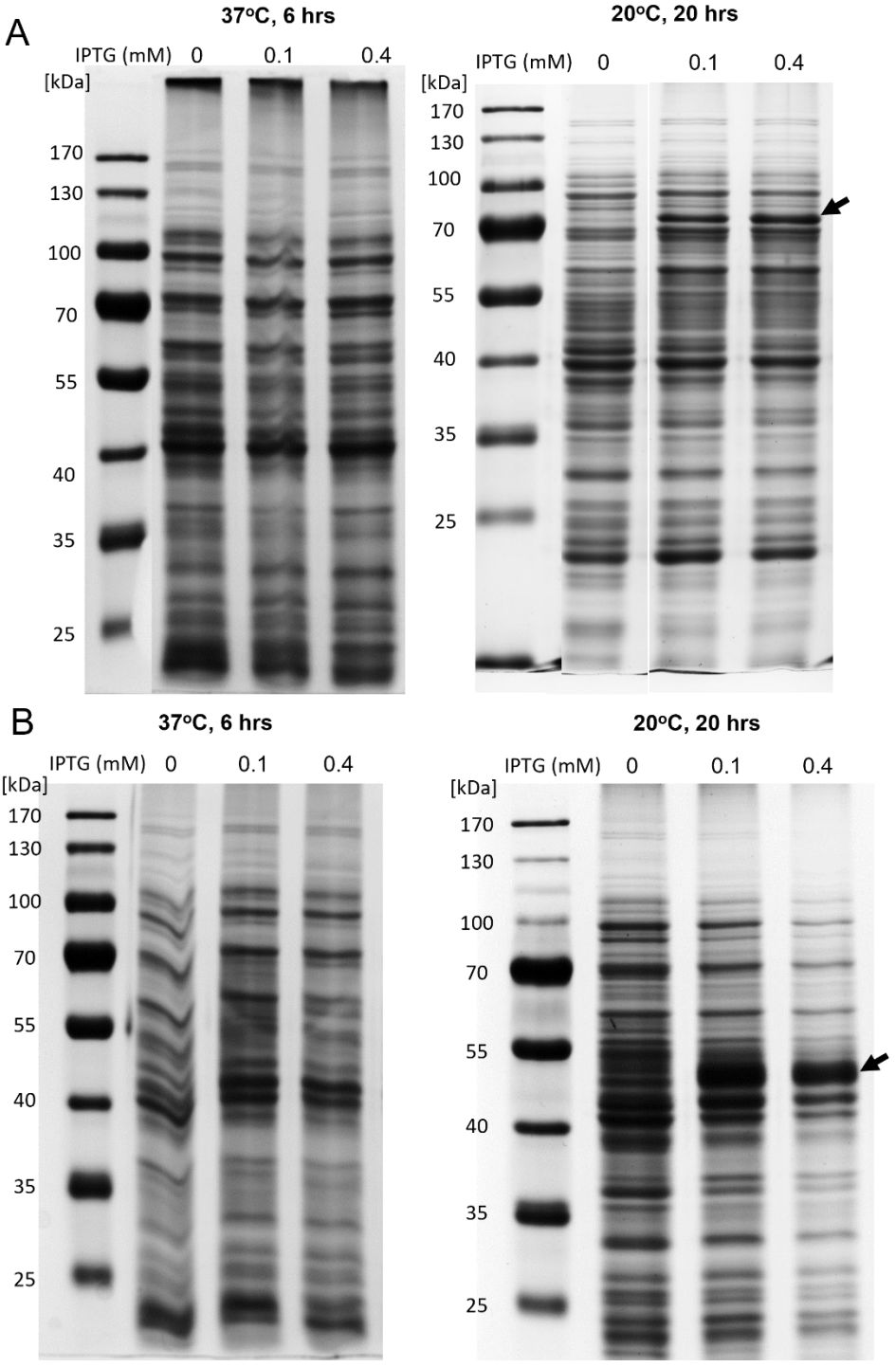

Figure 25. Optimization of recombinant TTL3 (A) and BRL2 kinase domain (B) expression*. CBB-G250 stained SDS/PAGE gels with soluble protein extract from 2 different cultivation conditions (6 hr incubation at 37°C and 20 hr incubation at 20°C). Protein extract from uninduced bacterial culture as a negative control. Position of induced protein band marked with a black arrow.*

BRL2 extracellular domain was highly expressed in the insoluble fraction

For expression of BRL2 extracellular domain, same conditions (20°C 20 hr and 37° 6 hr incubation) were tested without any evident expression in the soluble cytoplasmic fraction. Two alternative explanations were possible: either BRL2 ECD was not expressed at all, or it was expressed in the insoluble fraction. To maximize soluble protein expression, bacterial cultures were chilled on ice for 10 min after the induction and incubation temperature was lowered to 16°C. Recombinant protein expression was uninduced in the control sample and induced by 0.1 and 0.4 mM IPTG. Prior to centrifugal separation of soluble and insoluble fractions, an aliquot of total protein extract was taken. An aliquot of soluble protein extract was kept in a separate tube. Remaining solution was used for Ni-NTA purification. Total protein extract, soluble fraction and Ni-NTA eluate were boiled in a reducing SDS sample buffer and run on SDS/PAGE electrophoresis. Gels were stained in CBB-G250 and imaged.

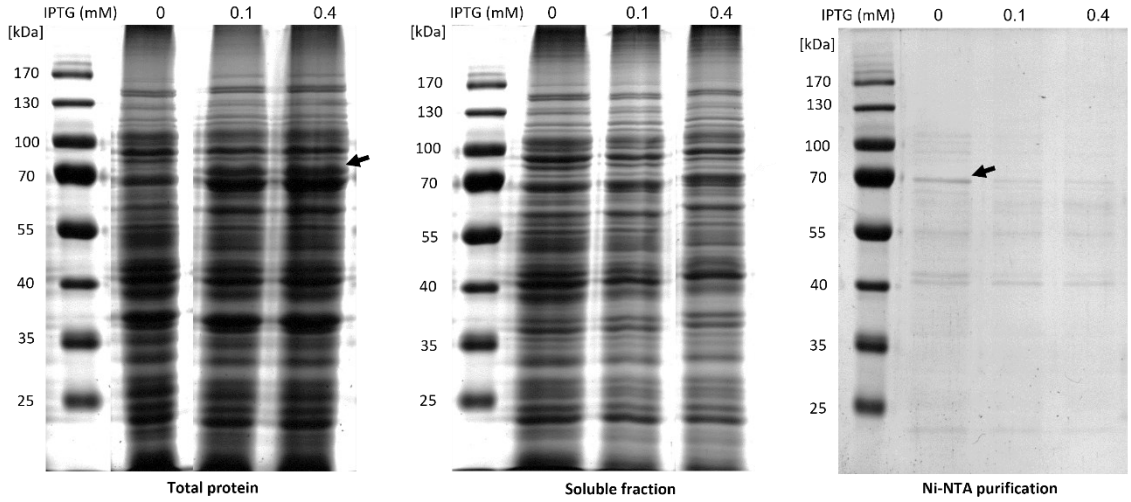

Figure 26. Recombinant BRL2 extracellular domain expression*. CBB-G250 stained SDS/PAGE gels with total protein extract, soluble protein extract and Ni-NTA purification eluate. Uninduced bacterial culture as a negative control. Position of induced protein band marked with a black arrow.*

In total protein extract containing proteins from both insoluble and soluble fraction, a strong protein band with apparent molecular weight between 70 and 100 kDa was observed in the IPTG-induced samples, which corresponds to predicted 84 kDa (Figure 26). In contrast, no difference in protein profile was observed between control and induced samples in the soluble fraction. This result suggests that produced BRL2 ECD is largely insoluble. To verify if at least some of the expressed protein is soluble, Ni-NTA purification was performed. A weak band was observed on a gel with eluate between 70 and 100 kDa. Interestingly, this band was stronger in the uninduced control than in induced samples. This band was cut out of the gel with a sterile scalpel and sent for sequencing to BIOCEV. Mass spectrometry confirmed it to be *At*BRL2.

Both TTL3 and BRL2 were purified by Ni-NTA for downstream experiments

For further use in in vitro interaction experiments, recombinant proteins must be purified. Purification by Ni-NTA agarose was tested in the same way as described for recombinant TCTP1. It was possible to purify both BRL2 intracellular domain and TTL3. However, some nonspecific bands appeared in TTL3 eluate, which could be potentially prevented by larger number of washes.

Along with recombinant TCTP1, BRL2 and TTL3 were planned to be used for in vitro interaction experiment. The experiment was planned as follows: HisMBP-tagged TCTP1, HisMBP control, BRL2-His and TTL3-His would be purified with Ni-NTA matrix. Using dialysis technique, elution buffer containing imidazole would be exchanged for a Tris-based buffer without imidazole. HisMBP-TCTP1 would then be incubated together with BRL2-His and TTL3-His. As a negative control, HisMBP tag only would be incubated with BRL2-His and TTL3-His. MBP-Trap matrix would be employed to purify protein complexes.

As can be seen in Figure 27, more-or-less pure recombinant proteins for this experiment could be obtained. However, due to lack of time, planned in vitro pull-down experiments were initiated but could not be fully completed to be included into my thesis. At the beginning of my diploma project, methods for bacterial protein expression were not yet established in the Laboratory of Pollen Biology.

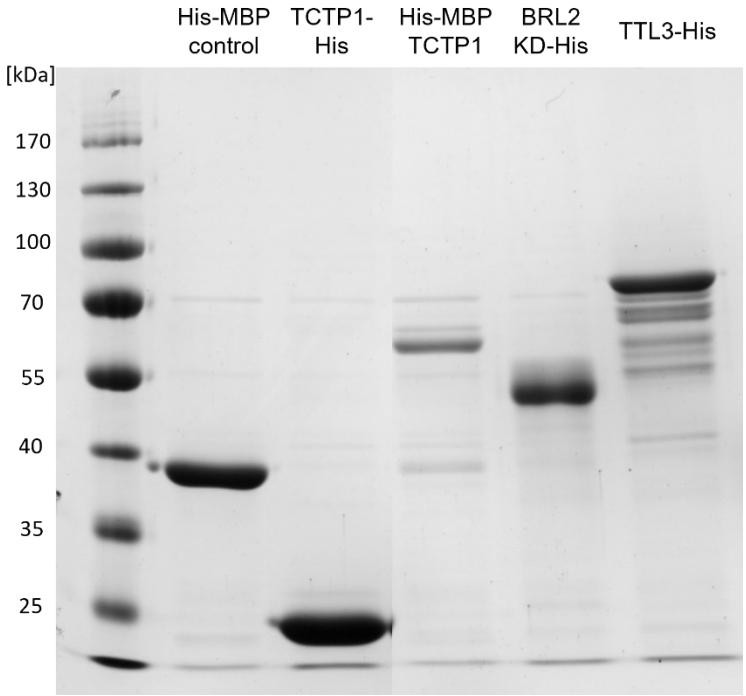

Figure 27. Ni-NTA purification of recombinant proteins for in vitro pull-down experiment*. CBB-G250 stained SDS/PAGE gels with Ni-NTA purification eluate of proteins intended to be further used in in vitro interaction experiments*

Discussion

In this thesis, TCTP1 homolog in model *Arabidopsis thaliana* was studied. Knowledge about TCTP in plants is rather scarce in comparison to animal model organisms. In this thesis, TCTP1 homolog in model organism *Arabidopsis thaliana* was studied. This work mainly focused on TCTP1 role in male gametophyte development, its putative interacting proteins and its potential homodimerization. T-DNA insertion line *tctp-1* was characterized with a focus on pollen tube growth and pollen tube targeting deficiency. To analyze TCTP1 expression and subcellular localization in mature pollen and pollen tubes, gDNA and cDNA-based constructs driven by 2.5 kb native promoter or pollen-specific Lat52 were cloned and transformed in *A. thaliana* (pTCTP1-TCTP1(gDNA)-GFP, pTCTP1-TCTP1(cDNA)-YFP and pLat52-TCTP1(cDNA)-YFP). Recombinant TCTP1 was produced in heterologous *E. coli* system and utilized in study of TCTP1 dimerization. Finally, potential interacting partners were expressed in *E. coli* system for future interaction experiments.

Mutant alleles are an important tool in plant biology. Phenotypic differences in mutant plants in comparison to wild type plants can provide a valuable insight into gene function. Characterization of *tctp-1* line was initiated in already published studies (Berkowitz et al., 2008; Brioudes et al., 2010; Hafidh et al., 2016b). As a part of this thesis, *tctp-1* mutant allele transmission was analyzed. While *tctp-1* allele transmission through female gametophyte was unaffected, a significant decrease in *tctp-1* transmission was observed through male gametophyte, confirming previously published results (Berkowitz et al., 2008; Hafidh et al., 2016b). This study revealed a yet undocumented difference in *tctp-1* transmission through the male gametophyte between apical and basal half of the silique. Analogous experiment pointed to an impaired pollen tube growth in *tip1* mutant (Schiefelbein et al., 1993). Decreased mutant allele transmission could also be caused by defective pollen tube targeting, like in *eru* mutant (Schoenaers et al., 2017). Pollen tube guidance was reported to be disturbed in *tctp-1* pollen previously (Hafidh et al., 2016b). In this work, ovule targeting by mutant pollen tubes was indeed decreased. Differences in frequencies of mutant pollen tubes arrest prior to fertilization or ovules targeted by multiple pollen tubes were not observed between *ms1-1* pistils pollinated by *tctp-1 +/-* pollen and control. However, interpretation of these results is not straightforward. As mutant pollen tubes grow slower and are outcompeted by wild type pollen tubes, defective targeting events might be too rare to detect with this experimental setup. It could be useful to create a *tctp-1 -/-* line complemented with a construct driven by a sporophytic promoter (such as 35S) and observe pollen tube growth and targeting. 35S promoter activity is assumed to be low or absent in the male gametophyte. Brioudes et al. (2010) did not observe any phenotypic defects in the male gametophyte and attributed previously published results to different cultivation conditions. Instead, embryo lethality of *tctp-1* homozygous individuals was reported (Brioudes et al., 2010). Seeds segregated in

tctp-1 +/- siliques in 3:1 ratio (green: white) (Brioudes et al., 2010). White seeds with delayed embryo development were observed in *tctp-1 +/-* siliques in previous study in our laboratory and in this thesis (Hafidh et al., 2016b). Their nonuniform distribution within *tctp-1 +/-* siliques uncovered in this work further supported TCTP1 involvement in pollen tube growth. To gather more evidence for this hypothesis, performed experiments could be repeated in another *tctp* mutant allele(s) in future. A different T-DNA insertion line (such as *tctp-2* used in Brioudes et al., 2010) or mutant lines created by CRISPR/Cas9 mediated mutagenesis (currently under characterization in our laboratory).

Mutant complementation is a powerful method that can confirm a proposed gene function. Embryo lethal phenotype was previously complemented in both *tctp-1* and *tctp-2* mutant lines with GFP-tagged TCTP1 construct under both native and sporophytic 35S promoter (Brioudes et al., 2010). Both N- and C-terminal GFP-tagged TCTP1 constructs rescued *tctp -/-* homozygous individuals. Functionality of C-terminal GFP-tagged TCTP1 was independently confirmed in a study of tunicamycin-induced programmed cell death (Hoepflinger et al., 2013). In this work, C-terminal GFP/YFP constructs under both native promoter and pollen-specific Lat52-promoter were cloned. cDNA based pTCTP1-TCTP1-YFP construct did not rescue embryo lethal phenotype. This could be explained by low expression of this construct. Due to lack of time, ability of remaining constructs to rescue phenotypic differences in *tctp-1* mutant line was not assessed. However, we can at least speculate about limitations of this experiment. C-terminal GFP tag could interfere with TCTP1 dimerization. Little is known about its importance in plants. In human, TCTP1 dimerization is crucial for its extracellular function in immune response (Kim et al., 2009). TCTP was identified in tobacco pollen tube secretome as a highly secreted protein (Hafidh et al., 2016b). Unpublished data in *Arabidopsis thaliana* pollen tubes from our laboratory indicate that TCTP1 is a secreted protein. As an alternative, N-terminal GFP-tagged TCTP1 construct could be cloned and transformed into plants for complementation analysis.

Available RNA-seq data show high *At*TCTP1 expression in different developmental stages. RT-qPCR confirmed *TCTP1* expression in all analyzed tissues (Berkowitz et al., 2008). 300 bp *TCTP1* promoter showed a constitutive transcriptional activity, but longer promoter fragments initiated transcription in a tissue-specific manner (Han et al., 2015). In this work, weak fluorescent signal was observed in roots and no fluorescent signal was observed in mature pollen of *A. thaliana* transformed with a cDNA based TCTP1-GFP construct driven by a 2.5 kb promoter. Multiple studies in plants point to *TCTP1* transcriptional regulation. For instance, *TCTP1* expression was upregulated by biotic and abiotic stress e. g. flooding stress (Chen et al., 2014), salt stress (Deng et al., 2016; Meng et al., 2017), low temperature (Deng et al., 2016) and high temperature stress (Meng et al., 2017). Apart from transcriptional regulation, gene expression can be regulated at post-transcriptional level as well. Post-transcriptional regulation is associated with *TCTP* since its discovery in mouse model (Yenofsky et al.,

1983). Previously published results indicated similar regulation mechanisms in plants. Brioudes et al. (2010) observed a different protein expression pattern in genomic GFP-tagged TCTP1 lines containing 5´ and 3´untranslated regions and in YFP-tagged TCTP1 lines lacking these elements. 5´ UTR and 3´ UTR contain RNA motifs known to regulate mRNA translation. In this study, a difference in lines transformed with a gDNA-based TCTP1-GFP and a cDNA-based TCTP-YFP was observed. Expression of both fusion proteins was driven by 2.5 kb native *TCTP1* promoter and both constructs contained 5´UTR and lacked 3´UTR. These results pointed to an importance of introns in regulation of gene expression. Intron-mediated enhancement of gene expression has been known for at least 35 years in plants (Callis et al., 1987). A computational tool of intron mediated enhancement IMEter predicted first *TCTP1* intron to be very likely enhancing *TCTP1* gene expression.

Protein subcellular localization can give an insight into its function and possible interacting partners. In this work, subcellular localization was analyzed in the roots, in mature pollen and in growing pollen tubes. In all three cell types, fluorescent signal was localized in the cytoplasm and no signal was observed in the nucleus. Presence of TCTP1-GFP fusion protein was confirmed by Western blot with anti-GFP antibodies. *At*TCTP1 subcellular localization was previously examined in a different system. Similarly, fluorescent signal was observed in the cytoplasm of epidermal cells in stable p35S-*At*TCTP1-GFP lines (Hoepflinger et al., 2013). TCTP subcellular localization has also been analyzed in other TCTP species. GFP-tagged cucumber CsTCTP1 and CsTCTP2 localized exclusively in the cytoplasm of *N. benthamiana* leaves and *A. thaliana* protoplasts (Meng et al., 2018). In contrast, tobacco *Nt*TCTP-GFP localized in the nucleus and colocalized with ER, Golgi vesicle, and exosome markers in *Nt*TCTP-GFP transformed tobacco epidermal cells (Hafidh et al., 2016b). Nuclear and ER localization of tobacco TCTP was documented in another study (Tao et al., 2015). Subcellular localization of TCTP might be dynamic and change in response to different stimuli. GFP-tagged tomato *Sl*TCTP homolog transformed into *Nicotiana benthamiana* epidermal cells localized to both cytoplasm and nucleus. However, its localization is exclusively cytosolic when tobacco plant is infected by Pepper yellow mosaic virus (Bruckner et al., 2017). TCTP subcellular localization was reported to change in different cell cycle phases in animal cell lines (Gachet et al., 1999). Protein-protein interactions might have an impact on subcellular localization and function. In tobacco, *Nt*TCTP binds to ethylene receptor NTHK1 localized in the ER (Tao et al., 2015). A post-translational modification sumoylation plays a role in nuclear transport (Munirathinam and Ramaswamy, 2012) of human TCTP. To my knowledge, this study is the first report of TCTP1 subcellular localization in pollen. An accumulation of fluorescent signal was observed around vegetative nucleus in mature pollen. In pollen tubes, fluorescent signal was cytoplasmic and appeared to form a filamentous structure. Actin is known to form filamentous structures in pollen tubes. TCTP colocalization with actin was previously documented in animal cell

lines (Bazile et al., 2009). However, TCTP has not yet been associated with actin in plants. It could be interesting to analyze a potential colocalization of TCTP with actin and other organellar markers in mature pollen and pollen tubes.

Based on transcriptomic and proteomic data, *TCTP1* expression is highly upregulated in pollen. TCTP1 protein was identified in the first published pollen proteome (Holmes-Davis et al., 2005). In this work, strong fluorescent signal was observed in mature pollen and growing pollen tubes of *A. thaliana* transformed with GFP-tagged TCTP1 under the control of native promoter. Mutant characterization results indicated a possible TCTP1 role in pollen tube growth. Interestingly, tip growth was impaired in root hairs of *TCTP1*-silenced *A. thaliana* lines (Berkowitz et al., 2008). In animals, TCTP has both intracellular and extracellular functions. According to BioGrid database, more than 250 proteins were found to interact with human TCTP using both high-throughput and low-throughput methods. Some TCTP functions and interactors are evolutionary conserved. TCTP1 is involved in regulation of translation elongation in human. It interacts with elongation factors eEF1A and eEF1Bβ (Cans et al., 2003; Langdon et al., 2004). Its interaction with eEF1Bβ was reported to be evolutionary conserved (Wu et al., 2015). Protein synthesis is critical for pollen tube growth and application of translation inhibitors leads to PT growth inhibition (Čapková-Balatková et al., 1980). *EF1Bβ* mutant in *A. thaliana* has a dwarf phenotype reminiscent of *tctp-1 -/-* nutrient rescued individuals (Hossain et al., 2012). However, no defects in pollen tube growth were reported. *EF1Bβ* has medium level expression in pollen according to Genevestigator. In our laboratory, interaction of TCTP1 with translation initiation factor eIF3i was reported. Silencing of *eIF3i* expression led to dwarf seedling phenotype and reduced fertility (Jiang and Clouse, 2001). TCTP in various organisms including *A. thaliana* binds calcium (Yong-Min et al., 2012). Calcium ion dynamics is critical for pollen tube germination and growth (summarized in Yang et al., 2021). As both high-affinity and low-affinity calcium binding sites are present on TCTP, it could influence calcium homeostasis in PT. Another possible function of TCTP in a pollen tube could be related to its cytoskeleton binding. There are reports of TCTP interaction with both actin filaments and microtubules in literature (Gachet et al., 1999; Bazile et al., 2009). Cytoskeleton organization is critical for pollen tube growth (summarized in Fu, 2015). Bazile et al. (2009) suggested TCTP to mediate the interaction between microtubule and microfilament cytoskeletal system within a cell. Apart from its intracellular functions, TCTP1 could have an extracellular function in pollen tube growth and/or guidance. Even though it does not contain a signal peptide, it was identified in secretome of tobacco pollen tubes (Hafidh et al., 2016b). Human TCTP is secreted via a non-classical secretion pathway (Amzallag et al., 2004). Secreted protein could hypothetically act in an autocrine manner or mediate male-female crosstalk.

TCTP1 pollen tube interactome could broaden our knowledge about its function in pollen tube growth and guidance. Potential TCTP1 interacting partners involved in male-female communication were identified in a co-immunoprecipitation experiment in our laboratory (unpublished results). BRL2 and TTL3 were selected for interaction verification by bimolecular fluorescence complementation and *in vitro* interaction experiments. As a part of this thesis, TCTP1, BRL2 and TTL3 were successfully expressed in bacteria. Recombinant TCTPs from multiple plant species including *Arabidopsis thaliana* were successfully produced in *E. coli* before (Brioudes et al., 2010; Li et al., 2013; Meng et al., 2017). A previous unsuccessful attempt to express TTL3 in *E. coli* was reported (Amorim-Silva et al., 2019). In this work, TTL3 was fused with a His tag, in comparison to GST tag used in Amorim-Silva et al. (2019). Use of a different tag could have an impact on protein expression. Heterologous expression of kinase domain of BRL2 was reported in literature (Clay and Nelson, 2002). This thesis is the first report of a successful expression of BRL2 extracellular domain. In this case, the recombinant protein accumulated mostly in the insoluble fraction and only leaky expression from T7 promoter led to soluble expression, which corroborates previous results with LRR (leucine rich repeat) domain of LRRK2 kinase (Vancraenenbroeck et al., 2012). Even though *in vitro* interaction experiment could not be performed due to lack of time, I would like to point out some of its limitations. In vitro pull-down will detect only direct interaction of two proteins. However, their interaction could potentially be indirect in a protein complex. Protein-protein interaction could be dependent on ligand binding and post-translational modifications. Upon activation, BRL2 kinase dimerizes and undergoes autophosphorylation. When expressed in *E. coli* system, BRL2 kinase domain possessed kinase activity (Clay and Nelson, 2002). Binding of its interacting partners depended on its phosphorylation (Ceserani et al., 2009). Studies of animal TCTP pointed to a role of TCTP phosphorylation in interaction with the mitotic spindle (Yarm., 2002). Calcium binding in *A. thaliana* affected TCTP1 microtubule binding (Yong-Min et al., 2012). If the interaction experiments indeed confirm an interaction of TCTP1 with BRL2 and/or TTL3, further experiments are necessary to explain its importance of TCTP1 in context of plant reproduction. Mutant characterization of *brl2* and *ttl3* mutants did not report any defects in plant reproduction so far.

TCTP in mammals forms homodimers (Yoon et al., 2000). Its self-association is crucial for its function in immune response (Kim et al., 2009). Interestingly, *At*TCTP1 dimerized with *Hs*TCTP in a bimolecular fluorescence complementation experiment (Brioudes et al., 2010). The mechanism of *Hs*TCTP dimerization was elucidated and a its structure was experimentally determined (Doré et al., 2018). A disulfide bridge is formed between terminal cysteine residues (C172 in *Hs*TCTP). When primary TCTP sequences from different eukaryotic species were aligned, we found out that terminal cysteine residue was conserved not only in animal but also in green plant lineage. This led us to formulate a hypothesis that *At*TCTP1 homodimerizes in a similar mechanism as *Hs*TCTP. We indeed confirmed terminal

cysteine residue was important in *At*TCTP1 dimerization. Recombinant *At*TCTP1 expressed in *E. coli* homodimerized in pET29 expression system but did not dimerize in pDEST-periHisMBP system. MBP-tag was attached to the N-terminus of TCTP1. Based on the homology model, N and C termini of TCTP protein are very close to each other. A possible explanation could be that N-terminal MBP tag sterically hindered dimer formation of HisMBP-tagged TCTP1. In this work, we confirmed that *At*TCTP1 can form dimers in *in vitro* conditions. we can only speculate about function of TCTP1 dimerization in plants. Disulfide bond formation can be important for native protein folding and function. For example, intramolecular disulfide bonds in RALF4 peptide are critical for binding to LRX receptor kinase in pollen tube plasma membrane and regulation of cell wall integrity pathway (Moussu et al., 2020). Even though exceptions were found, disulfide bond formation in plant cells is mainly catalyzed by protein disulfide isomerases in the endoplasmic reticulum (Marshall et al., 2010). Even though TCTP lacks a signal peptide in its primary sequence, tobacco *Nt*TCTP homolog colocalized with ER and Golgi markers. GFP-tagged TCTP1 lines generated in this work could be used for analysis of colocalization with organellar markers in *A. thaliana* pollen and pollen tubes. Similar to RALF peptide, TCTP dimer formation could be important for its extracellular function. In human, TCTP dimer is functional in immune response when it is secreted from the cell (Kim et al., 2009). In future, detection of TCTP1 dimers in protein extracts from plant tissue could be attempted. There is no commercially available antibody against *A. thaliana* TCTP1 yet. Recombinant TCTP1 created in this thesis could be used to raise the antibody or alternatively, FLAG-tagged lines could be generated for this purpose.

Conclusions

Goals of this thesis were fulfilled, with some only partially. More critically, valuable material was created and most likely will contribute to a future publication in an impacted journal (*A. thaliana* stable *TCTP1* transgenic lines and functional *E. coli* recombinant protein expression system).

Goal 1: Phenotypic characterization of tctp-1 T-DNA insertion line with focus on pollen tube growth and guidance

Characterization of *tctp-1* SAIL line pointed to TCTP1 role in pollen tube growth and guidance. Obtained results suggested an additional approach will be necessary to achieve a conclusive assessment of the pollen tube targeting phenotype.

Goal 2: Analysis of subcellular localization of TCTP1 in Arabidopsis thaliana mature pollen and pollen tubes

GFP/YFP-tagged TCTP1 localized in the cytoplasm of mature pollen and pollen tube. Signal accumulated around vegetative nucleus in mature pollen. Experiments pointed to a yet unreported influence of the intron sequence in the regulation of *TCTP1* expression in gametophyte and sporophyte.

Goal 3: Optimization of recombinant *At*TCTP1 expression in *E. coli* and its purification

*At*TCTP1 was produced in two expression system (pET29 and pDEST-periHisMBP) and cultivation conditions were optimized. Tagged protein was successfully purified with Ni-NTA IMAC and MBP-Trap.

Goal 4: Verification of *At*TCTP1 dimerization *in vitro*

*At*TCTP1 expressed in *E. coli* homodimerized *in vitro* via a disulfide bond. Site-directed mutagenesis of terminal cysteine (C168) residue confirmed it is important for TCTP1 dimerization in *Arabidopsis thaliana*, similar mechanism as in animals.

Goal 5: Recombinant expression of selected potential TCTP1 interacting partners BRL2 and TTL3 and in vitro pull-down experiment

BRL2 intracellular domain, BRL2 extracellular domain and TTL3 were expressed in *E. coli* expression system. Pull-down experiment was not performed due to time restraint.

Conferences

This work was presented as a poster at 26th ICSPR (International Conference on Sexual Plant Reproduction) in June 2022 in Prague, Czech Republic.

References

Agha, M. A., D. Lightfoot, and A. J. Afzal. 2017. Expression of Plant Receptor Kinases in E. coli. *In* R. B. Aalen [ed.], Plant Receptor Kinases: Methods and Protocols, 3–20. Springer New York, New York, NY.

Amorim-Silva, V., Á. García-Moreno, A. G. Castillo, N. Lakhssassi, A. Esteban del Valle, J. Pérez-Sancho, Y. Li, et al. 2019. TTL Proteins Scaffold Brassinosteroid Signaling Components at the Plasma Membrane to Optimize Signal Transduction in Arabidopsis. *The Plant Cell* 31: 1807–1828.

Amson, R., S. Pece, A. Lespagnol, R. Vyas, G. Mazzarol, D. Tosoni, I. Colaluca, et al. 2012. Reciprocal repression between P53 and TCTP. *Nature Medicine* 18: 91–99.

Amzallag, N., B. J. Passer, D. Allanic, E. Segura, C. Théry, B. Goud, R. Amson, and A. Telerman. 2004. TSAP6 Facilitates the Secretion of Translationally Controlled Tumor Protein/Histamine-releasing Factor via a Nonclassical Pathway. *Journal of Biological Chemistry* 279: 46104–46112.

Arcuri, F., S. Papa, A. Meini, A. Carducci, R. Romagnoli, L. Bianchi, M. G. Riparbelli, et al. 2005. The Translationally Controlled Tumor Protein Is a Novel Calcium Binding Protein of the Human Placenta and Regulates Calcium Handling in Trophoblast Cells1. *Biology of Reproduction* 73: 745–751.

Bae, H.-D., J.-S. Lee, H. Pyun, M. Kim, and K. Lee. 2019. Optimization of formulation for enhanced intranasal delivery of insulin with translationally controlled tumor protein-derived protein transduction domain. *Drug Delivery* 26: 622–628.

Bazile, F., A. Pascal, I. Arnal, C. Le Clainche, F. Chesnel, and J. Z. Kubiak. 2009. Complex relationship between TCTP, microtubules and actin microfilaments regulates cell shape in normal and cancer cells. *Carcinogenesis* 30: 555–565.

Berkowitz, O., R. Jost, S. Pollmann, and J. Masle. 2008. Characterization of TCTP, the Translationally Controlled Tumor Protein, from Arabidopsis thaliana. *The Plant Cell* 20: 3430–3447.

Betsch, L., V. Boltz, F. Brioudes, G. Pontier, V. Girard, J. Savarin, B. Wipperman, et al. 2019. TCTP and CSN4 control cell cycle progression and development by regulating CULLIN1 neddylation in plants and animals. *PLOS Genetics* 15: e1007899.

Bischof, J., M. Salzmann, M. K. Streubel, J. Hasek, F. Geltinger, J. Duschl, N. Bresgen, et al. 2017. Clearing the outer mitochondrial membrane from harmful proteins via lipid droplets. *Cell Death Discovery* 3: 17016.

Bloch, D., R. Pleskot, P. Pejchar, M. Potocký, P. Trpkošová, L. Cwiklik, N. Vukašinović, et al. 2016. Exocyst SEC3 and Phosphoinositides Define Sites of Exocytosis in Pollen Tube Initiation and Growth. *Plant Physiology* 172: 980–1002.

Boavida, L. C., and S. McCormick. 2007. Temperature as a determinant factor for increased and reproducible in vitro pollen germination in Arabidopsis thaliana. *The Plant Journal* 52: 570–582.

Bommer, U.-A., K. L. Vine, P. Puri, M. Engel, L. Belfiore, K. Fildes, M. Batterham, et al. 2017. Translationally controlled tumour protein TCTP is induced early in human colorectal tumours

and contributes to the resistance of HCT116 colon cancer cells to 5-FU and oxaliplatin. *Cell Communication and Signaling* 15: 9.

Borg, M., and F. Berger. 2015. Chromatin remodelling during male gametophyte development. *The Plant Journal* 83: 177–188.

Borges, F., G. Gomes, R. Gardner, N. Moreno, S. McCormick, J. A. Feijó, and J. D. Becker. 2008. Comparative Transcriptomics of Arabidopsis Sperm Cells. *Plant Physiology* 148: 1168–1181.

Branco, R., and J. Masle. 2019. Systemic signalling through translationally controlled tumour protein controls lateral root formation in Arabidopsis. *Journal of Experimental Botany* 70: 3927–3940.

Brewbaker, J. L. 1967. The Distribution and Phylogenetic Significance of Binucleate and Trinucleate Pollen Grains in the Angiosperms. *American Journal of Botany* 54: 1069–1083.

Brioudes F., A.-M. Thierry, P. Chambrier, B. Mollereau, and M. Bendahmane. 2010. Translationally controlled tumor protein is a conserved mitotic growth integrator in animals and plants. *Proceedings of the National Academy of Sciences* 107: 16384–16389.

Bruckner, F. P., A. D. S. Xavier, R. D. S. Cascardo, W. C. Otoni, F. M. Zerbini, and P. Alfenas-Zerbini. 2017. Translationally controlled tumour protein (TCTP) from tomato and Nicotiana benthamiana is necessary for successful infection by a potyvirus. *Molecular Plant Pathology* 18: 672–683.

Calderón-Pérez, B., B. Xoconostle-Cázares, R. Lira-Carmona, R. Hernández-Rivas, J. Ortega-López, and R. Ruiz-Medrano. 2014. The Plasmodium falciparum Translationally Controlled Tumor Protein (TCTP) Is Incorporated More Efficiently into B Cells than Its Human Homologue. *PLOS ONE* 9: e85514.

Callis, J., M. Fromm, and V. Walbot. 1987. Introns increase gene expression in cultured maize cells. *Genes & Development* 1: 1183–1200.

Caño-Delgado, A., Y. Yin, C. Yu, D. Vafeados, S. Mora-García, J.-C. Cheng, K. H. Nam, et al. 2004. BRL1 and BRL3 are novel brassinosteroid receptors that function in vascular differentiation in Arabidopsis. *Development* 131: 5341–5351.

C**ans C., B. J. Passer, V. Shalak, V. Nancy-Portebois, V. Crible, N. Amzallag, D. Allanic, et al**. 2003. Translationally controlled tumor protein acts as a guanine nucleotide dissociation inhibitor on the translation elongation factor eEF1A. *Proceedings of the National Academy of Sciences* 100: 13892–13897.

Cantrell, M. S., J. D. Wall, X. Pu, M. Turner, L. Woodbury, K. Fujise, O. M. McDougal, and L. R. Warner. 2022. Expression and purification of a cleavable recombinant fortilin from Escherichia coli for structure activity studies. *Protein Expression and Purification* 189: 105989.

Čapková-Balatková, V., E. Hrabětová, and J. Tupý. 1980. Effects of cycloheximide on pollen of Nicotiana tabacum in Culture. *Biochemie und Physiologie der Pflanzen* 175: 412–420.

de Carvalho, M., M. L. Acencio, A. V. N. Laitz, L. M. de Araújo, M. de Lara Campos Arcuri, L. C. do Nascimento, and I. G. Maia. 2017. Impacts of the overexpression of a tomato translationally controlled tumor protein (TCTP) in tobacco revealed by phenotypic and transcriptomic analysis. *Plant Cell Reports* 36: 887–900.

Cascallares, M., N. Setzes, F. Marchetti, G. A. López, A. M. Distéfano, M. Cainzos, E. Zabaleta, and G. C. Pagnussat. 2020. A Complex Journey: Cell Wall Remodeling, Interactions, and Integrity During Pollen Tube Growth. *Frontiers in Plant Science* 11: 599247.

Ceserani, T., A. Trofka, N. Gandotra, and T. Nelson. 2009. VH1/BRL2 receptor-like kinase interacts with vascular-specific adaptor proteins VIT and VIK to influence leaf venation. *The Plant Journal* 57: 1000–1014.

Chen, Y., X. Chen, H. Wang, Y. Bao, and W. Zhang. 2014. Examination of the leaf proteome during flooding stress and the induction of programmed cell death in maize. *Proteome Science* 12: 33.

Chou, M., C. Xia, Z. Feng, Y. Sun, D. Zhang, M. Zhang, L. Wang, and G. Wei. 2016. A translationally controlled tumor protein gene Rpf41 is required for the nodulation of Robinia pseudoacacia. *Plant Molecular Biology* 90: 389–402.

Clay, N. K., and T. Nelson. 2002. VH1, a Provascular Cell–Specific Receptor Kinase That Influences Leaf Cell Patterns in Arabidopsis. *The Plant Cell* 14: 2707–2722.

Crawford, B. C. W., G. Ditta, and M. F. Yanofsky. 2007. The NTT Gene Is Required for Transmitting-Tract Development in Carpels of Arabidopsis thaliana. *Current Biology* 17: 1101–1108.

Deng, Z., J. Chen, J. Leclercq, Z. Zhou, C. Liu, H. Liu, H. Yang, et al. 2016. Expression Profiles, Characterization and Function of HbTCTP in Rubber Tree (Hevea brasiliensis). *Frontiers in Plant Science* 7: 789.

Dibble, C. C., W. Elis, S. Menon, W. Qin, J. Klekota, J. M. Asara, P. M. Finan, et al. 2012. TBC1D7 Is a Third Subunit of the TSC1-TSC2 Complex Upstream of mTORC1. *Molecular Cell* 47: 535–546.

Dong, X., B. Yang, Y. Li, C. Zhong, and J. Ding. 2009. Molecular Basis of the Acceleration of the GDP-GTP Exchange of Human Ras Homolog Enriched in Brain by Human Translationally Controlled Tumor Protein. *Journal of Biological Chemistry* 284: 23754–23764.

Doré, K. A., J. Kashiwakura, J. M. McDonnell, H. J. Gould, T. Kawakami, B. J. Sutton, and A. M. Davies. 2018. Crystal structures of murine and human Histamine-Releasing Factor (HRF/TCTP) and a model for HRF dimerisation in mast cell activation. *Molecular Immunology* 93: 216–222.

Doucet, J., H. K. Lee, and D. R. Goring. 2016. Pollen Acceptance or Rejection: A Tale of Two Pathways. *Trends in Plant Science* 21: 1058–1067.

Fabrice, T. N., H. Vogler, C. Draeger, G. Munglani, S. Gupta, A. G. Herger, P. Knox, et al. 2018. LRX Proteins Play a Crucial Role in Pollen Grain and Pollen Tube Cell Wall Development. *Plant Physiology* 176: 1981–1992.

Feng, Y., D. Liu, H. Yao, and J. Wang. 2007. Solution structure and mapping of a very weak calcium-binding site of human translationally controlled tumor protein by NMR. *Archives of Biochemistry and Biophysics* 467: 48–57.

Fu, Y. 2015. The cytoskeleton in the pollen tube. *Cell Biology* 28: 111–119.

Fujii, S., K. Kubo, and S. Takayama. 2016. Non-self- and self-recognition models in plant self-incompatibility. *Nature Plants* 2: 16130.

Funston, G., W. Goh, S. J. Wei, Q. S. Tng, C. Brown, L. Jiah Tong, C. Verma, et al. 2012. Binding of Translationally Controlled Tumour Protein to the N-Terminal Domain of HDM2 Is Inhibited by Nutlin-3. *PLOS ONE* 7: e42642.

Gachet, Y., S. Tournier, M. Lee, A. Lazaris-Karatzas, T. Poulton, and U. A. Bommer. 1999. The growth-related, translationally controlled protein P23 has properties of a tubulin binding protein and associates transiently with microtubules during the cell cycle. *Journal of Cell Science* 112: 1257–1271.

Graidist, P., M. Yazawa, M. Tonganunt, A. Nakatomi, C. C.-J. Lin, J.-Y. Chang, A. Phongdara, and K. Fujise. 2007. Fortilin binds Ca2+ and blocks Ca2+-dependent apoptosis in vivo. *Biochemical Journal* 408: 181–191.

Guan, Y., J. Lu, J. Xu, B. McClure, and S. Zhang. 2014. Two Mitogen-Activated Protein Kinases, MPK3 and MPK6, Are Required for Funicular Guidance of Pollen Tubes in Arabidopsis. *Plant Physiology* 165: 528–533.

Gulbranson, D. R., E. M. Davis, B. A. Demmitt, Y. Ouyang, Y. Ye, H. Yu, and J. Shen. 2017. RABIF/MSS4 is a Rab-stabilizing holdase chaperone required for GLUT4 exocytosis. *Proceedings of the National Academy of Sciences* 114: E8224–E8233.

Gutiérrez-Galeano, D. F., R. Toscano-Morales, B. Calderón-Pérez, B. Xoconostle-Cázares, and R. Ruiz-Medrano. 2014. Structural divergence of plant TCTPs. *Frontiers in Plant Science* 5: 361.

Hafidh, S., J. Fíla, and D. Honys. 2016a. Male gametophyte development and function in angiosperms: a general concept. *Plant Reproduction* 29: 31–51.

Hafidh, S., D. Potěšil, J. Fíla, V. Čapková, Z. Zdráhal, and D. Honys. 2016b. Quantitative proteomics of the tobacco pollen tube secretome identifies novel pollen tube guidance proteins important for fertilization. *Genome Biology* 17: 81.

Haghighat, N. G., and L. Ruben. 1992. Purification of novel calcium binding proteins from Trypanosoma brucei: properties of 22-, 24- and 38-kilodalton proteins. *Molecular and Biochemical Parasitology* 51: 99–110.

Han, Y.-J., Y.-M. Kim, O.-J. Hwang, and J.-I. Kim. 2015. Characterization of a small constitutive promoter from Arabidopsis translationally controlled tumor protein (AtTCTP) gene for plant transformation. *Plant Cell Reports* 34: 265–275.

Hartley, J. L., G. F. Temple, and M. A. Brasch. 2000. DNA Cloning Using In Vitro Site-Specific Recombination. *Genome Research* 10: 1788–1795.

Hepler, P. K., and L. J. Winship. 2015. The pollen tube clear zone: Clues to the mechanism of polarized growth. *Journal of Integrative Plant Biology* 57: 79–92.

Hetz, C., and F. R. Papa. 2018. The Unfolded Protein Response and Cell Fate Control. *Molecular Cell* 69: 169–181.

Hinojosa-Moya, J. J., B. Xoconostle-Cázares, R. Toscano-Morales, F. Ramírez-Ortega, J. Luis Cabrera-Ponce, and R. Ruiz-Medrano. 2013. Characterization of the pumpkin Translationally-Controlled Tumor Protein CmTCTP. *Plant Signaling & Behavior* 8: e26477.

Hinojosa-Moya, J., B. Xoconostle-Cázares, E. Piedra-Ibarra, A. Méndez-Tenorio, W. J. Lucas, and R. Ruiz-Medrano. 2008. Phylogenetic and Structural Analysis of Translationally Controlled Tumor Proteins. *Journal of Molecular Evolution* 66: 472–483.

Hoepflinger, M. C., J. Reitsamer, A. M. Geretschlaeger, N. Mehlmer, and R. Tenhaken. 2013. The effect of Translationally Controlled Tumour Protein (TCTP) on programmed cell death in plants. *BMC Plant Biology* 13: 135.

Hoffmann, R. D., M. T. Portes, L. I. Olsen, D. S. C. Damineli, M. Hayashi, C. O. Nunes, J. T. Pedersen, et al. 2020. Plasma membrane H+-ATPases sustain pollen tube growth and fertilization. *Nature Communications* 11: 2395.

Hollien, J. 2013. Evolution of the unfolded protein response. *Biochimica et Biophysica Acta (BBA) - Molecular Cell Research* 11: 2458–2463.

Holmes-Davis, R., C. K. Tanaka, W. H. Vensel, W. J. Hurkman, and S. McCormick. 2005. Proteome mapping of mature pollen of Arabidopsis thaliana. *Proteomics* 5: 4864–4884.

Honys, D., D. Reňák, J. Feciková, P. L. Jedelský, J. Nebesářová, P. Dobrev, and V. Čapková. 2009. Cytoskeleton-Associated Large RNP Complexes in Tobacco Male Gametophyte (EPPs) Are Associated with Ribosomes and Are Involved in Protein Synthesis, Processing, and Localization. *Journal of Proteome Research* 8: 2015–2031.

Hossain, Z., L. Amyot, B. McGarvey, M. Gruber, J. Jung, and A. Hannoufa. 2012. The Translation Elongation Factor eEF-1Bβ1 Is Involved in Cell Wall Biosynthesis and Plant Development in Arabidopsis thaliana. *PLOS ONE* 7: e30425.

Hsu, Y.-C., J. J. Chern, Y. Cai, M. Liu, and K.-W. Choi. 2007. Drosophila TCTP is essential for growth and proliferation through regulation of dRheb GTPase. *Nature* 445: 785–788.

Inoki, K., Y. Li, T. Xu, and K.-L. Guan. 2003. Rheb GTPase is a direct target of TSC2 GAP activity and regulates mTOR signaling. *Genes & Development* 17: 1829–1834.

Iwano, M., M. Igarashi, Y. Tarutani, P. Kaothien-Nakayama, H. Nakayama, H. Moriyama, R. Yakabe, et al. 2014. A Pollen Coat–Inducible Autoinhibited Ca2+-ATPase Expressed in Stigmatic Papilla Cells Is Required for Compatible Pollination in the Brassicaceae. *The Plant Cell* 26: 636–649.

Jaglarz, M. K., F. Bazile, K. Laskowska, Z. Polanski, F. Chesnel, E. Borsuk, M. Kloc, and J. Z. Kubiak. 2012. Association of TCTP with Centrosome and Microtubules. *Biochemistry Research International* 2012: 541906.

Jeon, H.-J., S. Y. You, Y. S. Park, J. W. Chang, J.-S. Kim, and J. S. Oh. 2016. TCTP regulates spindle microtubule dynamics by stabilizing polar microtubules during mouse oocyte meiosis. *Biochimica et Biophysica Acta (BBA) - Molecular Cell Research* 1863: 630–637.

Jeong, M., M. H. Jeong, J. E. Kim, S. Cho, K. J. Lee, S. Park, J. Sohn, and Y. G. Park. 2021. TCTP protein degradation by targeting mTORC1 and signaling through S6K, Akt, and Plk1 sensitizes lung cancer cells to DNA-damaging drugs. *Scientific Reports* 11: 20812.

Jiang, J., and S. D. Clouse. 2001. Expression of a plant gene with sequence similarity to animal TGF-β receptor interacting protein is regulated by brassinosteroids and required for normal plant development. *The Plant Journal* 26: 35–45.

Kang, H. S., M. J. Lee, H. Song, S. H. Han, Y. M. Kim, J. Y. Im, and I. Choi. 2001. Molecular Identification of IgE-Dependent Histamine-Releasing Factor as a B Cell Growth Factor. *The Journal of Immunology* 166: 6545.

Karimi, M., A. Depicker, and P. Hilson. 2007. Recombinational Cloning with Plant Gateway Vectors. *Plant Physiology* 145: 1144–1154.

Kashiwakura, J., T. Ando, K. Matsumoto, M. Kimura, J. Kitaura, M. H. Matho, D. M. Zajonc, et al. 2012. Histamine-releasing factor has a proinflammatory role in mouse models of asthma and allergy. *The Journal of Clinical Investigation* 122: 218–228.

Kawai-Yamada, M., L. Jin, K. Yoshinaga, A. Hirata, and H. Uchimiya. 2001. Mammalian Bax-induced plant cell death can be down-regulated by overexpression of Arabidopsis Bax Inhibitor-1 (AtBI-1). *Proceedings of the National Academy of Sciences* 98: 12295–12300.

Kawakami, Y., K. Kasakura, and T. Kawakami. 2019. Histamine-Releasing Factor, a New Therapeutic Target in Allergic Diseases. *Cells* 8: 1515.

Kim, M., Y. Jung, K. Lee, and C. Kim. 2000. Identification of the calcium binding sites in translationally controlled tumor protein. *Archives of Pharmacal Research* 23: 633–636.

Kim, M., M. Kim, H. Y. Kim, S. Kim, J. Jung, J. Maeng, J. Chang, and K. Lee. 2011. A protein transduction domain located at the NH2-terminus of human translationally controlled tumor protein for delivery of active molecules to cells. *Biomaterials* 32: 222–230.

Kim, M., H. J. Min, H. Y. Won, H. Park, J.-C. Lee, H.-W. Park, J. Chung, et al. 2009. Dimerization of Translationally Controlled Tumor Protein Is Essential For Its Cytokine-Like Activity. *PLOS ONE* 4: e6464.

Kiraz, Y., A. Adan, M. Kartal Yandim, and Y. Baran. 2016. Major apoptotic mechanisms and genes involved in apoptosis. *Tumor Biology* 37: 8471–8486.

Koo, N., A.-Y. Shin, S. Oh, H. Kim, S. Hong, S.-J. Park, Y. M. Sim, et al. 2020. Comprehensive analysis of Translationally Controlled Tumor Protein (TCTP) provides insights for lineage-specific evolution and functional divergence. *PLOS ONE* 15: e0232029.

Lakhssassi, N., V. G. Doblas, A. Rosado, A. E. del Valle, D. Posé, A. J. Jimenez, A. G. Castillo, et al. 2012. The Arabidopsis TETRATRICOPEPTIDE THIOREDOXIN-LIKE Gene Family Is Required for Osmotic Stress Tolerance and Male Sporogenesis. *Plant Physiology* 158: 1252–1266.

Langdon, J. M., B. M. Vonakis, and S. M. MacDonald. 2004. Identification of the interaction between the human recombinant histamine releasing factor/translationally controlled tumor protein and elongation factor-1 delta (also known as eElongation factor-1B beta). *Biochimica et Biophysica Acta (BBA) - Molecular Basis of Disease* 1688: 232–236.

Lee, H., M.-S. Kim, J.-S. Lee, H. Cho, J. Park, D. Hae Shin, and K. Lee. 2020. Flexible loop and helix 2 domains of TCTP are the functional domains of dimerized TCTP. *Scientific Reports* 10: 197.

Lespagnol, A., D. Duflaut, C. Beekman, L. Blanc, G. Fiucci, J.-C. Marine, M. Vidal, et al. 2008. Exosome secretion, including the DNA damage-induced p53-dependent secretory pathway, is severely compromised in TSAP6/Steap3-null mice. *Cell Death & Differentiation* 15: 1723–1733.

Levine, A. J. 2020. p53: 800 million years of evolution and 40 years of discovery. *Nature Reviews Cancer* 20: 471–480.

Li, D., Z. Deng, X. Liu, and B. Qin. 2013. Molecular cloning, expression profiles and characterization of a novel translationally controlled tumor protein in rubber tree (Hevea brasiliensis). *Journal of Plant Physiology* 170: 497–504.

Li, F., D. Zhang, and K. Fujise. 2001. Characterization of Fortilin, a Novel Antiapoptotic Protein. *Journal of Biological Chemistry* 276: 47542–47549.

Lin, Z., X. Zhang, J. Wang, W. Liu, Q. Liu, Y. Ye, B. Dai, et al. 2020. Translationally controlled tumor protein promotes liver regeneration by activating mTORC2/AKT signaling. *Cell Death & Disease* 11: 58.

Liu, C., L. Shen, Y. Xiao, D. Vyshedsky, C. Peng, X. Sun, Z. Liu, et al. 2021a. Pollen PCP-B peptides unlock a stigma peptide–receptor kinase gating mechanism for pollination. *Science* 372: 171–175.

Liu, G. Y., and D. M. Sabatini. 2020. mTOR at the nexus of nutrition, growth, ageing and disease. *Nature Reviews Molecular Cell Biology* 21: 183–203.

Liu H., H.-W. Peng, Y.-S. Cheng, H.-Y. Yuan, and H.-F. Yang-Yen. 2005. Stabilization and Enhancement of the Antiapoptotic Activity of Mcl-1 by TCTP. *Molecular and Cellular Biology* 25: 3117–3126.

Liu, M., Z. Wang, S. Hou, L. Wang, Q. Huang, H. Gu, T. Dresselhaus, et al. 2021b. AtLURE1/PRK6-mediated signaling promotes conspecific micropylar pollen tube guidance. *Plant Physiology* 186: 865–873.

Long, X., Y. Lin, S. Ortiz-Vega, K. Yonezawa, and J. Avruch. 2005. Rheb Binds and Regulates the mTOR Kinase. *Current Biology* 15: 702–713.

MacDonald S. M., T. Rafnar, J. Langdon, and L. M. Lichtenstein. 1995. Molecular Identification of an IgE-Dependent Histamine-Releasing Factor. *Science* 269: 688–690.

Malard, F., N. Assrir, M. Alami, S. Messaoudi, E. Lescop, and T. Ha-Duong. 2018. Conformational Ensemble and Biological Role of the TCTP Intrinsically Disordered Region: Influence of Calcium and Phosphorylation. *Journal of Molecular Biology* 430: 1621–1639.

Malherbe, G., D. P. Humphreys, and E. Davé. 2019. A robust fractionation method for protein subcellular localization studies in Escherichia coli. *BioTechniques* 66: 171–178.

Marshall, R. S., L. Frigerio, and L. M. Roberts. 2010. Disulfide formation in plant storage vacuoles permits assembly of a multimeric lectin. *Biochemical Journal* 427: 513–521.

Mecchia, M. A., G. Santos-Fernandez, N. N. Duss, S. C. Somoza, A. Boisson-Dernier, V. Gagliardini, A. Martínez-Bernardini, et al. 2017. RALF4/19 peptides interact with LRX proteins to control pollen tube growth in Arabidopsis. *Science* 358: 1600–1603.

Meng, X. N., Q. M. Chen, H. Y. Fan, T. F. Song, N. Cui, J. Y. Zhao, S. M. Jia, and K. X. Meng. 2017. Molecular characterization, expression analysis and heterologous expression of two translationally controlled tumor protein genes from Cucumis sativus. *PLOS ONE* 12: e0184872.

Meng, X., Y. Yu, J. Zhao, N. Cui, T. Song, Y. Yang, and H. Fan. 2018. The Two Translationally Controlled Tumor Protein Genes, CsTCTP1 and CsTCTP2, Are Negative Modulators in the Cucumis sativus Defense Response to Sphaerotheca fuliginea. *Frontiers in Plant Science* 9: 544.

Mori, T., H. Kuroiwa, T. Higashiyama, and T. Kuroiwa. 2006. GENERATIVE CELL SPECIFIC 1 is essential for angiosperm fertilization. *Nature Cell Biology* 8: 64–71.

Moussu, S., C. Broyart, G. Santos-Fernandez, S. Augustin, S. Wehrle, U. Grossniklaus, and J. Santiago. 2020. Structural basis for recognition of RALF peptides by LRX proteins during pollen tube growth. *Proceedings of the National Academy of Sciences* 117: 7494–7503.

Munirathinam, G., and K. Ramaswamy. 2012. Sumoylation of Human Translationally Controlled Tumor Protein Is Important for Its Nuclear Transport. *Biochemistry Research International* 2012: 831940.

Oh, S.-A., T. N. T. Hoai, H.-J. Park, M. Zhao, D. Twell, D. Honys, and S.-K. Park. 2020. MYB81, a microspore-specific GAMYB transcription factor, promotes pollen mitosis I and cell lineage formation in Arabidopsis. *The Plant Journal* 101: 590–603.

Okamura, E., T. Sakamoto, T. Sasaki, and S. Matsunaga. 2017. A Plant Ancestral Polo-Like Kinase Sheds Light on the Mystery of the Evolutionary Disappearance of Polo-Like Kinases in the Plant Kingdom. *Cytologia* 82: 261–266.

Palanivelu, R., L. Brass, A. F. Edlund, and D. Preuss. 2003. Pollen Tube Growth and Guidance Is Regulated by POP2, an Arabidopsis Gene that Controls GABA Levels. *Cell* 114: 47–59.

Palanivelu, R., and D. Preuss. 2006. Distinct short-range ovule signals attract or repel Arabidopsis thaliana pollen tubes in vitro. *BMC Plant Biology* 6: 7.

Park, S. K., R. Howden, and D. Twell. 1998. The Arabidopsis thaliana gametophytic mutation gemini pollen1 disrupts microspore polarity, division asymmetry and pollen cell fate. *Development* 125: 3789–3799.

Pinkaew, D., A. Chattopadhyay, M. D. King, P. Chunhacha, Z. Liu, H. L. Stevenson, Y. Chen, et al. 2017. Fortilin binds IRE1α and prevents ER stress from signaling apoptotic cell death. *Nature Communications* 8: 18.

Qin, Y., A. R. Leydon, A. Manziello, R. Pandey, D. Mount, S. Denic, B. Vasic, et al. 2009. Penetration of the Stigma and Style Elicits a Novel Transcriptome in Pollen Tubes, Pointing to Genes Critical for Growth in a Pistil. *PLOS Genetics* 5: e1000621.

Reynolds, J. E., T. Yang, L. Qian, J. D. Jenkinson, P. Zhou, A. Eastman, and R. W. Craig. 1994. Mcl-1, a Member of the Bcl-2 Family, Delays Apoptosis Induced by c-Myc Overexpression in Chinese Hamster Ovary Cells1. *Cancer Research* 54: 6348–6352.

Rosado, A., A. L. Schapire, R. A. Bressan, A. L. Harfouche, P. M. Hasegawa, V. Valpuesta, and M. A. Botella. 2006. The Arabidopsis Tetratricopeptide Repeat-Containing Protein TTL1 Is Required for Osmotic Stress Responses and Abscisic Acid Sensitivity. *Plant Physiology* 142: 1113–1126.

Rozier, F., L. Riglet, C. Kodera, V. Bayle, E. Durand, J. Schnabel, T. Gaude, and I. Fobis-Loisy. 2020. Live-cell imaging of early events following pollen perception in self-incompatible Arabidopsis thaliana. *Journal of Experimental Botany* 71: 2513–2526.

Safavian, D., and D. R. Goring. 2013. Secretory Activity Is Rapidly Induced in Stigmatic Papillae by Compatible Pollen, but Inhibited for Self-Incompatible Pollen in the Brassicaceae. *PLOS ONE* 8: e84286.

Sanchez, J.-C., D. Schaller, F. Ravier, O. Golaz, S. Jaccoud, M. Belet, M. R. Wilkins, et al. 1997. Translationally controlled tumor protein: A protein identified in several nontumoral cells including erythrocytes. *Electrophoresis* 18: 150–155.

Sarwar, A. K. M. G., and H. Takahashi. 2014. Pollen morphology of Erica L. and related genera and its taxonomic significance. *Grana* 53: 221–231.

Schiefelbein, J., M. Galway, J. Masucci, and S. Ford. 1993. Pollen Tube and Root-Hair Tip Growth Is Disrupted in a Mutant of Arabidopsis thaliana. *Plant Physiology* 103: 979–985.

Schoenaers, S., D. Balcerowicz, A. Costa, and K. Vissenberg. 2017. The Kinase ERULUS Controls Pollen Tube Targeting and Growth in Arabidopsis thaliana. *Frontiers in Plant Science* 8: 1942.

Schroeder, J. T., L. M. Lichtenstein, and S. M. MacDonald. 1996. An immunoglobulin E-dependent recombinant histamine-releasing factor induces interleukin-4 secretion from human basophils. *Journal of Experimental Medicine* 183: 1265–1270.

Studier, F. W., and B. A. Moffatt. 1986. Use of bacteriophage T7 RNA polymerase to direct selective high-level expression of cloned genes. *Journal of Molecular Biology* 189: 113–130.

Susini, L., S. Besse, D. Duflaut, A. Lespagnol, C. Beekman, G. Fiucci, A. R. Atkinson, et al. 2008. TCTP protects from apoptotic cell death by antagonizing bax function. *Cell Death & Differentiation* 15: 1211–1220.

Takasaki, H., T. Mahmood, M. Matsuoka, H. Matsumoto, and S. Komatsu. 2008. Identification and characterization of a gibberellin-regulated protein, which is ASR5, in the basal region of rice leaf sheaths. *Molecular Genetics and Genomics* 279: 359–370.

T**ao, J.-J., Y.-R. Cao, H.-W. Chen, W. Wei, Q.-T. Li, B. Ma, W.-K. Zhang, et al**. 2015. Tobacco Translationally Controlled Tumor Protein Interacts with Ethylene Receptor Tobacco Histidine Kinase1 and Enhances Plant Growth through Promotion of Cell Proliferation. *Plant Physiology* 169: 96–114.

Tatebe, H., and K. Shiozaki. 2017. Evolutionary Conservation of the Components in the TOR Signaling Pathways. *Biomolecules* 7: 77.

Thaw, P., N. J. Baxter, A. M. Hounslow, C. Price, J. P. Waltho, and C. J. Craven. 2001. Structure of TCTP reveals unexpected relationship with guanine nucleotide-free chaperones. *Nature Structural Biology* 8: 701–704.

Thébault, S., M. Agez, X. Chi, J. Stojko, V. Cura, S. B. Telerman, L. Maillet, et al. 2016. TCTP contains a BH3-like domain, which instead of inhibiting, activates Bcl-xL. *Scientific Reports* 6: 19725.

Toscano-Morales, R., B. Xoconostle-Cázares, J. L. Cabrera-Ponce, J. Hinojosa-Moya, J. L. Ruiz-Salas, V. Galván-Gordillo, R. G. Guevara-González, and R. Ruiz-Medrano. 2015. AtTCTP2, an Arabidopsis thaliana homolog of Translationally Controlled Tumor Protein, enhances in vitro plant regeneration. *Frontiers in Plant Science* 6: 468.

Tsarova, K., E. G. Yarmola, and M. R. Bubb. 2010. Identification of a cofilin-like actin-binding site on translationally controlled tumor protein (TCTP). *FEBS Letters* 584: 4756–4760.

Vancraenenbroeck, R., E. Lobbestael, S. D. Weeks, S. V. Strelkov, V. Baekelandt, J.-M. Taymans, and M. De Maeyer. 2012. Expression, purification and preliminary biochemical and structural characterization of the leucine rich repeat namesake domain of leucine rich repeat kinase 2. *Biochimica et Biophysica Acta (BBA) - Proteins and Proteomics* 1824: 450–460.

Vedadi, M., J. Lew, J. Artz, M. Amani, Y. Zhao, A. Dong, G. A. Wasney, et al. 2007. Genome-scale protein expression and structural biology of Plasmodium falciparum and related Apicomplexan organisms. *Molecular and Biochemical Parasitology* 151: 100–110.

Vogler, H., G. Santos-Fernandez, M. A. Mecchia, and U. Grossniklaus. 2019. To preserve or to destroy, that is the question: the role of the cell wall integrity pathway in pollen tube growth. *Cell Biology* 52: 131–139.

Wang, L., L. A. Clarke, R. J. Eason, C. C. Parker, B. Qi, R. J. Scott, and J. Doughty. 2017. PCP-B class pollen coat proteins are key regulators of the hydration checkpoint in Arabidopsis thaliana pollen–stigma interactions. *New Phytologist* 213: 764–777.

Wang, X., B. D. Fonseca, H. Tang, R. Liu, A. Elia, M. J. Clemens, U.-A. Bommer, and C. G. Proud. 2008. Re-evaluating the Roles of Proposed Modulators of Mammalian Target of Rapamycin Complex 1 (mTORC1) Signaling. *Journal of Biological Chemistry* 283: 30482–30492.

Warren, C. F. A., M. W. Wong-Brown, and N. A. Bowden. 2019. BCL-2 family isoforms in apoptosis and cancer. *Cell Death & Disease* 10: 177.

Wu, H., W. Gong, X. Yao, J. Wang, S. Perrett, and Y. Feng. 2015. Evolutionarily Conserved Binding of Translationally Controlled Tumor Protein to Eukaryotic Elongation Factor 1B. *Journal of Biological Chemistry* 290: 8694–8710.

Xu, B., L. Liu, and G. Song. 2022. Functions and Regulation of Translation Elongation Factors. *Frontiers in Molecular Biosciences* 8: 816398.

Yang, H., C. You, S. Yang, Y. Zhang, F. Yang, X. Li, N. Chen, et al. 2021. The Role of Calcium/Calcium-Dependent Protein Kinases Signal Pathway in Pollen Tube Growth. *Frontiers in Plant Science* 12: 633293.

Yang, Y., F. Yang, Z. Xiong, Y. Yan, X. Wang, M. Nishino, D. Mirkovic, et al. 2005. An N-terminal region of translationally controlled tumor protein is required for its antiapoptotic activity. *Oncogene* 24: 4778–4788.

Yao, X., Y.-J. Liu, Q. Cui, and Y. Feng. 2019. Solution structure of a unicellular microalgae-derived translationally controlled tumor protein revealed both conserved features and structural diversity. *Archives of Biochemistry and Biophysics* 665: 23–29.

Yao, X., Y. Xiao, Q. Cui, and Y. Feng. 2015. 1H, 15N and 13C resonance assignments of translationally-controlled tumor protein from photosynthetic microalga Nannochloropsis oceanica. *Biomolecular NMR Assignments* 9: 325–328.

Yarm F. R. 2002. Plk Phosphorylation Regulates the Microtubule-Stabilizing Protein TCTP. *Molecular and Cellular Biology* 22: 6209–6221.

Yenofsky, R., S. Cereghini, A. Krowczynska, and G. Brawerman. 1983. Regulation of mRNA utilization in mouse erythroleukemia cells induced to differentiate by exposure to dimethyl sulfoxide. *Molecular and Cellular Biology* 3: 1197–1203.

Yong-Min K., Y.-J. Han, O.-J. Hwang, S.-S. Lee, A.-Y. Shin, S. Y. Kim, and and J-I. Kim. 2012. Overexpression of Arabidopsis Translationally Controlled Tumor Protein Gene AtTCTP Enhances Drought Tolerance with Rapid ABA-Induced Stomatal Closure. *Molecules and Cells* 33: 617–626.

Yoon, T., J. Jung, M. Kim, K. M. Lee, E. C. Choi, and K. Lee. 2000. Identification of the Self-Interaction of Rat TCTP/IgE-Dependent Histamine-Releasing Factor Using Yeast Two-Hybrid System. *Archives of Biochemistry and Biophysics* 384: 379–382.

Z**huo, K., J. Chen, B. Lin, J. Wang, F. Sun, L. Hu, and J. Liao**. 2017. A novel Meloidogyne enterolobii effector MeTCTP promotes parasitism by suppressing programmed cell death in host plants. *Molecular Plant Pathology* 18: 45–54.

Zou, X., L. Li, F. Liao, and W. Chen. 2021. iTRAQ-based quantitative proteomic analysis reveals NtGNL1-dependent regulatory network underlying endosome trafficking for pollen tube polar growth. *Plant Physiology and Biochemistry* 161: 200–209.

Supplement

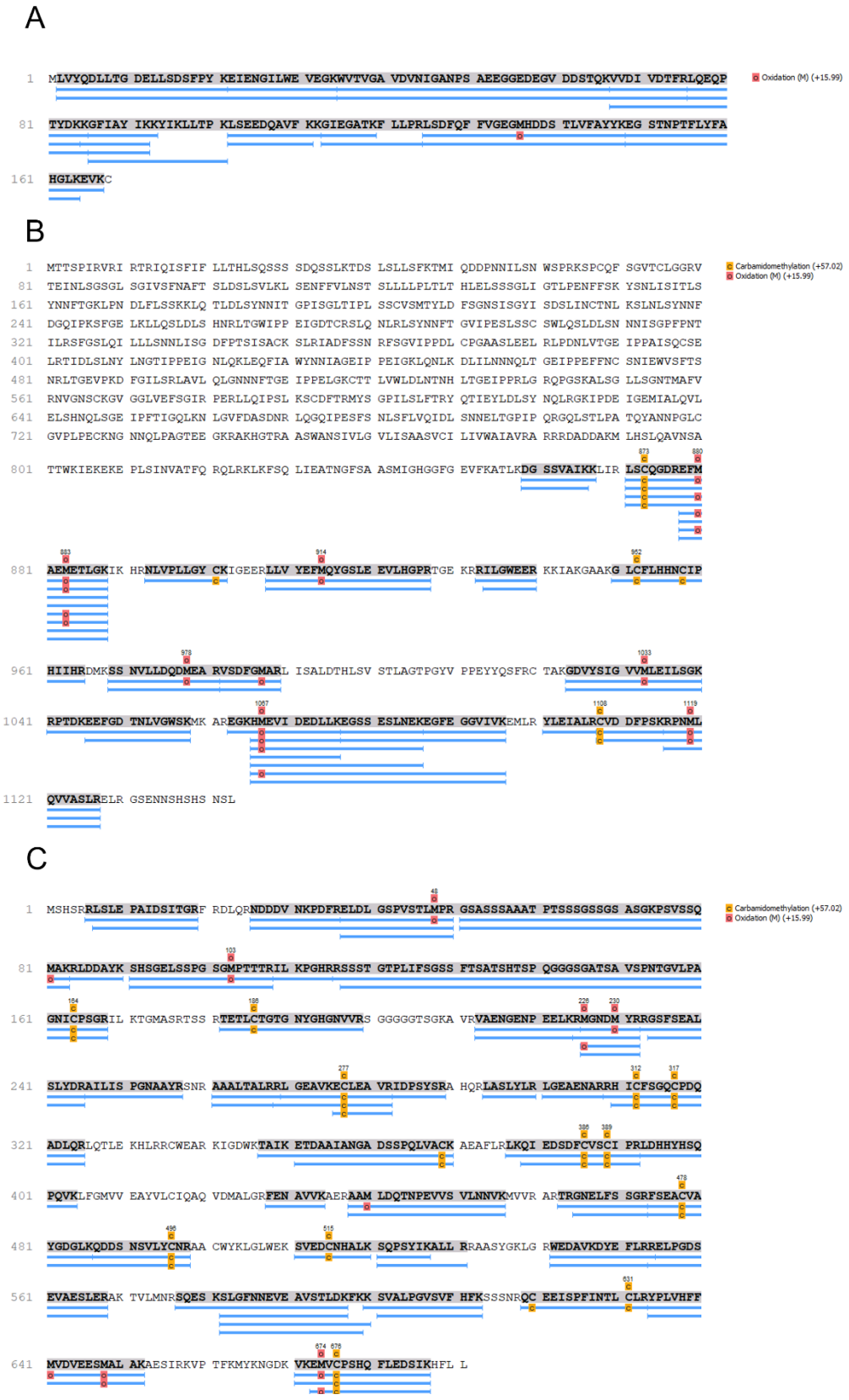

Figure S1. Alignment of LC-MS/MS identified peptides with (A) TCTP1, (B) BRL2 and (C) TTL3 sequence. *BRL2 was expressed as an intracellular kinase domain and aligns to this region (B). Detected modifications might be an artefact of sample preparation.*